Sex-Specific Changes in Bone Structure and Strength during Growth:

pQCT Analysis of the Mid-Tibia

by

Yasmin Ahamed

BSc, The University of British Columbia, 2004

A thesis submitted in partial fulfillment of the requirements

for the degree of

MASTER OF SCIENCE

in

THE FACULTY OF GRADUATE STUDIES

(Experimental Medicine)

University of British Columbia

December 2007

Abstract

Introduction: The process by which children's bones grow has not been fully chracterised. The current dogma is that girls fill in their medullary canal area by forming bone at the endosteum. It has been argued that the sex difference in how bone strength is conferred -- favoring boys -- may contribute to the relative protection that aging men have over aging women with respect to fracture incidence and the prevalence of osteoporosis.

Primary Objectives:

1) To compare bone surface changes at the periosteal and endosteal surface of the tibial midshaft in boys and girls.
2) To compare how bone density at the tibial midshaft is accrued in boys and girls.
3) To compare sex differences in bone strength accrual.

Methods:

Design and Participants: Participants were obtained from a 20-month randomized, controlled school-based physical activity intervention. As we found no difference in the effect of the intervention on pQCT bone outcome variables, both groups were combined for our current study. A total of 183 participants (93 boys, 89 girls) received a pQCT scan at baseline.

Results: Sex-specific comparisons of the pQCT bone outcome variables showed significantly greater rates of change (slope) for boys for the total area (ToA), cortical area (CoA), medullary canal area (MedA) and strength-strain index (SSI) measures, $p<0.001$. No significant differences were observed for CoD, $p=0.904$. The magnitude of these differences is 60.8% for ToA, 55.7% for CoA, 75.6% for MedA, 1.3% for CoD, and 54.7% for SSI. Examination of differences between the sexes (intercept) revealed significant differences with greater gains observed for boys for all measures $p<0.001$ except for CoD where girls exhibited greater gains $p<0.001$.

Conclusion: Girls showed a similar pattern of cortical bone growth at the tibial midshaft- periosteal apposition dominated over endosteal resorption. Boys' increased changes and pattern of growth were of a greater magnitude at both surfaces compared to girls. This resulted in a greater increase in strength as measured by SSI in boys which can partly be explained by their larger size. Girls exhibited greater increases in CoD; however, no significant difference in the change in CoD was observed between the two.

Table of contents

List of Figures

List of Tables

List of Terms

pQCT	Peripheral quantitative computed tomography. XCT-2000 model is used in the research used in this thesis.
ToA	Total bone cross-sectional area (mm^2) as measured with pQCT.
CoA	Cortical bone cross-sectional area (mm^2) as measured with pQCT.
CavA	Area of the marrow cavity (mm^2) as calculated with pQCT outcomes of ToA and CoA. (CavA = ToA – CoA)
CTh	Cortical thickness (mm) as measured with pQCT determines the distance between the outer and inner border of the cortical shell.
CoD	Cortical bone mineral density (mg/cm^3) as measured with pQCT.
SSI	Polar strength-strain index (mm^3) as measured by pQCT. Also commonly known as the density-weighted polar section modulus. Ultimate failure load of bone. In this thesis bone strength is estimated with pQCT-derived SSI.
DXA	Dual energy x-ray absorptiometry. Hologic QDR 4500W model is discussed in this thesis.
TBBMC	Total Body Bone Mineral Content (g) as measured with DXA.
BMC	Bone mineral content (g) as measured by DXA.
aBMD	Areal bone mineral density (g/cm^2) as measured by DXA. The ratio of bone mineral content to the projectional area of bone (g/cm^2) as measured by DXA.
vBMD	Volumetric bone mineral density (g/cm^2). The amount of bone mineral averaged over a certain volume as measured by pQCT. Can be cortical (CoD), trabecular (TrbD) or total bone mineral density (ToD).
NN	Narrow neck. Refers to the narrowest region of the femoral neck.
CSA	Cross-sectional area (cm^2) as measured by pQCT.
CSMI	Cross-sectional moment of inertia (cm^4) as measured by pQCT.
Z	Section modulus (cm^3) as measured by pQCT. Provides an estimate of bone bending strength.
Bone mass	Amount of bone material within a cross-section or region of interest (e.g. BMC by DXA).
Bone structure	Properties of bone such as size, shape and distribution of material that contribute to bone strength.
Voxels	Used to make up an image in pQCT, Volume elements arranged on a fixed regular grid that defines 3D bone.
Multilevel Modeling (MLM)	Statistical method that summarizes hierarchical data measured or data being collected at more than one level within groups.
Healthy Bones Study (HBS)	Elementary school-based jumping intervention aimed to increase bone accrual in a mixed ethnic group of children.
Sexual Maturation Rating (SMR)/ Tanner Staging	A self-report method of assessing the stage of reproductive (or sexual) maturity in girls and boys. In this thesis Tanner stage for girls refers to breast stage and pubic hair and Tanner stage for boys refers to pubic hair.

Prepuberty	Period prior to puberty onset. Usually marked by accelerated physical growth. Classified by Tanner stage 1.
Early puberty	Period where changes in growth and sexual maturation start to become apparent. Classified as Tanner stage 2 or 3.
Peri-puberty	Period around puberty, after pre puberty but before post puberty. Classified by Tanner stages 2 or 3.
Puberty	Period of time (usually between the ages of 10 and 15) during which sexual development occurs, allowing reproduction to become possible. Classified by Tanner stage 4
Post Puberty	Period where full sexual maturation has been attained. Classified by Tanner Stage 5
Premenarcheal	Refers to a girl who has not yet experienced her first menstrual period.
Postmenarcheal	Refers to a girl who has experienced her first menstrual period.
Peak Height Velocity (PHV)	Maximum rate of gain (cm/yr) in height during adolescence.
Age at Peak Height Velocity (APHV)	An indicator of somatic maturity that reflects the age of maximum gain in height during adolescence.
Maturity Offset/ Biological Age	Accounts for maturational differences observed between adolescents of the same sex and chronological age. Maturity offset = (APHV- chronological age at time of measurement)

Acknowledgements

This thesis is a product of the support and help of many people whom I have had the pleasure of working with. I must first start of by thanking my supervisor, Dr. Heather McKay. Her constant support, patience, love for research, and her vast knowledge has been instrumental in the success of her lab and in the success of her students. Heather, I thank you for your patience, for always taking the time out to be there for me, and for helping me to achieve my goals. I appreciate how you strive for the best in everything that you do and for the opportunities you have provided me with. You truly are an inspiration who inspires me to achieve greatness. Second, I have to thank Dr. Karim Khan for his constant support and encouragement. Thank you Dr. Khan for always reminding everyone in the lab that the work we do is important and that we will one day make a difference. I appreciate your honesty and your ability to see the best in everyone. Your guidance and objective advice has been instrumental in the career choices I have made. I am also in debt to Dr. Penny Brasher who is a brilliant statistician and amazing teacher. Penny I have enjoyed our meetings and would look forward to showing you my results so that we could take the analysis to the next level. I have learnt so much from you. I appreciate your patience and your honesty. I would like to thank Dr. Saija Kontulainen for her pQCT analysis guidance and for her constant support and friendship. I am amazed at times at your enthusiasm and love for your research and I wish you much future success. Last but certainly not least, I must thank Dr. David Cooper. Dave there are no words to fully describe how much I appreciate you. I have enjoyed the countless hours we have spent discussing our research and science. Your excitement and passion for your research and your hard work motivates all those whom are lucky enough to work with you. Thank you for always answering my questions and for being a true friend. You have contributed immensely to my growth as a researcher and I could not have asked for a better mentor. You are an amazing scientist/researcher that will make great contributions to the scientific community. I wish you all the best in all your future endeavours.

The research in our lab would not be possible without our wonderful support staff. Dr. Melonie Burrows, although new to the BHRG I feel like we have formed a close friendship. I admire your personal strength and wish you much success in your aim to advance your research career. I would like to give a very special thanks to Margie Bell for all the advice you have given me over the years, both on a professional and personal level. I have enjoyed the talks we have had over tea and I thank you for motivating me, believing in me and for your honesty. I feel lucky to have met you. Finally, this study would not have been possible without all of the wonderful participants who have dedicated their time so that we could obtain such wonderful data.

I am very fortunate to have such a loving and supportive family and for my network of friends. My mom has always stressed the importance of education and hard work. Mom, you have instilled in me the passion and confidence to be the best that I can be and I thank you for all your love and guidance. I would like to give a special thanks to my siblings, Ashifa and Sophia for always making me laugh and for always cheering me on. You both mean the world to me. I would also like to thank Jen Faddegon for being a most wonderful friend. I will miss our Friday night dinners where we would discuss our research and our life goals. Thank you also to Rosey Sharma, Zubin Amarsi, Jennifer Zhang, Nadya Castro, Dexter Tan, and Jason Reyes for being wonderful friends and for forcing me to take breaks.

My final thank you is left for my significant other, Jagdeep Heer. Although you have resided in Australia for the past few years, you always managed to take the time to call to see how I was doing and to provide your support. I appreciate your ability to always make me laugh, for your encouragement throughout this entire process and for pushing me to see beyond my self-imposed boundaries. I admire your ability to embrace change and for your attempts to make the impossible possible.

I wish you all much success and happiness in all that you do.

1 Introduction

It has been estimated that in Canada, the number of proximal femur fractures in the aging population will be 88,124 (range: 78,649-103,954) per annum by 2041 (206). In addition, the number of Canadians that will die from this type of fracture has been projected to increase from 1570 in 1993/1994 to 7000 by the year 2041 (206). The costs associated with osteoporosis and osteoporosis related fractures is staggering (151). In 2003, the costs of Canadian health care services directly associated with osteoporosis were reported to be an estimated $1.3 billion (151). Osteoporosis-related femur fractures alone cost the Canadian health care system $650 million/year and this amount is expected to rise exponentially to $2.4 billion/year by 2041 (206, 274).

In the literal sense, osteoporosis means porous bone. In 1994, the National Osteoporosis Foundation and the World Health Organization defined osteoporosis as a "systemic skeletal disease characterized by low bone mass and microarchitecture deteroration" (80). This occurs by trabecular thining and increased porosity of cortical bone. These events occurring in combination result in increased bone fragility and thus increase the susceptibility to fracture (80). It is not a disease that can be attributed to a single cause but rather is comprised of various mechanisms that differ between individuals. Some individuals with this disease experience maladaptation to loading; estrogen, calcium and Vitamin D deficiencies; altered parathyroid hormone (PTH) secretion; genetic defects or a combination of these to name a few (221). Thus, it comes to no surprise that there is no current cure for this disease. As the general population ages, the impact of this disease and its associated fractures on health care costs and the burden to society will be staggering (33).

Bone mineral status at any time in life is dependent on the amount accumulated during the growing years and the amount lost in adulthood (6). Thus, childhood and adolescence is considered a critical time period for bone mineral accrual (216). Pubertal growth marks a valuable period where gains in bone acquisition and the completion of skeletal growth occur (256). It is also the period of sexual maturation, where increases in height, weight, and changes in body composition occur (256). All these factors influence overall bone size and strength (156). Thus, increasing the amount of total bone attained during peak bone mineral accrual is likely to be associated with less severe biomechanical consequences that are apparent during bone loss (221).

In the 1960 and 1970's, Garn et al., were the first to conduct radiographic studies of the second metacarpal examining bone surface changes during growth in children (92). These cross-sectional studies revealed that although growing boys and girls can both exhibit endosteal and periosteal apposition within the diaphysis of the second metacarpal; girls undergo greater endosteal apposition while boys undergo greater periosteal apposition during adolescent growth (84, 91, 92). This suggests a strength advantage for boys as adding bone to the endosteal surface where bone is placed closer to the neutral axis in a long bone is less mechanically advantageous (268). This

biological difference has been viewed as a contributing factor to women's increased bone fragility (221). The strength of bone and thus its ability to resist fracture is dependent on its mass, geometry, and the intrinsic properties of bone (44). Garn's classic studies were conducted using two-dimensional planar measurement techniques and thus were unable to directly assess bones cross-sectional geometry. Due to the reasons mentioned above, understanding the defects that lead to osteoporosis and osteoporosis-related fractures requires the study of skeletal surfaces during growth as the structural bases of bone fragility in the aging population may have some origin in growth (15, 30, 221).

The primary aim of my thesis was to extend the work of Garn and colleagues and 1) compare bone biological events on the periosteal and endosteal surfaces of the mid tibia, 2) to compare how bone density is accrued and 3) to compare bone strength accrual in boys and girls. Participants were obtained from the Healthy Bones Study who participated in an exercise intervention study from 1999-2001. No effect of the intervention was found at peripheral quantitative computed tomography (pQCT) bone outcomes at the tibia. Three dimensional images of the tibial midshaft were obtained from the years 2001-2007.

2 Literature Review

In this chapter I review the normal process of growth and development, generally and of the skeleton, specifically. This overview focuses on 5 key areas: 1. maturity and sex-related differences in skeletal development, 2. basic bone cell biology and the dual-nature of bone to act as both a tissue and an organ, 3. longitudinal bone growth and development focusing on the lower level extremities of the appendicular skeleton, 4. bone biomechanics particularly bone geometry and strength, and 5. measuring the properties of bone in children. Lastly, I discuss statistical modeling techniques that can be applied to bone growth and development.

2.1 Maturity and Sex-Related Differences During Growth

In this section, I discuss the difference between chronological and maturational age. I then provide a description of methods commonly used to assess physical maturity in growing children and examine the accuracy and feasibility of these measurements. I close with a description of the University of Saskatchewan Bone Mineral Accrual Study that assessed longitudinal growth.

2.1.1 Variation in Somatic Growth and Development

One of the greatest challenges in the study of adolescent bone growth is the variation in maturational status of children who are the same chronological age (10). An individual's *chronological age* is their actual age (current date-birth date) (233). On the other hand, maturational or biological age identifies the maturity level of each child and is much more complex. Maturation is defined as the tempo (magnitude or velocity) and timing (age) of biological and physiological changes associated with increases in body size or dimensional growth that inevitably occurs in every child during normal development (165). However, the pattern of these occurrences may vary substantially between individuals of the same chronological age and between boys and girls (10, 73, 159, 247). Indeed, children of the same chronological age may differ as much as 6 years developmentally (165).

Rapid acceleration of growth and development occurs at puberty after which a child attains the maturational characteristics of an adult. A variety of biological changes occur at this time including the appearance of secondary sex characteristics (10), sexual maturation, increases in height, weight and changes in body composition, increases in skeletal mass and the cessation of longitudinal skeletal growth (247). However, there is no relationship between the onset of puberty and length of time required to obtain full maturational status. For example, a girl entering puberty early would not necessarily reach full maturity sooner (early maturer) than a girl who entered puberty later (10.). Therefore, it is important to assess maturational age when measuring children prospectively or when assessing their response to an intervention.

2.1.2 Assessing Maturity in Children

The accurate assessment of sexual maturity is crucial to appropriately monitor normal growth, the effects of a lifestyle or pharmaceutical intervention, the progression of a disease, or to compare differences across individuals (233). A number of methods have been used to assess maturity. Those most commonly used in clinical and research practice are described below.

First, skeletal age can be determined by a hand-wrist radiograph which evaluates the size and morphology of the carpal and metacarpal bones. This is the preferred maturational index as fusion of the ossification centers occurs in a fairly uniform manner (165, 188, 233). That being said skeletal age is rarely used in non-clinical studies because of the costs associated with obtaining radiographs, the need for specialized equipment and the specialized training of technicians to conduct and evaluate the scans. There are also safety concerns associated with exposing healthy children to ionizing radiation (10, 159, 165, 188, 247). In addition, skeletal age serves only as an estimate of maturational age, as every child is compared to a pre-specified standard derived from a scoring system that may or may not fully represent them (18). There are many approaches that can be used to determine skeletal age and they differ in the scoring system used and the reference populations from which they have been based. Thus, the skeletal age can vary depending on the scoring system used (18).

Second, physician or self-assessed sexual maturation using Tanner Staging (1-5) (Glossary: Maturity Definitions) is based upon the known pattern of development of secondary sex characteristics (10, 256). This includes breast and pubic hair development in girls and the development of pubic hair and genitalia in boys (10, 159). Tanner Stage 1 corresponds with pre-puberty, Stages 2 and 3 correspond with early- and peri-puberty, Stage 4 corresponds to puberty and sexual maturity is reached at Tanner Stage 5 - post-puberty (256, 259). Girls' maturity is also assessed based on the occurrence of menarche – or their first menstrual period. Girls are considered pre-menarcheal if they have not yet experienced their first menstrual period and post-menarcheal once menarche has been achieved.

Self-assessment by Tanner Staging is relatively low cost, non-invasive, and practical to use in clinical and research settings. This method has similar precision as assessing skeletal aging with hand-wrist radiographs (73, 164). Correlations between physician assessments and self-assessments by adolescent girls were 0.81 for breast stage and 0.91 for pubic hair stage (73). Despite the many advantages of self-assessment by Tanner Staging, it appears that it cannot be used reliably with overweight or obese children and adolescents (27). It is possible that overweight adolescent girls overestimated their maturational level as they were not able to adequately distinguish between adiposity and true breast tissue. Tanner Staging is also limited as it provides data as 5 discrete stages and there are no intermediate stages (refer to paragraph above for staging designation). Thus, an adolescent's maturational stage can easily be over or underestimated. Also, Tanner Staging is not appropriate for gender comparisons as stages are not equivalent across sexes – that is a girl at a Tanner Stage 4 for breast or pubic hair development is not at the same maturity level as a boy at Tanner Stage 4 for pubic hair development. This is a common error made in many

studies that compare groups by Tanner Stage (18). Finally, an equivalent marker to menarche is not available for boys (19).

Third, Age at Peak Height Velocity (APHV) is a biological maturity indicator that reflects the age at which the maximum growth in height during adolescence occurs and is used to determine the timing of growth (160, 171). Peak Height Velocity (PHV) can account for variations and changes in the rate of growth at any chronological age. In both boys and girls, PHV occurs at a maturational point equivalent to 92% of adult stature (27). However, it is only possible to determine PHV with longitudinal data consisting of serial measurements of height surrounding the years close to the occurrence of PHV (188, 247) – which is not always feasible. The University of Saskatchewan Bone Mineral Accrual study was a 7-year longitudinal study where the chronological age at which PHV achieved was determined for 60 boys and 53 girls (12). On average PHV occurred at Tanner Stage 3 (peri-puberty) in girls and Tanner Stage 4 (puberty) in boys confirming that girls reach PHV at an earlier stage than boys, on average.

In 2002, Mirwald et. al. developed an equation that used sitting height and leg length to predict age at PHV based on the known relationship between age at takeoff for growth of the legs versus growth at the trunk (188). Cross-validation with two other longitudinal growth studies showed that age at PHV could be predicted to within 1 year of the actual value 95% of the time (188). However, prediction error increased the further a child was from actual age at PHV. The advantages of using this equation are that only one measurement period is required, it is non-invasive and it is a practical solution to determine biological maturity. Despite this, it cannot be used to assess maturity prior to the growth spurt, and can only classify adolescents either prior to or after PHV is obtained (188). Finally, this equation was developed using data from Caucasian children and it has not been validated for children of other ethnicities.

2.1.3 Sex Related Differences in Sexual Maturation

Many chronological ages are represented within each Tanner stage. MacKelvie et al. reported that girls reached early puberty (Tanner Stage 2) between 8.8 and 11.8 years of age (160). However, this can vary from between 8 and 13 years old (256). A longitudinal study examining the association between the age of peak bone mineral content velocity, peak height velocity, and onset of menarche in girls found that menarche onset and peak bone mineral content velocity occurs approximately one year after peak height velocity. The average age of menarche was 12.7 years in these studies (12, 179) but menarche can occur anytime from ages 10.5-15.5. Menarche commonly occurs after early puberty (Tanner Stage 3) (259). It is important to mention that these ages for menarche refer to normal reference values for healthy girls. These values cannot be applied to competitive athletes or those who restrict their caloric intake - as the onset of menstruation is likely to be delayed (256). In boys, genitalia and pubic hair development occurs at 11.6 years, on average, but can occur anytime between 10.5 to 14.5 years of age (Tanner Stages 2 and 3). Testicular enlargement begins during Tanner Stages 2 and 3 (ages 9.5-13.5 years, on average) and is complete by 12.7 to 17 years of age when boys reach Tanner stage 5 or sexual maturity (256). Boys undergo puberty at a later age (2 years on average) and for a longer duration (2 years on average) compared with

girls, which accounts in part for the difference in greater adult height in men compared with women (18, 92). This sex difference is also observed for skeletal maturation as girls' maturity has been shown to preceed boys by 1.6 years, on average (Figure 2-7) (12). Earlier skeletal maturation for girls leaves them at an overall disadvantage as boys develop larger and longer bones (186, 255). Further, greater muscle mass in boys also contributes to greater skeletal stability and strength (233, 259).

2.2 Bone Growth and Development

In this section I provide an overview of the functions of the human skeletal system and describe the composition and structural properties of bone. This leads into a discussion of three bone processes - modeling, remodeling or turnover, and growth - that are responsible for building and maintaining bone structure.

2.2.1 Whole Bone Structure and Skeletal Function

The skeletal system includes 206 separate bones and a significant number of associated cartilages (172). The skeleton performs numerous functions, some of which include protecting internal organs, allowing movement of body parts, providing sites for haematopoesis (217) and maintaining calcium levels (83). Bones have been referred to as both a tissue and organ due to their microscopic and macroscopic properties (130). At the microscopic level, bone can be viewed as a tissue (83, 130) as it is composed of cortical and trabecular bone, haemopoetic and connective tissues. At the macroscopic level, the human skeleton can be divided into axial and appendicular components. The axial skeleton is made up of 80 bones and its primary function is to protect, support and in come cases strengthen the body wall. It consists of flat and irregular bones such as the skull which is comprised of the cranium, face, auditory ossicles, and the hyoid; the thoracic cage which consists of the sternum and ribs; and the vertebral column which are made up of the vertebrae, sacrum, and coccyx. The appendicular skeleton contains 126 bones and includes bones of the upper and lower extremities (172). The appendicular skeleton allows us to move and manipulate objects and is comprised of long, short and sesamoid bones such as the femur, tibia, fibula, ulna, radius, humerus, metacarpal, scapula, clavicle and patella, to name a few (130, 172, 233).

2.2.2 Cellular and Tissue Composition of Bone

Embryonic mesoderm gives rise to multipotent mesenchymal cells that can differentiate into distinct cell populations that give rise to specific connective tissues such as cartilage and bone. During embryonic development, mesenchymal cells travel to sites where skeletal formation is required and communicate with growth factors such that mesenchymal cells differentiate into osteogenic cells (109). Signaling agents such as retinoid are responsible for determining the numbers of cells that will aggregate to a specific site to become a specific skeletal structure (265). This is a highly controlled process where growth factors function to prevent bone from forming in an incorrect location (109) and signaling agents ensure that the bone structure formed is of the correct size (265). Osteogenic cells then differentiate into *osteoblasts* which are defined as bone forming cells that regulate the influx of calcium and phosphorus in and out of bone. Osteoblasts secrete a basophilic matrix (2, 266) made up of inorganic and organic

components (83, 130). This basophilic matrix is referred to as the bone matrix or *osteoid* and eventually mineralizes to form bone (167, 266). The mineralized inorganic component consists of hydroxyapatite (calcium and phosphorus crystals), sodium, magnesium and carbonate. It provides bones with compressive strength and rigidity (2). The organic component is primarily composed of Type I collagen which is essential for bone's tensile strength and provides a location for the deposition of inorganic crystals (2). The final amount of Type I collagen is what ultimately determines the overall size and shape of bone. During bone mineralization, some osteoblasts get trapped in the osteoid and become osteocytes. Conversely, others line the bone surface and act as an ionic barrier (167, 266). During early fetal development, much of the skeleton is made up of cartilage. Cartilage is produced from both chondroblasts and chondrocytes. Chondroblasts are immature cartilage producing cells that secrete and maintain extracellular cartilage matrix (167, 266). The development and maturation of chrondrocytes is influenced by many genetic and non-genetic factors such as circulating hormones (IGF-1, estrogen, and testosterone) (200), nutrition, mechanical influences and growth hormone (GH) (82, 120, 217). Cartilage is made up of type II collagen, elastic fibers and contains chondrocytes. The importance of cartilage lies in its ability to provide an outline of the bone structure upon which the bony matrix is deposited.

Ossification occurs by expansion and formation of hydroxyapatite swellings within the osteoid. These swellings then fuse together to form bone tissue called woven bone (21, 173). Bone tissue is comprised of woven and lamellar bone. The distinctive difference between them is their collagen arrangement. Woven bone is referred to as immature bone that forms rapidly and is found in the embryonic stages of fetal development, in newborns and in the metaphyseal region of growing bone. Woven bone has been found in fracture repair and bone diseases such as osteogenesis imperfecta (43, 130, 217). Within woven bone, collagen fibrils and mineral content are arranged in an irregular fashion and have isotropic mechanical characteristics. Thus, the behavior of woven bone is the same regardless of the orientation of forces as the properties of bone are uniform. In addition, woven bone has large vascular spaces (233) and has been proven to be mechanically weak during testing (43, 217). By contrast, lamellar bone is slow forming and is referred to as mature bone. Formation begins 1 month after birth at which point active replacement of woven bone begins. From age 4 years onwards, most bone is lamellar bone (217). Collagen fibrils and mineral content are arranged in an orderly fashion in thin sheets called lamellae that have anisotropic mechanical characteristics (217). Therefore, the strength and thickness of bone varies depending on the orientation of forces applied to the bone (43, 229). Lamellar bone is found throughout the mature skeleton in cortical (dense or compact) and trabecular (spongy or cancellous) bone. Bone formation occurs by intramembraneous and endochondral ossification (233). The difference between these two modes of ossification is that cortical bone arises from vascular connective tissue and trabecular bone from avascular connective tissue (233). Cortical and trabecular bone are structurally and functionally different and can be distinguished by their differences in porosity and density (Figure 2-1) (14, 43). Approximately, 80% of total bone mass is comprised of cortical bone. Despite a high mineral content (70%) (217), cortical bone has low porosity (10%) (2), and its function is primarily mechanical (217). Cortical bone has an ordered arrangement, runs parallel to the bone shaft (233) and is found principally in the diaphysis of

long bones that surrounds the medullary cavity. Cortical bone has two surfaces; an inner or endosteal surface and an outer or periosteal surface (Figure 2-1) and can withstand bending, torsional, and compressive forces. The endosteal surface is associated with a thin layer of metabolically active cells that surrounds the bone marrow. The periosteal surface is covered by a tough vascular membrane that interfaces with soft tissue, is surrounded by blood vessels, and is involved in appositional bone growth (233). Both have osteogenic potency and thus are involved in bone tissue turnover (130). However, the rate at which bone is lost and gained differs between the endosteum and periosteum. The periosteum is the primary site of bone formation and undergoes varying rates of apposition throughout the life span. On the other hand, the endosteum is the primary site of bone resorption and undergoes apposition only during adolescent growth. The rate and magnitude of these changes occurring at these bone sites differs between sexes.

The most complex form of cortical bone is Haversian bone (217). Haversion bone is comprised of lamellar bone arranged circumferentially around a vascular channel (Haversian canal) oriented along the long axis of bone (2). Each canal contains a blood vessel, nerve, and lymph vessel that is surrounded by bone matrix and osteoblasts (58). Haversian canals are connected to osteocytes in the matrix by interconnecting canals referred to as canaliculi. Collectively, these structures make up the Haversian system and is created by bone remodeling (*section 2.2.7)* (58). During childhood, or prepubescent growth (the period from infancy to the onset of puberty, up to 10 years in age), cortical bone gain at the periosteum is directly proportional to cortical bone loss at the endosteum (84). However, during adolescence (the developmental period of transition from the beginning of puberty to adult, occurs from approximately 10-19 years of age), the rate of endosteal and periosteal apposition may vary (91). Some reasons for this are attributed to sex differences, variability in the rate of maturity (84), level of physical activity, genetic abnormalities resulting in irregular bone growth and development and protein-calorie malnourishment which can affect the rate of apposition and resorption (91). Trabecular bone is primarily found at the metaphysis and epiphysis of long bones (Figure 2-1). Trabecular bone is highly porous (~90%) (2) and houses large spaces between thin trabeculae that allow bone marrow, blood vessels, haemopoetic marrow, and connective tissue to be in contact with bone (130, 217). The large surface area and multiple trabeculae lead to greater cellular activity. Thus, trabecular bone has a high rate of bone remodeling compared with cortical bone. Importantly, trabecular bone serves to reduce skeletal weight without decreasing strength (217).

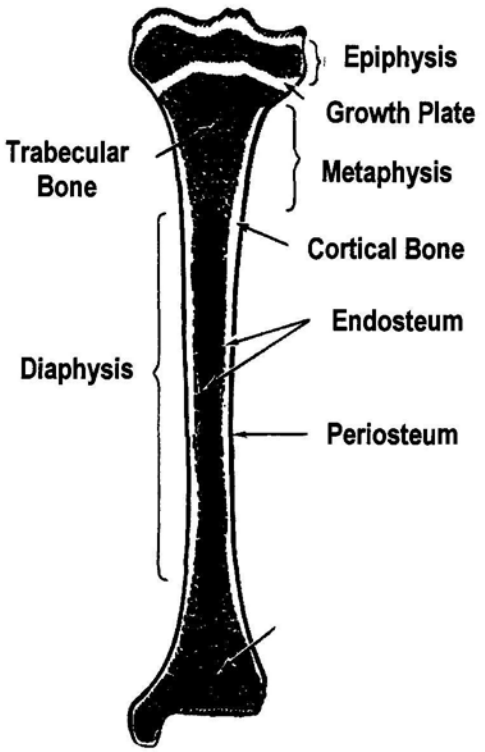

Figure 2-1: Growing Long Bone. Adapted from Jee et al. In Tissue and Cell Biology (127)

2.2.3 Anatomy of Lower Extremity Bones

The bones of the lower extremity consist of the femur (thigh bone), the patella (knee cap), the tibia and fibula (leg bones) and the tarsals, metarsals and phalanges (ankle and foot bones) (172). These bones are much larger than those of the upper extremity because of increased stresses that are placed on them when transferring body weight to the ground during locomotion (172). The femur is located at the upper portion of the lower extremity (thigh) and is the heaviest and longest bone in the human body. It articulates with the tibia (leg) via the femoral condyles at the knee joint (172, 233). The patella is a large sesamoid bone (forms in the tendon) that has been described as being triangular in shape and as having a rough convex surface. Its anterior surface is an attachment site for quadricep tendons and also for ligaments (172). Located on the medial side of the fibula, the tibia is the main bone of the leg as it carries a significant portion of the body weight of an individual. The tibia is comprised of an expanded proximal condylar surface, shaft, a distal end, and contains cortical (shaft) and trabecular bone (proximal and distal ends) (233). The medial and lateral condyles of the tibial plateau articulate with the corresponding structures of the distal femur. The fibula is much thinner than the tibia and functions as a muscle attachment site. The head of the fibula attaches to the posterior portion of the tibial condyle. The interosseous crest at both the tibia and fibula contains an interosseous membrane that extends between them providing increased surface area for muscle attachment and increased stabilization. The inferior tibial surface acts as a hinge joint with the talus (most proximal ankle bone). The medial malleolus of the tibia provides medial support for the joint whereas the lateral malleolus of the fibula provides lateral stability to the ankle. The fibula does not transfer significant amounts of weight to the ankle

and foot because it has no attachments to the knee joint (172). Certain parts of the tibia such as the tibial tuberosity and the anterior crest can be felt through the skin (172) and are used as landmarks in human studies.

For the purpose of my thesis, my focus will be on the growth and development of the tibia in children as they progress through puberty.

2.2.4 Growth plate: Emphasis at the Tibia

Bone growth begins in the embryo and continues until skeletal maturity is reached. The growth plate, sometimes referred to in Greek terminology as the "physis" which means "growth", forms after birth. Physes are located at the proximal and distal ends of bones and develop between the epiphysis and metaphysis (200) (Figure 2-1). The primary function of the tibial growth plate is for longitudinal growth (70, 233) and diametric expansion of the tibial shaft (233). Long bones grow in length by endochondral ossification whereby hyaline cartilage in the growth plate is converted into bone tissue. Bones increase in width via periosteal bone formation (2, 91). Longitudinal bone growth varies by age and sex and is achieved through the coordinated activity of recruitment, differentiation and maturation of growth plate chrondrocytes and osteoblasts (217).

The growth plate is comprised of 4 layers, commonly referred to as "zones", each with specific functions required for growth and expansion. The first layer is termed the "germinal zone" followed by the "proliferative zone", "cartilage transformation zone" and "ossification zone" (233). The organization of chondrocytes located within the growth plate is dependent on the layer they are in (200). The "germinal zone" is located closest to the epiphysis and contains randomly allocated chondrocytes, type II collagen, and proteoglycans (200). Type II collagen functions as a barrier to prevent calcification (200). Chondrocytes are small in size and make contact with the epiphysis for vascularization (233). In the proliferative zone these vascularized cells increase in size, number and undergo mitosis. Chondrocytes are organized into columns parallel to the axis of the longitudinal bone. Type II collagen fibrils are oriented longitudinally (200). Cartilage formation, diaphysis expansion, and shaft lengthening happen in the proliferative zone of the growth plate. In the "cartilage transformation zone", chondrocytes stop dividing but further increase in size which is required for bone turnover. Mineral is deposited into the matrix and calcium phosphate is converted into hydroxyapatite. Some cells in this zone undergo degradation whereas others migrate to the "ossification zone" and become osteoblasts. A new layer of bone is formed by osteoblasts at the final "ossification zone". An increase in the number of cells during bone formation expands the diameter of the growth plate. In order to maintain appropriate proportions, the diaphysis undergoes modeling (refer to *section 2.2.6)* in the transverse direction as well as undergoing longitudinal expansion. During growth resorption and formation work in unison to maintain a balance between removal and formation of bone at these sites (233). At maturity, the growth plate thins out and the epiphysis and metaphysis surfaces thicken. Ossification continues until a vascular connection between the epiphysis and metaphysis leads to the final sealing of the growth plate (108).

Growth plates at the proximal and distal ends of long bones have differential growth rates which also vary between skeletal sites (172, 233). Generally, the distal tibia fuses earlier than the proximal tibia such that the proximal end contributes slightly more (57% on average) to overall tibial length (3, 95) (Figure 2-1). This contribution varies with age - from 50% in girls and boys aged 7 years to 80% in girls aged 14 years and boys aged 16 years (218). In a cross-sectional radiographic study, complete epiphyseal fusion at the distal tibia occurred earlier in girls (12-16 years) and later in boys (14-19 years) (60). A similar study examining the proximal tibia found complete epiphyseal fusion at a mean age of 13 years in girls, whereas boys experienced this 2 years later at 15.5 years (219). However using a different measurement technique complete fusion in boys occurred approximately 8 years later at age 21 (183). Regardless of site, girls undergo ossification and thus fusion earlier than boys and these differences can be observed 3 weeks post birth until skeletal maturation is reached (219).

Further, the nature of growth plate activity during skeletal growth results in it being relatively weak and can thus fracture more readily in growing children. Approximately 15% of children experience growth plate fractures during growth (203). However, this is observed to a greater extent in boys over girls (197). A proposed explanation for this is that boys may be involved in more physical activity or more aggressive physical activity than girls (197). It may be also be that boys' extended period of longitudinal growth increases their susceptibility to fracture (1).

2.2.5 Adolescent Growth of the Lower Limb

Puberty onset occurs at approximately 11 years for girls and 13 years for boys, on average, and is marked first by accelerated growth in the lower limb for 2 years (70). The growth spurt in lower limb length precedes the growth spurt in trunk length by approximately 6 months in both sexes. It is the magnitude and timing of these events that determine the final growth response (120). Sex steroids influence the rate and magnitude of these events in boys and girls during this critical period of growth (90, 91, 131). Sex steroids are crucial during pubertal growth as they are directly required for epiphyseal fusion and also indirectly inhibit growth hormone (GH) secretion (82). After 13 to 15 years of age, lower limb growth slows dramatically and growth primarily occurs at the trunk (as represented by measured sitting height) (261-263). The velocity of growth at the trunk during peri-puberty (2.0 cm/year, on average) is much slower than growth velocity of the lower limbs (3.5 cm/year, on average) (70). Tibial and femoral growth between boys and girls is almost identical during the first five years of life. From 5 years of age to the onset of puberty, growth velocity declines to 1.3 cm per year, on average. During puberty, growth at these lower limb sites increases to 1.6 cm per year. This velocity varies by region and greater increases have been reported at the femur (70). Bass et al., reported a 40% increase in growth of the lower limbs in prepubertal girls, compared with a 24% increase at the spine (representing trunk growth) (15). These findings are of particular relevance to my study as tibial length accounts for 80% of leg length. However, the growth between the femur and tibia are interdependent (70, 71).

2.2.6 Bone Modeling

Bone modeling is the process by which bone alters its shape by coordinated resorption and/or formation through the action of osteoblasts and osteoclasts (87). Osteoblasts, as mentioned in *section 2.2.2* are cells that form the bone matrix and are responsible for it's mineralization (130, 217) whereas, osteoclasts are cells that resorb the bone matrix (217). The overall function of bone modeling is to sculpt bone by adding it in some places and removing it in others. This is a fundamental process during growth, whereby osteoclasts remove bone in one location while new bone can be formed simultaneously elsewhere (200, 233). During bone modeling, the net formation and resorption of bone by the combination of osteoblast and osteoclast activity results in diaphysis enlargement and the redistribution of the bone matrix to accommodate changes in load placed on the bone (233). Although, bone modeling occurs throughout life it is most active during childhood and adolescence and declines once maturity has been reached (229, 233). The importance of modeling lies in its ability to change the shape, develop a marrow cavity, and increase the diameter of long bones (217, 233). Some factors which explains why bone modeling occurs at a greater rate during adolescent growth than in adulthood is due to the increase in circulating (GH, PTH, sex hormones) (83, 210) and local hormones (growth factors, and cytokines) (83) and the increase in mechanical loads on bone produced from increased body weight and muscle mass that occurs during childhood growth (210). Therefore, bone modeling is advantageous as it alters the diameters of the endosteal and periosteal cortical bone layers which increase bone mass and ultimately increases bone strength (130). It is important to note that bone modeling can involve resorption, formation, or a combination of both (230).

2.2.7 Bone Remodeling

Remodeling occurs by a coordinated process by which osteoclasts remove damaged or old, worn bone that was formed earlier and then activates osteoblasts to replace it with newly formed bone (233). Remodeling occurs on bone surfaces such as cortical (endosteal, periosteal, intra-cortical) and trabecular bone. In adults, approximately 5% of cortical bone and 25% of trabecular bone is remodeled per year (171). However, this may vary slightly depending on the bone being remodeled. Two types of bone remodeling occur throughout life. Microdamage remodeling occurs in response to fatigue damage (72, 90), whereby damaged, microcracked tissue resulting from trauma or accumulated mechanical stress is replaced (46, 52, 85, 169, 170, 209). In this form of remodeling, activity will be greatest in the location of greatest microdamage or strain (190). Stochastic remodeling occurs at the same rate in all long bones and functions in bone maintenance (45, 90),. It also ensures optimal levels of mineral concentration to optimum levels in the blood stream (130, 204). Therefore, remodeling is necessary for normal bone growth and development, to prevent bone failure when increased stresses are applied to the bone as well as for bone repair during fractures (233). Unlike modeling, bone remodeling is site specific and occurs in one location over a relatively short period of time (210). Cortical and trabecular remodeling continues throughout life and occurs by a specific cycle of cellular activity where resorption is closely coupled with formation (Figure 2-2). This results in no net change in the size and shape of bones (92). Remodeling follows a process of *activation, resorption, and formation* (ARF) which occurs by organized cellular activity based on the basic multicellular unit (BMU) (2, 130, 208, 230). BMU's are

comprised of osteoclasts, osteoblasts and other cell types of varying origins (230). The function of BMU's is dependent on the type of bone being remodeled.

Trabecular bone has a higher remodeling rate compared to cortical bone due to its greater surface to volume ratio. The trabecular surface is in contact with the marrow cavity which contains osteoclast precursors. These precursors lead to the differentiation and activation of osteoclasts. Once the bone is removed and cavities are formed, osteoblasts are activated and recruited to the particular site where they refill these cavities (207) (Figure 2-2(C)). In cortical bone, osteoclasts are *activated* and recruited to *resorb* bone in a specific pattern referred to as the "cutting cone". *Resorption* continues longitudinally along the length of the bone until the edge of the bone is reached (126). Acid secretions are released by the osteoclasts to demineralize bone and collagenaze works to break down collagen (214, 233). Osteoblasts are then activated and bone *formation* begins when new bone matrix (osteoid) is deposited forming a "closing cone". The entire cone is not filled so as to leave enough space for vasculature within a central canal (216, 230). The new bone consists of osteons and unmineralized bone matrix (130, 217). Mineralization of new bone and the conversion of osteoblasts to mature osteocytes can take up to 6 months (233). Cortical bone is continuously being altered through the process of remodeling. Despite the fact that bone remodeling is a life long process, the rate at which cortical and trabecular bone remodels varies by age and sex. For example, approximately 50% of the all cortical bone in the femoral midshaft is remodeled at 2 years of age. The remodeling rate at this site decreases to 2-5% annually in healthy elderly individuals (2). In contrast, remodeling of trabecular bone follows an inverse relationship and the rate increases throughout life (2). In later life, bone resorption is favored over bone formation which leads to a decline in bone mass and strength (75, 130). This has been observed to occur to a greater extent in postmenopausal women compared to men of the same age (244). During growth and into the third decade of life when changes in bone size are occurring, remodeling occurs at a greater rate and magnitude than during the mid-adult years (211). Animal studies have aimed to increase the rate of remodeling to enhance bone formation by increasing loading activities at different ages. Weight bearing or loaded activity increased the rate of remodeling and enhanced periosteal formation in the young (140, 142) but not older animals (46, 141, 143, 202, 220). Thus, it may be that the role of exercise is to preserve rather than enhance bone mass in the mature skeleton.

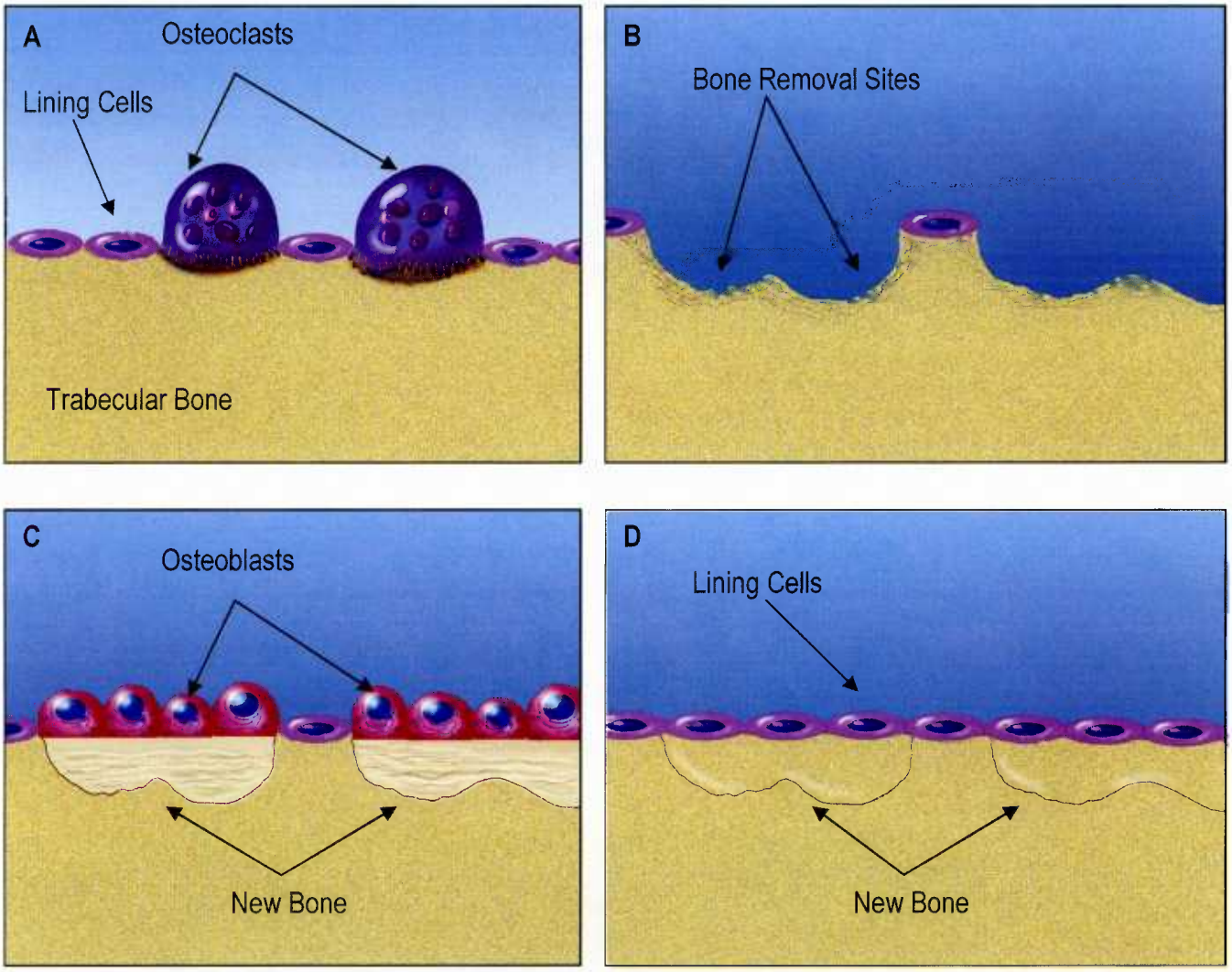

Figure 2-2: Visual depiction of bone remodelling. A) bone resorption by osteoclasts that act on trabecular surface and break down mineral and matrix. B) appearance of small cavities upon completion of resorption. C) bone formation by osteoblasts that fill cavities with unmineralized bone. D) bone surface restoration occurs by protective bone cells or lining cells covering the trabecular surface. New bone is mineralized and modelling is complete at this stage. Adapted from Arnett et al. In Methods in Bone Biology (4).

2.3 Bone Biomechanics: Bone Strength and Geometry

In this section, I describe both the material and mechanical properties of bone and focus on stress, strain, stiffness and strength. I then describe the influence of these properties on whole bone strength. Finally, I discuss studies that have examined bone geometry and structure and those that have investigated age and sex-related differences in bone strength.

2.3.1 Material Properties of Bone

True bone strength can only be determined by measuring the ultimate failure load of a bone and is dependent on its mass, geometry and on the physical properties of the tissue itself (44). A common surrogate measure used in vivo within participants is the strength strain index (SSI) obtained by peripheral quantitative computed tomography (pQCT). Bone is a two-phase porous composite material comprised of inorganic and organic components (45, 130). As mentioned in *section* 2.2.2, the organic component is comprised of primarily Type I Collagen and provides tensile

resistance in response to tensile forces whereas; the inorganic component is comprised of bone mineral and provides resistance to compressive forces (130). At the tissue level bones' material properties are independent of structure and geometry (74). At the organ level bones' material properties contribute to bone strength and geometry (168). I describe 4 key material properties (stress, strain, stiffness, and strength) to facilitate a greater understanding of the fundamental principles of bone biomechanics.

Under loading conditions, bone will experience deformation from its original dimensions. This is defined as ***strain***, and is calculated by the change in the entire length of the bone divided by its original length (74, 114). It is measured as the change in bone length after force is applied divided by the original bone length (μstrain) (74). These forces can be external such as the pulling on a muscle at its origin (212) or internal such as during walking, running or jumping (130, 212). The internal resistance in response to a force being applied to bone is referred to as ***stress***. The stress is equal in magnitude but opposite in direction to the force applied and is distributed over the entire cross-sectional area of bone (74). This occurs in an attempt to resist the externally applied force. Stress is measured by the force per area of bone on which it is applied (45, 74). The relationship between stress and strain is reflected by bone's ***stiffness***, the force required to cause bone deformation (74, 130). These material properties of bone are the characteristics at the tissue level that contribute to overall bone strength and can be determined by the stress strain curve (Figure 2-3) (74).

Stress and strain are considered to be the most important parameters with respect to their effect on altering bone geometry (212). The stress-strain curve plots where a section of bone exposed to known forces undergoes known deformations under controlled laboratory conditions. Stiffness is represented by the linear elastic region or the slope of the curve (74, 130). It is calculated by dividing the stress by the strain at any point along the linear part of the curve (Figure 2-3). Any force applied to bone within the linear elastic region will result in a non-permanent deformation. Thus, when the load is removed the bone will return to its original form and the energy expended is recovered (74). Saturation of the linear portion of the curve is referred to as the elastic limit. The energy stored by the bone at this point is referred to as the resilience (74). After this point, the plastic region of the curve is non-linear and all forces applied will result in permanent bone deformation (Figure 2-3) (74, 130). ***Strength*** is defined as the load that causes the point of failure of the bone structure and is calculated by determining the maximum stress at the point where the bone fails (74, 130) (Figure 2-3). The area under the curve is a measure of the absorptive energy or toughness of the bone (74). There is a positive relationship between the increased toughness of bone and resistance to fracture (130).

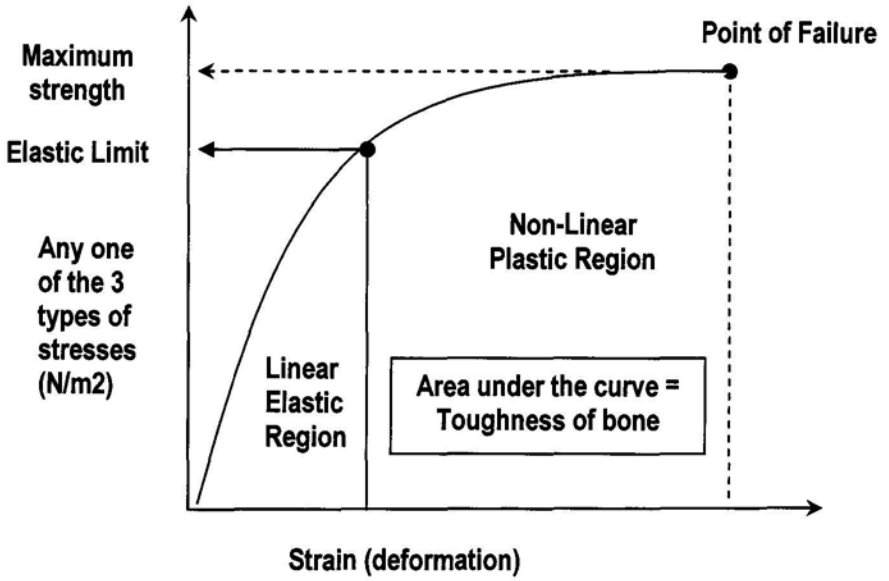

Figure 2-3: Stress-strain curve of a bone specimen produced during mechanical testing under controlled laboratory conditions. This curve can also be used to represent whole bone properties. Adapted from Einhorn (74)

There are three types of stress patterns that can be produced, depending on the direction of the applied forces (43, 61, 74). *Tensile stresses* (positive elongation) (212) occurs when two forces are directed away from each other in the same axis. In this case, intermolecular attractive forces prevent the bone segments from being separated from each other (74). *Compressive stresses* (negative elongation) (212) occur when two forces are directed towards each other in the same axis (74). *Shear stresses* occur when two forces are parallel to each other but not along the same line (74). Most bones experience complex loading activities which cause these stresses to combine. Bending occurs as a result of tensile and compressive stresses (74) and primarily occur at the shafts of long bones (54, 74). For instance, at the diaphysis, bending occurs as a result of tension stress on the convex side as compression stress occurs on the concave side (212).

The stress and strain generated depends on the character of the bone on which the stress is applied. For instance, stress applied to normal mineralized bone yields a relatively small strain. However, the opposite occurs if this same stress is applied to poorly mineralized bone (74). Thus, the denser the bone, the less stain is induced and vice versa (114). Forces produce stresses of varying intensities which in turn produce strains of varying magnitudes (212). There are similarities in the loads that animals can sustain despite variations in size and the density of bone. In all animals, bones considered to have normal bone mass bend and deform by approximately 1000-1500 microstrain (0.10-0.15%) under ordinary loading conditions such as walking or breathing (212). When exposed to peak loads, deformation occurs at 3500 microstrain (0.35%). Point of failure leading to fracture occurs when bones are exposed to repeated loads of approximately 7000 microstrain (0.70%) or greater (212).

Frost's mechanostat theory explains how varying strains influence bone mass. Frost suggested that skeletal physiology is regulated by negative feedback loops that are influenced by mechanical and non-mechanical factors (86, 89). For instance, when loads produce strains in bone above a given threshold, osteocytes are activated to release signals which ultimately lead to an increase in bone mass and architectural modification resulting in site-specific adjustment and bone deformation. This decreases strain and closes the feedback loop (223). The opposite will occur when the strain is lower than the threshold which can occur due to disuse or immobilization (Figure 2-4) (86, 114, 211). A functional model of bone development based on Frost's theory is shown in Figure 2-4. The mechanical and non-mechanical factors cannot override one another as they have different roles (Figure 2-4). During longitudinal growth, hormones and nutrition play a role in influencing mechanical loads by acting on growing bone and muscle mass but they do not have the same effect as mechanical strain has on bone (223). It is important to note with this functional model that the amount of bone strain determines the amount of bone mass and architecture and not vice versa (223).

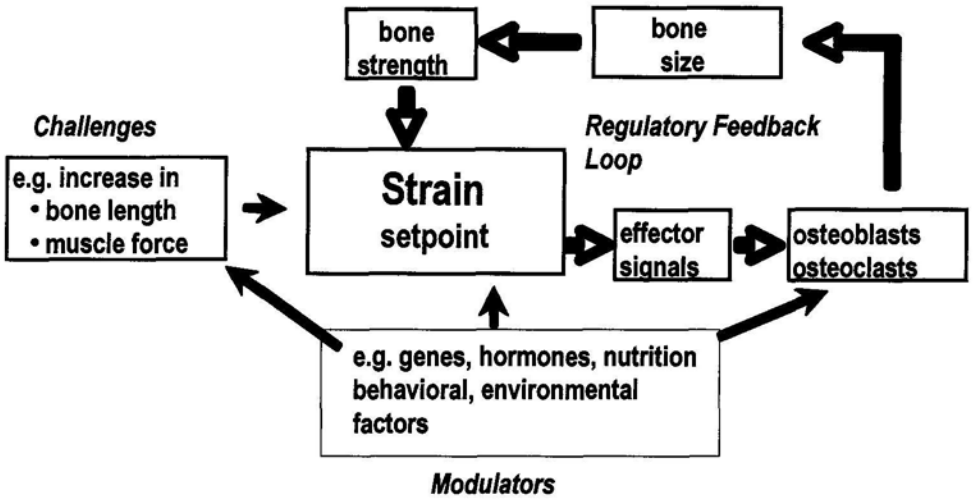

Figure 2-4: Functional model of bone development based on Frost's mechanostat theory. Modified from Rauch and Schonau (223).

2.3.2 Structural/Geometric Properties of Bone

When *whole bones* are exposed to loading conditions the response produced can be attributed to a combination of interactions between bones' material and geometric properties. Geometric properties are characterized by bone diameter, shape, cortical wall thickness, trabecular architecture and cross sectional area (74, 130). Bones of the appendicular skeleton are long and slightly curved and are loaded by bending (combination of compressive and tensile forces) (74). However, compressive force predominates in the diaphysis of a long bone (2). Resistance to bending, shear, twisting and torsion stresses is mainly due to the cross sectional properties of cortical bone rather than mass or density of bone tissue (74). During bending, both the cross-sectional area and the distribution of bone mass around the neutral axis or center of bone influences mechanical behavior (130). Ideally, the

greatest resistance to bending occurs when mineralized tissue is placed the furthest distance from the neutral axis as possible. This distribution results in a geometry of bone that has a large diameter and maintains minimum skeletal weight (decreased energy consumption during movement) as the cross-section is not entirely filled with bone (Figure 2-5 (A)). The bone also has greater resistance to bending as the bending resistance is proportional to the squared power of the distance from the neutral axis of bone (130). This is referred to as cross-sectional moment of inertia (CSMI mm^4 or I), and is defined as the geometric parameter that respresents the distribution of the cross-sectional area with respect to the neutral axis of bending (Figure 2-5 (A)) (130). CSMI can be used to calculate bone section modulus (Z), which provides an estimate of bone bending strength (242). $Z= (A_i \times r_i^2)/ r_{max}$) and is calculated as the integral sum of the products of area (A) of each voxel and the squared distance (r^2) of the corresponding voxel to the bending (x, y) or torsion (z) axes (234). This is divided by r_{max} which is the maximum distance of a voxel from the bending axis to the outer bone surface, in the plane of bending.

A large CSMI is most efficiently achieved by distributing a large portion of bone mass away from the neutral axis as this results in a stronger and stiffer bone (130). However, increasing CSMI can be achieved by increased periosteal apposition as this leads to increased bone diameter and greater resistance to loading as well as increased endosteal formation. Exercise has also been reported to enhance bone geometry without concomitant changes in bone mass (125, 131). Thus net bone strength is a combination of bone tissue's material properties and the structural properties of whole bone (130). Strength Strain Index (SSI) takes into account both section modulus (Z) and cortical density (CoD). The ratio of CoD and normal physiological density (ND = 1200 mg/cm^3) provides an estimate of the elasticity of the material. The derivation of SSI demonstrates how both bone density and bone geometry contribute to bone strength.

$SSI = \sum[(A_i \times r_i^2)(CoD/ND)]/ r_{max}$ where i =1,...n.....

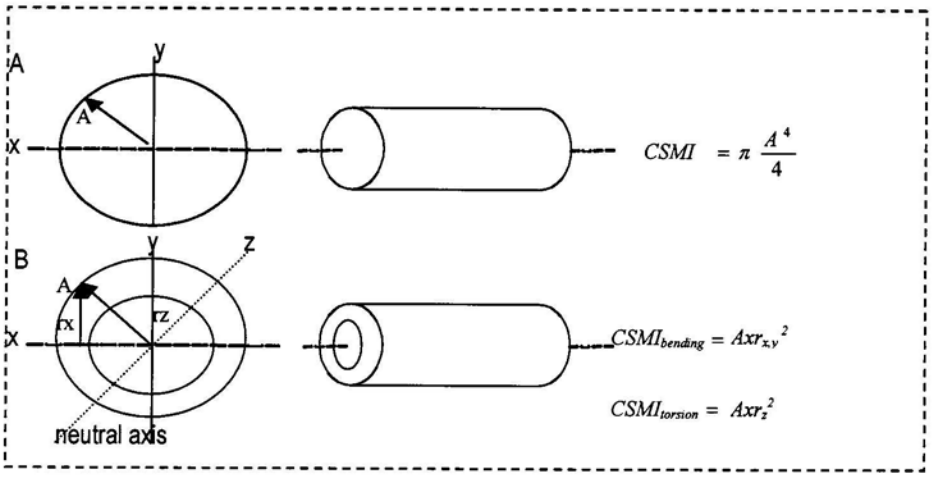

Figure 2-5: Cross-sectional moment of inertia (CSMI, mm^4) for a cylindrical beam. A) solid cylinder where A= the outer area of the cylinder, B) cylinder with a thin shell, similar to a long bone which has a dense cortical bone located at a distance from the neutral axis where r=the squared distance from the corresponding bending (x,y) or torsion (z) axis. Reproduced from Hayes et al (113).

2.3.3 Studies Examining the Effect of Age on Bone Strength and Geometry

"Wolff's Law" postulates that bone adapts to mechanical loading throughout life and this influence shapes and structures bone tissue. Our current understanding is that this is achieved via the processes of modeling and remodeling (212, 231). Wolff's law further suggests that the function of modeling or remodeling cells is to ensure that a bones' material and mechanical properties are appropriate for the applied stress (130); however, this should be interpreted with caution. Although remodeling increases with age, bone mineralization can occur to a point where the bone becomes brittle (232).

That being said, the extent to which bones respond to mechanical loads varies with age. For instance, compared to adult bone, children can undergo greater plastic deformation (greater bone deflection and energy absorption) in response to loading without fracture (65) Currey conducted mechanical testing on human specimens to determine age-specific differences in bone. Specimens of the femoral midshaft ranging from 2-48 years of age were subjected to loads applied at the periosteal-endosteal direction to ensure compression of bone on the periosteal surface (65). The results of this study showed marked differences in the mechanical properties of young and adult femoral bone. Young specimens had weaker bone bending strength and were less stiff than adults. However, young bone had greater plasticity. Thus young bone, was able to undergo greater bone deformation and had greater energy absorption that adult bone (65). These results are consistent with other studies (271, 272). This may be one of the reasons why mechanical loading is capable of positively influencing the growing skeleton by increasing bone mass and strength in children (22). In children, the structural response of bone to exercise, a form of loading, varies depending on sex and maturity level. At pre-puberty, the effects of exercise appear to be independent of sex as both girls and boys exhibit periosteal apposition. At puberty however, boys were found to undergo greater periosteal apposition than girls in response to exercise (66). These changes although occurring to a lesser magnitude in girls compared to boys result in greater bone strength in both sexes. Bone in older individuals cannot undergo as much plastic deformation and thus has less energy absorption than has been shown in children (Figure 2-3) (63, 64). This is of clinical importance as this increases the chance that bone with low bone mass will undergo failure when impact loads such as a fall are imposed on it. There have been many reasons suggested to explain this. One of which includes that older individuals undergo slower bone turnover (24) resulting in highly mineralized bone that is more dense and porous (48, 62, 65, 69). This results in bone with an increased number of microcracks or that has undergone microdamage (232). Microcracks increase exponentially with age in both cortical (59, 232) and trabecular bone (191) and occur to a greater extent in women than in men within the appendicular skeleton (232).

Courtney et al. conducted a study examining age-related damage in cortical bone at the femoral diaphysis obtained from female donors. Two groups of women, the first comprised of young (mean age 26 ± 5 years) and the other older (mean age 72 ± 6 years) subjects, were loaded to a 1% strain level at the femora. Results indicated that the older subjects developed twice as many microcracks than age matched controls and three times as many microcracks than younger subjects, $p<0.01$ (59). In addition, cracks obtained in the older subjects grew at a faster rate than those

in the younger subjects (59). The results from this and other studies have shown that microcrack accumulation in response to loading leads to greater tissue fragility which results in decreased bone strength and stiffness (47, 59). This helps to explain why fractures associated with minimal trauma are commonly seen in the elderly and in those with osteoporosis (232).

The results from this study have also been demonstrated in animals. Animal studies have shown that the level of cortical bone modeling and remodeling greatly declined once skeletal maturity was reached (143). A study was conducted to determine if aging dogs undergo similar accumulation in microdamage as is seen in aging humans. The left humerus was obtained from 43 canine specimens of varying ages and then was sectioned and stained to determine level of microdamage in young and older canine specimens. The results from this study indicate a significant increase in microdamage in aged compared to young bone, $p<0.05$; however, the quantity of microdamage was less than what is seen in human bone. This may explain why older dogs do not have increased skeletal fractures as is seen in adults (81). In addition, this study demonstrated an age-related decline in the number of osteons produced and an increase in the number of microcracks in cortical bone (81).

2.4 Sex Differences in Bone Growth and Biomechanics

In this section I discuss sex differences in bone development. I focus on Garn's landmark studies at the second metacarpal where he showed sex specific differences in cortical bone formation. I then provide a review of dual energy x-ray absorptiometry (DXA) and peripheral quantitative computed tomography (pQCT) studies that examined the contribution of sex to bone mineral/mass accrual.

2.4.1 Bone Development from Birth to Adulthood

After birth the rate of growth differs between various skeletal regions. Rapid bone acquisition is observed during fetal development to the first 12 months of life in both sexes (115). Landmark studies that compared developmental differences between boys and girls were first conducted by Stanley Garn in the early 1960s. These studies are especially relevant to the questions posed in my thesis so I devote a large part of this section to an overview of his findings.

To my knowledge, Garn was the first to use radiogammetry to obtain thousands of images of the second metacarpal. From these images, Garn determined total bone diameter and medullary canal diameter by inferring cross-sectional area to examine changes occurring on the endosteal and periosteal surfaces. In addition, he measured cortical wall thickness. He compared these measures cross-sectionally across the developmental years and between boys and girls. Despite the importance of these early findings – there were limitations in that all comparisons were cross-sectional. Longitudinal studies, such as the study undertaken in the current thesis, are essential to more aptly represent these developmental events

Overall, Garn showed that bone was added throughout life at the periosteum during three distinct phases - prior to adolescence, adolescence to mid adulthood and later adulthood (92). However, the magnitude of periosteal apposition differed in each stage (92). Once adulthood was reached, periosteal apposition occurred very slowly - with an approximate gain of 2% from age 30-80 years. Prior to adolescence, bone resorption took place at the enodosteum. From adolescence to mid adulthood, formation was the prominent event on this surface. In older adults, bone loss occurred at the endosteal surface (91, 92). Garn also reported marked sex differences in these events. The rate of periosteal apposition, and thus total periosteal diameter, was greater for men compared with women, irrespective of age. Whereas, the rate of endosteal apposition during the pubertal years and of endosteal resorption in later adulthood was greater in women compared with men (92).

Garn's radiographic studies were key to establishing some basic premises and launching a program of inquiry regarding developmental events in the growing skeleton. He showed that at the diaphysis of the second metacarpal; approximately 2 mm/yr of bone was formed on the periosteal surface in both sexes during the first year of life. Apposition declined to 0.5mm/yr after this early growth period (92). The magnitude and length of time at which gain in periosteal diameter occurs is greater in boys than in girls and is particularly apparent during pubertal growth. Garn determined bone resorption at the endosteal surface by measuring the width of the medullary cavity. Boys demonstrated a 6% greater increase in endosteal resorption compared with girls by 10 years of age (92). During the pubertal growth spurt, total periosteal apposition for boys was reportedly 2.84 mm compared with a 1.68 mm increase in girls (92). Endosteal apposition was found to start during the pubertal growth spurt and continue through 30 years of age in both sexes; however the extent of this was greater in females than in males (92). Garn also demonstrated that from 18 months to pre-puberty the rate of bone acquisition, endosteal resorption and periosteal apposition slowed substantially (92, 115). In addition, he found sex differences in cortical thickness during growth. From the first year of life onwards, cortical thickness increased in both sexes but the magnitude of this increase was greater in boys than girls at all ages. An exception to this was during the earlier adolescent growth spurt in girls where the gain in cortical thickness occured earlier and was more pronounced for a short time period until boys caught up and exceeded girls (92). Garn suggested that cortical thickness is affected by nutritional status and genetics (92). In summary, Garn attributed the sex differences observed at the endosteum and periosteum to the differential response to sex hormones as the outer bone surface responds to testosterone and the inner bone surface responds to estrogens (92). This may account for greater bone strength in boys (242). However, it is important that these results be verified with more advanced imaging.

The Bone Health Research Laboratory at VCHRI conducted a 20 month prospective study using pQCT that examined the rate of endosteal apposition at the mid-tibia in 127 growing children (59 boys) with a mean age of 11.9 ± 0.6 years. We found no significant changes (neither an increase nor decrease) in endosteal apposition in postmenarcheal girls; however, boys exhibited significant endosteal resorption. This was depicted by an increased

medullary cavity area (132). There is a need to further clarify these findings in longer term prospective trials using more advanced statistical modeling techniques – as I undertook for this thesis.

Garn and others have speculated that endosteal apposition at the metacarpal (92) and at the femoral midshaft (15) were associated with the timing of increased estrogen production (15). In addition, other radiographic studies of the second metacarpal showed significant increases in endosteal apposition during the first trimester of pregnancy. Women with more children had more cortical bone at the endosteal surface compared with women who had fewer children (92). It has been proposed that the estrogen-related increase in endosteal apposition at many skeletal regions during post-puberty in girls (92) and in premenopausal women is to promote calcium and mineral storage for reproductive needs later in life (92, 235, 237). This notion has been supported by many animal experiments which have found an increase in bone mineral in the developing female skeleton (35, 36, 136). Bone at the endocortical surfaces is thought to be resorbed during pregnancy and lactation to support the increased demands for calcium during fetal development and infant growth (134). Although an interesting hypothesis, some biological findings refute this notion. Garn et al. compared women living in developed countries who had short (or no) lactation periods with women living in impoverished countries who experienced low dietary calcium intakes and long periods of lactation. There was no difference in endosteal resorption between these groups (92). In addition, the more children a woman had was not positively associated with increased bone loss at the endosteal surface (92). Ritchie et al have shown that the increased fetal calcium demand was met by increased intestinal absorption by the mother and by renal calcium conserves (228). The evidence to support the hypothesis that pregnancy and/or breast feeding has a detrimental effect on the skeletal mass of mothers is equivocal (92, 123, 228). An alternative explanation that accounts for the endocortical differences observed between the sexes may primarily be due to changes in estrogen status in the female during the pubertal growth spurt and before and after pregnancy rather than the increased demand of calcium during pregnancy and lactation (123).

2.5 Measuring the Properties of Bone

In this section, I discuss imaging tools used to measure bone. The focus of this section will be on the advantages and disadvantages of Dual Energy X-ray Absorptiometry (DXA) and Peripheral Quantitative Computed Tomography (pQCT) imaging instruments.

2.5.1 Historical Technique used to Examine Bone: Radiogrammetry

Historically, film radiogrammetry was used to measure cortical bone diameter, thickness and estimate cross sectional area (CSA) at the diaphysis of metacarpals, radius and femur (92, 101). The success of radiogrammetry is dependent upon visual examination of the image and the absence of morphologic variations, fractures, and cortical bone defects, to name a few (92). Smaller measurement sites resulted in the greatest measurement error whereas smaller "readout capability" and an experienced technician resulted in less measurement error (92, 130); however, this is true for a measurement with almost any instrument. With the evolution of advanced imaging techniques, radiogrammetry is rarely used today because of its inability to take into account the geometric properties of bone (162, 165, 188, 247).

2.5.2 Dual Energy X-ray Absorptiometry (DXA)

Currently dual energy x-ray absorptiometry (DXA) is the most widely used diagnostic imaging technique to assess bone mineral content (BMC) and bone mineral density (BMD) (130, 198). DXA is also commonly used to quantify the process of growth or to evaluate and monitor bone disorders that may affect bone accrual. DXA assesses bone mineral content (BMC, grams)[1], bone area (BA, cm^2), and areal bone mineral density (aBMD, $grams/cm^2$). Areal BMD is thus defined as the ratio of BMC to projected BA. DXA is also often used in pediatric and adult research studies to monitor change over time (bone loss or gain) or to evaluate the effect of an intervention (e.g. exercise or pharmaceutics) on bone mass (148). DXA provides an integral measure that includes both cortical and trabecular bone components (198). Total body DXA also provides an estimation of soft tissue mass for the whole body and its regions. The separation between bone and soft tissue is determined by a decline in the energy of a photon beam as it progresses from bone to soft tissue (93, 130). The degree to which the x-ray beam is attenuated depends on photon energy, the length of the beam path, and the part or tissue under study (130). Although DXA is a very precise tool with very short scan times, it is limited in that it measures bone within a pre-specified two dimensional area and does not account for bone's three dimensional properties (94, 130). Most published pediatric studies used the DXA QDR 2000 or 4500 (Hologic Inc) as the radiation exposure is low and thus safer to use on a younger cohort.

---

[1] BMC and bone mass are used interchangeably in this thesis.

2.5.3 Advantages and Disadvantages of DXA

DXA is relatively inexpensive when compared with other imaging devices, it is easy to use, fast, painless in healthy and mobile participants and emits low levels of radiation (93, 130). It measures bone mineral, lean and fat mass at various sites at the axial and appendicular skeleton (130). Thus, DXA is commonly used to measure both adults and children (189). DXA is also accurate and precise as demonstrated by its short and long term reliability. The precision of BMD with repeated measurements was 0.5-1.5% at the lumbar spine (94, 144, 205) and 1-2% at the proximal femur (178). Clinical adult measures of BMD can be compared to reference norms of those of the same age and sex (with the exception of total body scans in males). The coefficient of variation (CV), in vivo for repositioning with the Hologic 4500 QDR in our laboratory was less than 2% for bone mass, lean mass, and fat mass as determined for 14 healthy (8 women, 7 men, aged 26-50 years) participants (unpublished data). One of the major disadvantages of DXA is that it measures bone properties in two dimensions rather than in three dimensions (130). Although, aBMD in part accounts for bone size differences among individuals, it does not account for the depth or thickness of bone (148, 198). The World Health Organization (WHO) defines osteopenia as a BMD -1 standard deviation from sex specific peak and osteoporosis as -2 standard deviations from peak. However, misclassification can occur as larger bones will appear to have greater bone density (242) and small individuals will appear to have low aBMD - even though they may have normal volumetric (v)BMD (53, 130, 148, 242, 243). Also, DXA cannot differentiate between cortical and trabecular bone and is less sensitive to detecting bone loss compared with instruments such as quantitative computed tomography (QCT) (49). With respect to soft tissue measures, errors in fat mass estimates occurred in larger individuals or those with tissue depths >12 cm (140, 270).

2.5.4 Peripheral Quantitative Computed Tomography (pQCT)

Peripheral QCT is a relatively new instrument that is more prevalent in Europe and is not used clinically in North America. Peripheral QCT uses an x-ray source to measure the appendicular skeleton, specifically the wrist and forearm (radius and ulna) and lower leg (tibia). Peripheral QCT is most often used in a research setting to advance knowledge of disease and other factors that affect bone in animals and humans (142, 235, 248). Peripheral QCT assesses volumetric bone density, geometry and structure and provides an estimate of bone strength (5). A rotation mechanism conducts a transverse scan following successive partial displacements every 12° for a total of 180° or 15 rotations. X-rays are absorbed during each transverse scan which produces multiple absorption profiles. These profiles are mathematically combined to produce an image through a process called "filtered backprojection". Each individual's measured points or voxels ultimately combine to make up an image that corresponds to a linear attenuation coefficient (μ) with dimensions (1/cm) of the measured part. Attenuation coefficients are dependent on the energy of the x-ray beam as well as on the material absorbed by the x-ray. Attenuation coefficients from each voxel obtained from the cross-sectional image is then transformed into density values by comparing values to a calibration equation that relates the attenuation value to the volumetric density of a reference hydroxyapatite phantom (257).

Peripheral pQCT evaluates both trabecular bone (in the distal region) and cortical bone (in the mid-region). It provides a measure of total area (ToA), trabecular area (TrA) and cortical area (CoA) (all mm^2), medullary canal area [MedA = (ToA-CoA)], CTh (mm), and density of these same compartments (ToD, TrD and CoD, respectively) (all mg/mm^3). The system also provides a bone strength index at distal sites (BSI, mg^2/mm^4) which is calculated using pQCT measures of ToA and ToD [BSI = ToA * ToD^2], a polar strength-strain index (mm^3) also known as the density-weighted polar section modulus or strength-strain index (SSI, mm^3) at midshaft regions (Table 4-1) (93, 130). The CV (%) in vivo with the XCT 2000 in our laboratory for repositioning was less than 2% for each bone parameter when 13 healthy adults (10 women, 3 men; mean age 27 years) were measured twice over a short period of time. In addition to bone, pQCT can quantify muscle cross sectional area (MCSA) at sites within the appendicular skeleton (257). For the leg the MCSA measurement site is located at 66% of the total tibial length proximal to the distal end. The analysis of MCSA involves two steps. The first is to separate muscle from bone and fat and the second is to separate muscle from bone. This can be done with user defined threshold algorithms provided by the XCT program during analysis. Precision of pQCT derived MCSA has not been determined for children but a precision error of 1.93% for MCSA has been reported in women (199).

The most common pQCT instruments are the Norland Stratec XCT 2000 (Stratec Medizintechnik GmbH, Pforzheim, Germany) and the Densiscan 1000 (Scanco Medical, Basserdorf, Switzerland). The Bone Health Research laboratory houses a Norland Stratec XCT 2000 which was used to collect the data for the current study. Peripheral QCT is quickly becoming an attractive instrument to investigate bone health in children, adolescents and the elderly (130). Despite this, as is seen in any imaging device, pQCT has its share of advantages and disadvantages.

2.5.5 Advantages and Disadvantages of QCT/pQCT

Peripheral QCT measures for the cross-sectional properties of bone by directly measuring its geometric and densitometric properties (8). This has important implications for studies of pediatric bone growth as the ends of long bones in children and adolescents are constantly changing (198). When QCT and pQCT outcomes from human and animal exercise studies were compared to DXA outcomes, computed tomography (CT) was found to be more sensitive in detecting changes (124, 125). Two studies that examined postmenopausal bone loss showed a 2% annual loss when measured by QCT compared with a 1% annual loss measured by DXA (93, 106). Precision for pQCT ranged from 0.5 % for trabecular density to 2.2% for cortical density (248). In addition, artifacts such as calcified tissue can be excluded from measurement by pQCT – this is not possible with DXA (139).

The Norland Stratec XCT 2000 provides a wide range of flexibility during scan acquisition and analysis. The operator can pre-set the scan resolution and field size (which influences the image voxel size), choose the number of slices at the site of interest, and position the anatomical reference line. During analysis, the operater may choose the analysis protocol and exclude image artifacts if present. (5). This poses both an advantage (as the appropriate protocol for each study and region of interest can be selected) and a disadvantage as acquisition and analysis methods that may vary between regions in various studies are most often not reported by investigators. In addition, there are very few pQCT studies of pediatric bone and, as such, there are no standards for pediatric scan acquisition and analysis and pediatric norms are currently unavailable (97, 98).

Despite its many advantages, pQCT scans are not clinically available in Canada and only three pQCT instruments are currently in use nation-wide. Also, pQCT emits marginally more radiation than DXA, although exposure is to less sensitive peripheral tissue (93). In addition, the more clinically relevant hip and spine cannot be assessed with this technique. The final disadvantage of pQCT is the Partial Volume Effect (PVE) – especially when assessing small bones. I describe this effect below.

2.5.5.1 The Partial Volume Effect

As mentioned previously, each point on the scanned image is made up of voxels (see glossary of terms) (257). Voxels are directly proportional to scan field size and determine overall scan resolution. Thus, small field sizes result in smaller voxels and improved resolution. However, smaller voxels requires a longer scan time and, as such, increases the radiation dose to the participant and the propensity for movement artifacts – especially when assessing children. In pediatric studies it is common to use a voxel size of 0.4 or 0.5 mm (78). Voxels are complicated by the PVE as they may be partially filled or filled with tissues of varying densities. Although, voxels of all sizes are affected by the PVE, this is observed to a greater extent in larger sized voxels.This is particularly true when assessing the relatively narrow expanse of cortical bone. For example, if a voxel at the endocortical border of the cortex is partly empty or filled with less dense trabecular bone, cortical density may be underestimated (239, 240). This

underestimation is exaggerated in thinner cortices despite identical bone mineral mass per unit volume (Figure 2-6) (239). Thus, bone size influences the placement of these voxels and the overall results (240). PVE can be minimized by choosing analysis modes and thresholds that include the majority of filled voxels or by assessing skeletal sites with thicker cortical shells (>2 mm) such as the midshaft (7, 110). Also, cortical thickness must be considered when measuring cortical density (239)

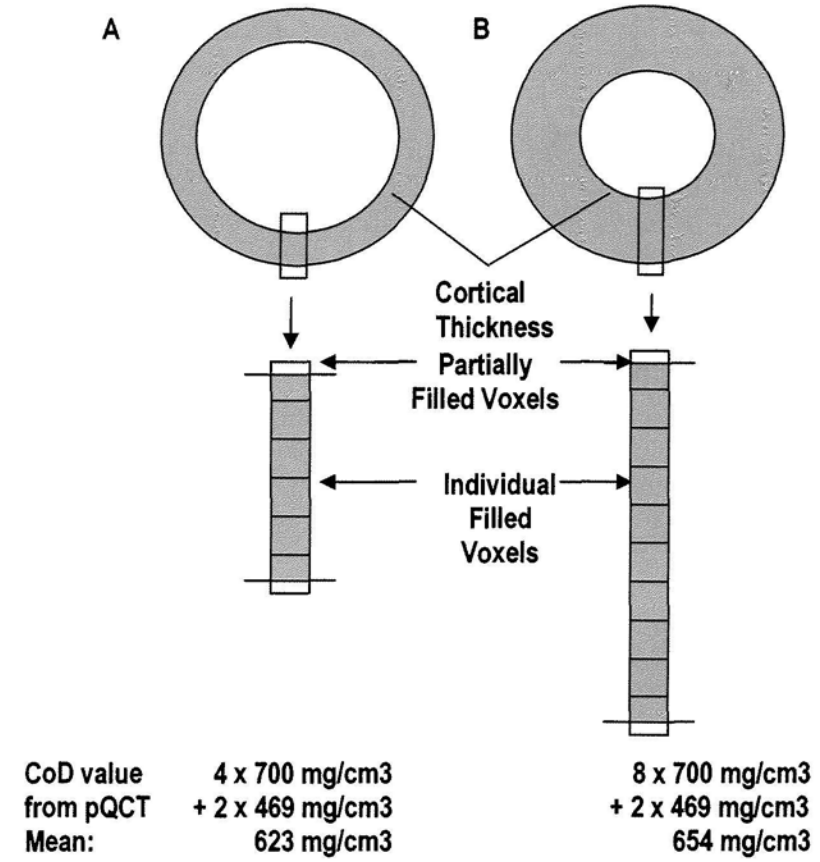

Figure 2-6: Partially filled voxels located at both ends of grey boxes and shown in white. In (A) thinner cortical wall sites (<2mm) reduces overall CoD values whereas, in (B) thicker cortical shells (>2mm) does not influence CoD values as much. Adapted from Schoenau et al. (240).

2.5.6 Bone Mineral Accrual as Measured by DXA

Bone development is marked by the process whereby bone mineral is accrued throughout the skeleton (224). This occurs at different rates throughout growth and development and in different parts of the skeleton, until maturity is reached (116). As childhood and adolescence are key periods of bone acquisition, attempts to increase bone mineral accrual during this period may have important clinical implications later in life (29, 30). Children who do not maximize their bone mass (or more importantly strength) during the growing years may have an increased risk of

skeletal fragility later in life (226, 227). They may also be at increased risk of fracture during youth (102, 115). By 15 years of age, girls have attained 90% of their mother's total bone mass (180). At 18 years in girls and approximately 20 years in boys, 85-90% of adult bone mass has been accrued (100, 175). The growth spurt period accounts for 15% of adult height (121, 175), 35-37% of total body (including the spine) bone mineral accrual (121, 175), and 27% of femoral neck bone mineral density (BMD) accrual (30). Thus, many pediatric intervention studies target childhood as key time to intervene with exercise (38, 160-163, 181, 182, 193) calcium supplementation (25, 28, 56) or both (153, 253) so as to maximize bone mass accrual.

2.5.6.1 Sex Differences in Bone Mass Accrual

There is a demonstrated sex difference in how bone mass is accrued [6, 7]. Bonjour et al., conducted a cross-sectional examination of bone mass accrual (QDR 2000) in 207 healthy Caucasian children aged 9-18 years. They reported site and sex-specific differences in bone mass accrual at the femoral neck (FN) and lumbar spine (LS). Boys between 15-18 years of age demonstrated a steady increase in bone mass at the FN and L2-L4 LS sites. However, in girls 15-16 years of age, growth slowed dramatically at these sites (30). This was positively associated with the age of menarche onset which occurred at approximately 15 years of age in girls (30).This study showed that the rate and magnitude of bone mass accrual during growth is not consistent between the sexes and differs between skeletal sites (30). Various other studies demonstrated sex specific differences in BMC across pubertal stages with BMC generally increasing from pre to post puberty (77, 104, 252). As girls enter puberty approximately 2 years earlier than boys, girls demonstrated significantly larger gains in BMC compared with boys the same chronological age. These differences reversed when children were aligned on a common biological landmark (16). This finding supports the fact that healthy males reportedly have higher bone mass throughout life (267). The University of Saskatchewan Pediatric Bone Mineral Accrual (U of S) study was a landmark trial that prospectively measured 113 boys and 115 girls between the ages 8-15 years at baseline (QDR 2000) for 7 years (16). The key findings from this trial are highlighted in (Figure 2-7).

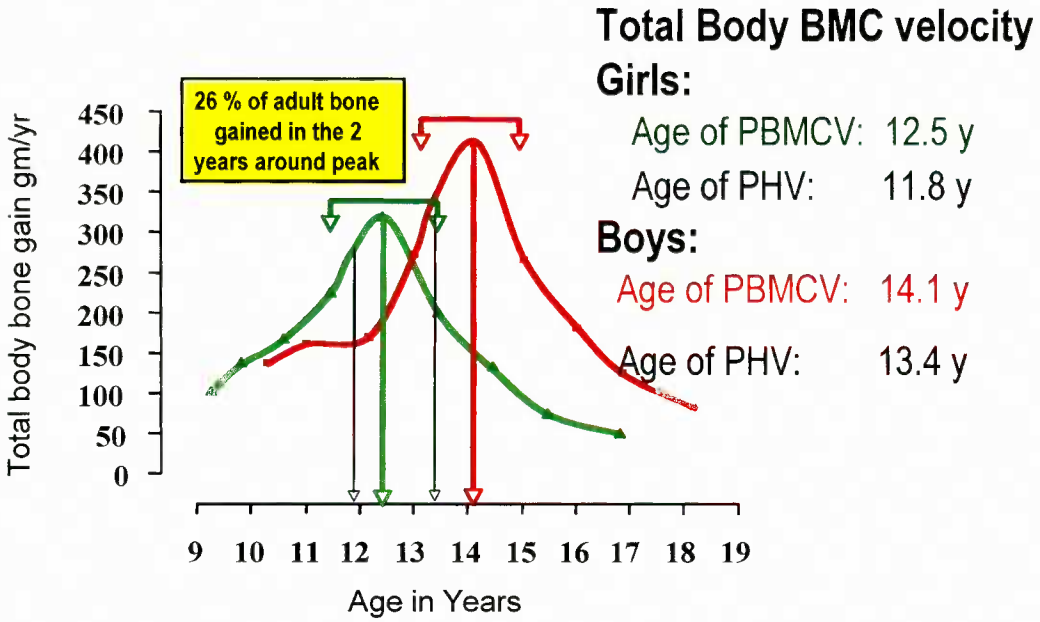

Figure 2-7: Graph illustrating total body peak BMC velocity curves (TB PBMCV) and ages at PBMCV and PHV for boys (red) and girls (green) by chronological age. Approximately 26% of adult BMC is accrued in the 2 years surrounding PBMCV in both sexes. Adapted from Bailey et al (12).

Briefly, data were modeled using a cubic spline fit and age at peak bone mass accrual occurred approximately 1.6 years earlier in girls compared with boys and lagged behind peak linear growth by approximately 7 months in both boys and girls (12). The magnitude of total body peak accrual adjusted for size was significantly greater for boys (394 g/yr) compared with girls (342 g/yr, $p<0.001$). There was also a significant difference in bone mass accrual between children who were the most physically active (409 g/yr) compared with those who were least active (331 g/yr) $p<0.001$ (12). A subsequent analysis of these same data used a multilevel model and demonstrated that boys had significantly more bone mass at the total body (TB) and the femoral neck (FN) sites, compared with girls $p<0.05$. After controlling for maturity or biological age (by determining APHV) and size within the model, these differences diminished to a 1.8% and 2.4% difference at age of PHV=0 for boys compared with girls at the TB and FN sites, respectively (16). Maturational age and fat mass coefficients predicted BMC at the TB and LS (lumbar spine) sites. However, sex was found to be a significant predictor of BMC at the TB and FN sites, $p<0.05$ (16). A biological age by height interaction for TB and a biological age by height, lean mass, and fat mass interaction at the LS was found. However, no interaction effects for the FN were found. In addition, significant predictors of TB BMC at PHV=0 were height (70%), lean mass (26%), and fat mass (3%). Significant predictors of FN BMC were height (60%), and lean mass (37%). Lastly, height (82%) and lean mass (17%) were found to be significant predictors of LS BMC (16). In another study conducted on girls from this cohort, the timing of peak BMC accrual approximated the age of menarche in girls (179). The findings highlighted in this section show the profound difference in accrual maturity between same

sex children and between boys and girls of the same chronological age. It also emphasizes the need to adequately control for maturational differences when comparing children.

2.5.7 Bone Strength and Geometry: Sex-Related Changes

It is commonly accepted that size plays a role in bone strength with larger bones having greater strength (242). Many studies have shown that boys undergo greater periosteal apposition than girls and have larger bones than girls (92, 132, 133, 242). However, it is not known whether this sex difference in periosteal apposition is primarily due to differences in body size. This is a possibility as size differences between individuals is often not controlled for within the research design, statistical analysis method or measurement technique (243).

Gilsanz et al., conducted a QCT study on 30 pairs of pre-pubertal (8.2-12.8 year old) Caucasian boys and girls whom were matched with each other by age, height and weight to determine sex-specific differences in bone geometry of the vertebrae (L1-L3) and femoral midshaft (99). Hand/wrist radiographs were employed to control for maturity. Sex differences in cross-sectional area (CSA) at the lumbar spine but not at the femoral shaft were found. Specifically, girls had significantly smaller vertebrae (-11%) compared with boys. In both sexes, children with higher body mass had higher vertebral CSA. There was no significant difference in trabecular bone density at the femur or the vertebrae in either sex (99). The results from this study suggests that sex differences in bone mass in children may be due to differences in relative bone size (96, 97, 194). Differences at the vertebrae but not at the femora can be attributed to the fact that growth and development at these sites are regulated differentially (51). It is important to note that the results from this study cannot be generalized beyond pre-pubertal Caucasian children.

2.5.7.1 Sex Differences in Bone Geometry and Strength

It has been suggested that sex differences in volumetric BMD (defined as the average BMD contained between the periosteum and endosteumcompartments) exist (239). A cross-sectional pQCT study examined gender differences in cortical vBMD at the proximal radius during puberty and early adulthood (239). The scanner was placed at 65% of the length of the forearm (239). Participants (n=362; 6-23 years) were obtained from the Dortmund Nutritional and Anthropometric Longitudinal Design (DONALD) study (135). When maturity (Tanner Staging) and cortical thickness were controlled for there were no sex differences in children at Tanner Stages 1-3. However, girls had significantly higher cortical vBMD (+3.4%) at Tanner Stages 4 and 5 compared with boys. This was also seen in adult women (n=88, 29-40 years) (+4.2%) compared with adult men (239). This study demonstrated sex differences at the proximal radius with a greater discrepancy between sexes in post puberty and young adulthood with greater gains occurring in females (239). It was suggested that this was due to less intracortical remodeling and thus less cortical porosity in girls and women (239). Results from this study are in keeping with other reports (99, 184, 239).

Another study recruited participants (n=318 healthy children, n=336 adults) from the DONALD study (135) to test Frost's theory that the greatest voluntary loads on bone come from muscles (88). Thus, researchers examined sex

differences in the muscle bone system interaction at the radius during puberty (237). Peripheral QCT (XCT 2000, Stratec) was used to determine cortical area and muscle area, measures representing bone strength and muscle strength, respectively. A single slice measurement at 65% of ulnar length was obtained as this site corresponds to the highest circumference and CSA in the forearm muscles (237). At pre-puberty, there was no difference in the muscle - bone relationship. However, at Tanner Stage 4 girls exhibited significant increases in cortical area relative to muscle area compared with boys. This difference which disappeared in adulthood, was attributed to greater endosteal apposition in girls (237). Although this study provides support for radiographic (91, 174) and other studies (87, 235) that showed mature girls have more cortical area at the radius than boys it is more likely accounted for by the rapid acceleration in muscle mass accrual in boys at adolescence. That said, gender differences in cortical area may also be related to sex hormones, especially the estrogen surge in girls during puberty (239).

Macdonald et al. examined sex differences in bone geometry and strength at the tibial midshaft in boys (n=69, mean age 11.9 years) and girls (n=59, mean age 12.0 years) by pQCT (XCT 2000, Norland/Stratec, Germany) (257). Girls were grouped into one of three maturity categories; "early" (pre-menarcheal at both baseline and 20 months), "peri" (pre-menarcheal at baseline and post-menarcheal at 20 months) and "post" (post-menarcheal at both baseline and 20 months) (157). For boys, those in Tanner Stages 2 or 3 at baseline were considered "early"-pubertal, those at Tanner Stage 4 were considered "peri"-pubertal and those at Tanner Stage 5 were considered "post"-pubertal (156). Bone geometry and strength was compared 1) across maturity within sexes and 2) between sexes within maturity group. After controlling for body weight, absolute change and percent change in CoA and section modulus (Z), 20 month change was significantly greater for early and peri girls compared with post girls ($p<0.05$) (156). Peri girls also had significantly greater gains in CTh compared to post girls ($p<0.05$) (156). There were no significant differences in these variables in boys over the 20 month period regardless of maturity group. Second, boys had significantly greater gains in ToA, CoA, and Z across all maturity groups compared with girls. The greatest differences were seen at post-puberty where boys had an 11%, 10%, and 14% increase in ToA, CoA, and Z, respectively, compared with post-pubertal girls. These findings suggest that bone modeling decreases in post puberty in girls and occurs at a relatively constant rate across maturity groups in boys (212). It would be important to follow these children forward to see when the rate of geometric changes diminishes in boys. Furthermore, boys exhibited a strength advantage irrespective of maturity, achieved by increased periosteal expansion that placed bone further from the center of bone or neutral axis (156). This may have implications for the propensity to fracture in later life, however, longer term prospective trials are needed to determine this

A study conducted on the same cohort as the current study utilizing in the same maturity categories as described above (Early, Peri, Post), examined sex differences in cortical bone surfaces across pubertal groups and *change* in these outcomes over 20 months (132). Bone outcomes assessed at the 50% site of the tibia were for the total bone cross-section (ToA), and for the cortical compartment CoA. The ratio of these two variables (CoA/ToA) was derived to estimate cortical thickness. Marrow Cavity Area (CavA (mm^2) was determined by subtracting CoA from ToA (132) to determine the amount of apposition or resorption at the endosteal surface. At baseline, girls had no significant difference between ToA and CoA across maturity groups. For boys, ToA was 21% greater in post compared with early boys. CoA was 13% and 21% greater in peri and post boys, respectively, compared with early boys (132). When examining change, both ToA and CoA significantly increased over 20 months in boys and girls at all maturity levels. For girls, greater gains in ToA were observed in peri compared with post girls (+ 5%). CoA increased by 5% and 8% in early girls compared with peri and post girls. There was a significant increase in the CoA/ToA ratio in the early group and increases in CavA in the early and peri groups. For boys, there was no significant difference for change in ToA. However, CoA increased 3% and 9% in peri boys compared to early and post boys, respectively across 20 months. An increase in the CoA/ToA ratio was observed for the early and peri boys, CavA increased in early and peri boys; these gains were greater than those observed in girls (132). Thus, both boys and girls demonstrated increases in CoA at the tibial midshaft across 20 months; however, boys showed a greater increase in periosteal apposition (represented by greater change in ToA) and endosteal resorption (represented by a greater increase in CavA). These differences represent an increase in bone size that would substantially favor bone strength in boys. The results for ToA and cortical thickness provide support for Garn's metacarpal studies. Counter to Garn's findings, there was no evidence of endosteal apposition in girls regardless of maturity group as was demonstrated in the increase in CavA (132). However, these discrepancies can be attributed to the fact that there are site-specific differences between these studies.

2.5.8 Increase in Fracture Risk During Pubertal Growth

There is a positive association between the occurrence of long bone fractures and the timing of peak height velocity (PHV) (223). One possible explanation is a transient fragility caused by the lag between the rapid increase in longitudinal bone growth and peak bone mineral accrual and bone strength accumulation (223). Peak growth in stature precedes bone mineral accretion by approximately 1 year in both sexes (12, 13, 115, 138) and at any age bone length is closer to the adult value than bone mineral content (242). The midshaft and distal ends of the tibia are common sites for lower limb fractures (233). These fractures occur as a result of a rotational force imposed on the bone when the foot is stationary. A common type of injury is epiphyseal separation, mainly seen in 9-14 year olds. However, fractures are relatively infrequent at the distal tibia (accounting for only 3% of all growth fractures), as this region is well protected by muscles and ligaments that surround the distal end of the tibia (233). Increased forearm fractures at the distal radius in girls during the pubertal growth spurt have also been reported (13).

Frost's mechanostat theory provides a partial explanation for the increased fracture rate during growth. It states that bones are continuously being overloaded and this causes them to become increasingly fragile during longitudinal growth (223, 254). In addition, an increase in bone remodeling leads to an increase in cortical porosity which offers an additional explanation as to the increased fracture rate during periods of accelerated growth (254). Thus, during the adolescent growth spurt, boys and girls may undergo a period of increased bone fragility due to both rapid remodeling and the lag time between peak height gains and peak bone gains (210). Fractures in growing bone heal quickly for the most part and growth resumes its natural course; however, if not monitored correctly, tibial fractures can lead to asymmetric growth, and limb shortening (233).

2.5.9 Association Between Bone Gained During Growth and Bone Lost During Aging

It is well known that all individuals, irrespective of sex, experience bone loss with advancing age (15, 92, 130). A significant correlation between declines in bone mass at the lumbar spine and increased age exists (76). It is thought that bone accrual during skeletal growth is an important factor that influences bone fragility and fracture observed in the aging population (15); however, there are currently no long term prospective trials that have assessed bone in the same cohort from childhood to old age. Areal BMD is commonly used as an indicator of bone loss and subsequent fracture risk in elderly persons (15). Seeman et al. conducted a study examining the relationship between bone density in daughters (n=41) of women (n=74) who had sustained an osteoporotic-related femoral hip fracture. Bone density at the lumbar spine, femoral neck, and femoral shaft was measured in both groups using dual-photon absorptiometry. Z-scores obtained were compared to values from normal controls (246). When age, height, weight, and menopausal status were controlled for, a significant relationship between bone density from osteoporotic mothers and their daughters was found. As was expected, mothers had greater declines in bone density compared with controls and than their daughters at all sites ($p<0.001$). Interestingly, daughters had significantly lower bone density at the femoral neck and shaft compared to controls ($p<0.001$). Another study examined the relationship between LS BMC (T12-L5 sites) in osteoporotic patients (n-25) and their first-degree relatives (n=35) (76). BMC was measured in both groups and compared to 127 healthy controls by QCT (Siemans Limited, Erlangen West Germany). Results indicated that LS BMC was lowest in ostroporotic patients. Relatives of these patients also had significantly lower BMC values compared to controls regardless of sex ($p<0.001$). In addition several of these participants had BMC values below 100 mg/cm^3 which are well below the value at which LS fractures can occur. An additional study examining the same question in daughters of women with osteoporosis provides support for this study (245). In summary, in a generational comparison, FN bone density was lower in the adult daughters of women who had sustained hip fractures (246) and LS BMC was lower in daughters and first-degree relatives of those with osteoporosis (76, 245). Thus it is thought that low peak BMC and aBMD is a strong indicator of fracture risk in later life (76, 245, 246). This can be attributed largely to genetic factors but a combination of nutritional and environmental influences can potentially exaggerate this (76); however, it should be noted that these studies had small sample sizes and thus, perhaps greater site-specific differences would have been observed if the sample size was larger.

2.6 Modeling Longitudinal Data

In this section, I provide a description of selected analysis techniques that researchers have used to describe their longitudinal data and discuss the issues associated with each. I will also describe some of the common modeling techniques used to represent hierarchical data.

2.6.1 Conventional Analysis Methods

An inherent assumption when using conventional statistical methods is that all data are independent (37). Despite this, conventional methods such as ANOVA, ANCOVA, or Linear Regression analysis have often been utilized to analyze longitudinal data including repeated, correlated, and thus, non-independent measurements. Studies that have used these approaches include the Coalfields Healthy Heartbeat School Project and The Prevention Education Program (PEP) (longitudinal cardiovascular risk studies) (215, 241) and the 15 year Amsterdam Growth and Health Longitudinal Study (129). An advantage of repeated measures ANOVA (RANOVA) and MANOVA is that it accounts for repeated measures. In addition ANOVA as well as ANCOVA are capable of conducting between group comparisons (37); however, the disadvantages of using these analysis techniques when conducting longitudinal studies far outweigh their advantages. For instance, all continuous data must be collected in a fixed, equally spaced manner (37). Furthermore, ANOVA is not flexible as time dependent covariates cannot be fitted and participants with missing observations can not be included in analysis (17, 152). This poses a major problem when researchers utilize traditional individual level statistics for their data that is comprised of repeated measures (152). Due to these disadvantages, these methods are usually not appropriate for modeling growth data.

In the past, growth data has been modeled by a process referred to as "growth curve fitting" or "growth modeling" whereby a mathematical model is adjusted to accommodate the particular data set. This method works occasionally but is dependent on many factors such as the type of variable being measured, precision of the measurement tool, and the age range and frequency of the observations to name a few (17). An example of this is the Preece-Bains Growth Model (PBGM) (276). The PBGM is a family of curves that conform to the shape of a human growth curve. It has been used by many to investigate the growth of children (23, 26, 41). The model is most often applied to analyze longitudinal data but has also been used on cross-sectional data, although not as well (276). For instance, when determining APHV using cross-sectional data, the model can accurately estimate APHV in males; however, in females the shape of the velocity curves are variable and APHV is underestimated. A disadvantage of using the PBGM is that it does not account for changes in the rates of growth such as those observed during the adolescent growth spurt (111). This is particularly apparent when the model is applied to infer longitudinal growth parameters from cross-sectional data (276).

On the other hand, multilevel modeling, also referred to as random effects models and hierarchical linear models, can be used to accurately describe growth data and present individual growth trajectories for each participant. The

University of Saskatchewan Bone Mineral Accrual Study (details in *section 2.5.6.1*) has used the technique previously to investigate BMC accrual in growing children (16, 17).

2.6.2 Multilevel Modeling Used to Describe Linear Growth in Children

Multilevel modeling (MLM) is defined as a statistical method that summarizes hierarchical data or data that are collected at more than one level within groups (37, 152). One example is data collected on students (level 1) who are "nested" within classes (level 2) that are "nested" within school (level 3) (152). MLM has many advantages including its ability to account for repeated measurements and within group correlations. It is also flexible in that data can be collected at variable times throughout the data collection period and all participants can be included in the model as long as they have complete data for a minimum of one time period. In addition, not all participants need to be assessed at the same time or for the same number of occasions (37). This is particularly useful when measuring growth variables in children as they undergo rapid change during pubertal development and thus sampling observations at different time points capture important changes that may be occurring (17, 37). When one measures and determines the influence of covariates on biological growth, it is important that the trajectory (slope and intercept) of each individual subject be determined. Although the pattern of growth will appear the same for each child, the tempo and timing will vary between children either slightly or dramatically based on genetic and/or environmental influences (17). The model also determines if the variation can be attributed to time-varying (i.e. height, weight, etc.) or time-invariant (sex, group, etc.) covariates (37).

When utilizing MLM, it is important to note that the total number of parameters included in the model should be one less than the number of total observations. Given an appropriate sample size, increasing the number of explanatory variables increases the complexity of the model but may also increase the accuracy of the results. However, this should only be considered if improved accuracy far outweighs the disadvantage of increased complexity (37). MLM can be used to summarize continuous (i.e. growth and developmental) data that are a smooth function of time or transitional (i.e. terminal illness such as the transition from HIV to AIDS) data relevant to the observation period under study (37). I provide details of trials that used conventional analysis methods as well as trials that used MLM to analyze their longitudinal data (Table 2-1).

2.7 Additional Types of Modeling

There are many other types of models that have been used to describe repeated measures data. Although not common in the published literature, covariance structure analysis can be used to model growth and developmental data (196, 275). It estimates the strength and direction of derived hypothesized constructs. Advantages of this model are its flexibility and its ability to distinguish between measurement variability and measurement error (37). Multivariate modeling can be used to model two or more outcome variables simultaneously (264). An example of this is a study that investigated the impact of behavioral disorders on increasing BMI on pubertal girls. In this study, researchers modeled BMI and pubertal development during the growth period while simultaneously measuring behavior disorders which were used as a covariate (42).

Two other important models are the marginal and conditional effects models. In marginal effects models, the average response for all individuals is regressed on selected covariates. For conditional effects models, also referred to as transition or Markov models, the average response is dependent on the pattern of previous responses and is also regressed on selected covariates. This model can take into account the individual's previous response or last two responses. Since the predicted values are dependent on previous values, any error that arises from the individual responses must be specified. This may pose a disadvantage and may lead to erroneous results if an error has been missed or has not been specified. However, advantages of this model are that it can be used to predict data if the participant is no longer a part of the study but previous data have been obtained. It is also useful in epidemiological studies as it can be used to estimate the incidence of disease or disorder (37).

Table 2-1: Examination of analysis techniques utilized for DXA and pQCT based longitudinal studies with BMC as the primary outcome variable. Outcomes relevant to this thesis are presented.

First Author Project Country	Methods	Intervention	Statistical Approach	Results	Other
Baxter-Jones et. al. (2003) (16) University of Saskatchewan Bone Mineral Accrual (U of SK) Study. Saskatoon, Canada.	Subjects: Healthy Boys & Girls Sample Size: N=85 Boys N=67 Girls Recruitment: Originally from 2 elementary schools Age Range (Yrs): 8-19 Maturity: All participants aligned by PHV (common maturational landmark) Design: Prospective mixed longitudinal design. Measurement tool(s): DXA (Hologic 2000, Hologic, Inc., Waltham, MA, U.S.A.). Bone Measurement Sites: TB, LS & PF.	Aim: To identify the independent effects of sex on BMC accrual in growing children. Program: Participants obtained from the U of S Study.	Cross-Sectional: Students t-tests. Results expressed as Mean ± SEM Age at PHV: Growth fitting curves were fitted to each subject by the cubic spline procedure. Longitudinal: Multilevel (random effects) modelling. Statistical Software: GraphPad Prism version 3.00 for Windows, GraphPad Software, San Diego, CA, USA; MlwiN version 1.0, Multilevel Models (MLM) Project, Institute of Education, Univ. of London, London UK; SPSS version 10.0, SPSS Inc, Chicago, IL, USA.	Mean APHV: Girls: 11.8 yrs Boys: 13.4 yrs Chronological Age Boys vs. Girls: Boys ≥ 14yrs were taller & had higher TB BMC values, from 10-12 yrs had greater lean mass., at 9-11 & 14-18 yrs had higher FN BMC vlaues. Girls ≥ 9 yrs had greater fat mass, at 12,13,17, & 18 yrs had higher LS BMC vlaues. Biological Age Boys vs Girls: Boys were taller and leaner than girls pre and post PHV. Boys had signifiantly higher TB, FN, and LS BMC. Girls had greater fat mass from +1 yr post PHV onwards.	Conclusion: Height and lean mass predicted BMC at all sites. Although the sex effect found was small and less than measurement error. Sig. Contribution(s) to Research: Aligned each participant on a common maturational landmark. Utilized MLM to account for the hierarchical nature of the data.

Table 2-1 Continued

First Author Project Country	Methods	Intervention	Statistical Approach	Results	Other
Mølgaard (1999) (189) A one year follow-up of a cross-sectional BMC study conducted on school children. Copenhagen, Denmark	Subjects: Healthy Boys & Girls Sample Size: N=140 Boys N=192 Girls Recruitment: 5 schools in Copenhagen Age Range (Yrs): 6.5-19.5 Maturity Range: Tanner Stage 1-5 Design: Not given Measurement tool(s): DXA Hologic 1000/W (Hologic Inc, Waltham, Massachusetts, USA). Bone Measurement Sites: TB	Aim: To determine the relationship between age, puberty, and growth in overall bone size and BMC. Intervention: None .	Change in anthropometric and DXA variables corrected to one year: calculated as final-baseline/difference in age Change in calcium: (Change in BMC*1000*0.322/365 days) Assumption: 32.2% of BMC consists of calcium. LMS (Box-Cox Power (L)), Median (M), & CV (S) Method: Used to derive smooth centile curves for change in BMC and BA. Linear Mixed Model: Determined the influence of maturity stage on BMC and BA change. Statistical Software: Not given	Age of Peak BA Accretion (Yrs): Girls: 12.3 Boys: 13.4 Age of Peak BMC Accretion: Girls:12.5 yrs Boys: 14.2 yrs Change in BA peaked earlier than change in BMC. Boys and Girls: -Change in BMC and BA significantly associated with Tanner stage, $p<0.001$ -change in BA was highest at Tanner Stage 3, $p<0.0001$ but not significantly different from Tanner stage 2, $p=0.15$ -change in BMC was highest at Tanner Stage 3 but not significantly different from Tanner Stage 2 in girls, $p=0.09$ and tanner Stage 4 in boys, $p=0.08$.	Conclusion:This study showed a difference between peak bone size and growth in BMC. There was a positive association between pubertal stage and gain in BMC and BA. Limitations: Used a 2 dimensional measurement instrument to determine the process of growth in a three dimensional structure. The data set used consisted of a limited number of children in each age and sex group. Sig. Contribution(s) to Research: This is the first long. study to report TB BA in a wide range of children

Table 2-1 Continued

First Author Project Country	Methods	Intervention	Statistical Approach	Results	Other
Specker (2003) (253) Physical Activity and Calcium Supplementation Trial South Dakota, USA	Subjects: Healthy young children. Sample Size: N=239 Recruitment: 11 child care centre. Age Range (Yrs): 3-5 Design: 1 yr RCT, placebo-controlled, partially blinded trial. Participants randomized to calcium or placebo group and by fine motor activity group and gross motor activity group. Measurement tool(s): DXA (Hologic QDR 4500W with HSA). pQCT (XCT 2000 Norland/Stratec Madison WI, USA Bone Measurement Sites: TB from DXA and distal 20% site from pQCT.	Aim: To determine whether calcium intake modified the bone response to increase physical activity in this group of children. Intervention: Supplements: 2 chewable 500 mg calcium pills or lactose pills. Fine motor activity: non-strenuous activity causing child to sit. Gross Motor Activity: physical activity comprised of 20 minutes of jumping, hopping, and skipping. Frequency & Duration: Supplements: 2X a day for 5 days for 50 weeks. Activity intervention: 30mins/day for 5 days for 50 weeks.	Student t-tests: Group comparisons. ANOVA: Between group comparisons General Linear Model: Used for pQCT bone variables to determine between group comparisons at the distal site. ANCOVA: To test for an interaction effect between calcium and activity group on changes in BMC and bone geometry at 12 months. -covariates: gender, age, childcare center, change in ht and wt, percent TB fat, and compliance with the program. Statistical Software: Experimental Pediatric Whole Body Version 8.2 Software for DXA TB Bone Analysis. None Mentioned for Non-Bone Analysis	Leg BMC DXA Placebo: Fine motor grp = gross motor group. DXA Calcium: Gross motor grp > fine motor grp (p=0.05) pQCT Distal 20% site Gross motor group had sig. greater periosteal and endosteal circumferences irrespective of group (p=0.05). There was an interaction effect between activity and calcium for CoA and CTh.	Conclusion:The effect of calcium in leg BMC is only seen if in combination with gross physical acitivty. Limitations: The complaince rate for calcuim supplementation was lower than that for placebo (56 ±25%) vs (74 ±12%). This does not coincide with the compliance with type of activity which was almost identical (72 vs 75%). Calcium may have had a main effect if providers complied as much as during administration of the placebo. Sig. Contribution(s) to Research: Provides support for adult activity trials which have found the same results.

Table 2-1 Continued

First Author Project Country	Methods	Intervention	Statistical Approach	Results	Other
Wang (2005) (273) Growth patterns at distal radius and tibial shaft trial Jyvaskyla, Finland	Subjects: Healthy pubertal girls. Sample Size: N=258 Recruitment: No information Age Range (Yrs): 10-13 Maturity Range: Tanner I-III Design: 2 yr longitudinal study where bone geometry and density was measured at baseline, at 1 yr and 2 yr follow-up. Participants obtained from a calcium, vitamin D, and milk supplementation intervention. Measurement tool(s): pQCT (XCT 2000 Stratec Germany) Bone Measurement Sites: 4% distal radius and 60% tibial shaft sites.	Aim: To clearly identify the different patterns of growth at the metaphysis and diaphysis at the radius and tibia. Intervention: None Thresholds: Total CSA: 169 and 280 mg/cm^3 At the tibial shaft CoA: 710 mg/cm^3 SubCoA: 100 mg/cm^3 CavA: density <100 mg/cm^3 CTh: determined by cortical ring model.	Shapiro Wilk Test: To test for normality. Hierarchical Linear Model: Used to explore changes in BMD and geometric properties during puberty. Time relative to menarche entered as an explanatory variable Statistical Software: SPSS version 11.0. MLwiN 1.0 (Multiple Project: Institute of Education, University of London, London, UK) XCT Stratec version 5.40 and Geanie 2.1(Bonaylze) for bone analysis	Peaks in bone outcome variables: Distal radius: CSA: 16 months before menarche BMC: 9 months before menarche. vBMD: declined 11 months before but increased after menarche Tibial shaft: CSA: 20 months before menarche. BMC: 10 months before menarche vBMD: increased during and after puberty CavA: increased until menarche and then decreased. CoA velocity: peaked at 13 months before puberty then declined. CTh: increase from early to late puberty.	Conclusion: Differences in growth patterns in diameter nad density at the distal radius and tibial shaft exist. Specifically, that cortical bone tissue dominates at the shaft wherease trabecular bone was found to dominate at the distal radius. Limitations: Pooling intervention participants may have biased the outcomes as studies have shown the effects these supplements on endocortical remodellng. (28, 56). Also, determining maturational status by determining APHV would have been a better indicator than Tanner Staging. Sig. Contribution(s) to Research: clearly showed differences in bone geometry and density at different skeletal regions and sites in pubertal girls.

Key: yrs = years; grp = group; BA = bone area (g/cm^3); DXA = dual energy x-ray absorptiometry; BMC= bone mineral content (g); LS = lumbar spine; PF = proximal femur; TB = Total Body; pQCT= Peripheral Quantitative Computed Tomography; CTh = cortical wall thickness (mm); CoA = cortical bone cross-sectional area (mm^2); SubCoA = subcortex; vBMD = volumetric bone mineral density; CSA= cross-sectional area; MedA= medullary canal area; CavaA= Marrow Cavity Area; PHV = Peak Height Velocity; APHV = Age at Peak Height Velocity; +1 PHV = One year from Peak Height Velocity RCT= randomized controlled trial; ANOVA= analysis of variance; ANCOVA= analysis of covariance;

3 Research Questions

In this chapter, I outline the rationale, research aims and research objectives that provide the framework of this thesis. I also outline the objectives and hypotheses of my research.

3.1 Rationale

As previously mentioned in the introduction, osteoporosis is a systemic disease that places significant social, emotional and economic burden on individuals, their families, society and the health care system (151). As the aging human skeleton inevitably experiences a decline in bone mass, an indicator of bone strength (122), detailed knowledge of how bone develops, is maintained and enhanced is required in order to combat osteoporosis and related fracture. It is well known that bone strength is inversely related to fracture (122). It has also been well documented in cross-sectional (20, 39, 84, 91, 92) and short (8, 157, 158, 163) and long term (12, 16, 23, 129) longitudinal studies that the majority of bone mineral is accrued during the pubertal years (29, 30).

Garn's landmark studies noted that during puberty, boys undergo greater periosteal apposition and girls experience greater endosteal apposition – and this remains the current dogma. Thus, bone strength is conferred differently between the sexes, favoring boys (92). It is only recently, with the evolution of imaging techniques and with increased precision in measurement tools, that we are better able to describe bone structure and strength in the long bones of growing children with high precision and accuracy. Further, longer term longitudinal (rather than cross-sectional) trials are necessary to more definitely characterize these sex differences in bone strength accrual.

Peripheral QCT is a relatively new imaging instrument that is able to assess volumetric bone density and bone strength. It also provides an accurate means to investigate sex differences in bone geometric properties in the appendicular skeleton. Peripheral QCT is also able to discern the contribution of the different parameters that comprise bone strength- bone geometry and volumetric density. The relevance of this study to the health of individuals is through enhanced knowledge of those mechanisms that underpin bone strength. Through this knowledge we can, in the future, effectively evaluate the effect of dedicated interventions so as to enhance peak bone accrual/strength and conserve this strength throughout life.

3.2 Research Aim

My research aim is to describe sex differences in bone structure and strength in a growing long bone.

3.3 Research Objectives

My *primary research objectives are:*

1) To compare bone biological events on the periosteal and endosteal surfaces of the tibial midshaft in boys and girls.
2) To compare how volumetric bone density at the tibial midshaft is accrued between boys and girls.
3) To compare sex differences in bone strength accrual.

3.4 Research Hypothesis

H_1 Boys and girls exhibit endosteal formation during adolescence but the magnitude of this is greater in girls. Experimentally this will be represented by a reduction in the cross-sectional area of the medullary canal (MedA).

H_2 Boys and girls exhibit periosteal formation during adolescence but the magnitude of this is greater in boys. Experimentally this will be represented by an increase in periosteal diameter as measured by total area (ToA).

H_3 Boys and girls exhibit gains in volumetric bone density during adolescent growth. The magnitude of this increase is greater in girls (CoD).

H_4 Boys and girls will exhibit increases in bone strength accrual during adolescent growth. The magnitude of this increase will be greater in boys (SSI).

4 Methods

In this section, I outline the study design and provide an overview of the Healthy Bones Study school-based exercise intervention. Discussion of this intervention is relevant as the cohort that I followed prospectively for the current study were participants in this intervention. I also provide a detailed explanation of cohort recruitment and the measurements that are relevant to this thesis. My contribution to the study was measuring all children across 2 years at the dual energy x-ray absorptiometry (DXA) station (data not used in the current thesis), analyzing pQCT and DXA scans from 2004-2006, determining APHV for all children, data checking and cleaning and statistical analysis of the data. In addition, I conducted the majority of anthropometric measurements across 3 years (2004-2006) of measurement.

4.1 Study Design and Overview of Measurement Time points

The Healthy Bones Study (HBS) was a randomized, controlled, school-based exercise intervention that assessed children in Grades 4 and 5 (at baseline) from 14 elementary schools in the Richmond School District. These children were measured prospectively across 7 years with a maximum of 10 measurement periods to date. I provide the study timeline for the HBS (Figure 4-1). The primary objective of the intervention study was to investigate the effects of a 20-month exercise intervention on bone mass.

Time 1 (baseline) measurements were undertaken in September – October, 1999 prior to the start of the exercise intervention. The intervention was then implemented by teachers for one academic year (7 months) within physical education. The first follow-up was June 2000 (Time 2), at the end of the first academic year. A second year baseline was obtained in September - October 2000 (Time 3) and the intervention was implemented once again during the next academic year. Year 2 follow-up data were collected in May-June, 2001 (Time 4) (Figure 4-1). The intervention was withdrawn at the end of the school year (June 2001). Data were once again collected at the start of the next school year (September - October 2001, Time 5) and pQCT were added to the measurement protocol to assess bone (which previously included only DXA). Subsequently, participants have undergone annual measurements at the end of every school year (June 2002-06) (Time 6-10) (Figure 4-1). Ethics approval was obtained for all measurement periods from the University of British Columbia Clinical Research Ethics Board (Certificate Number: C99-0313).

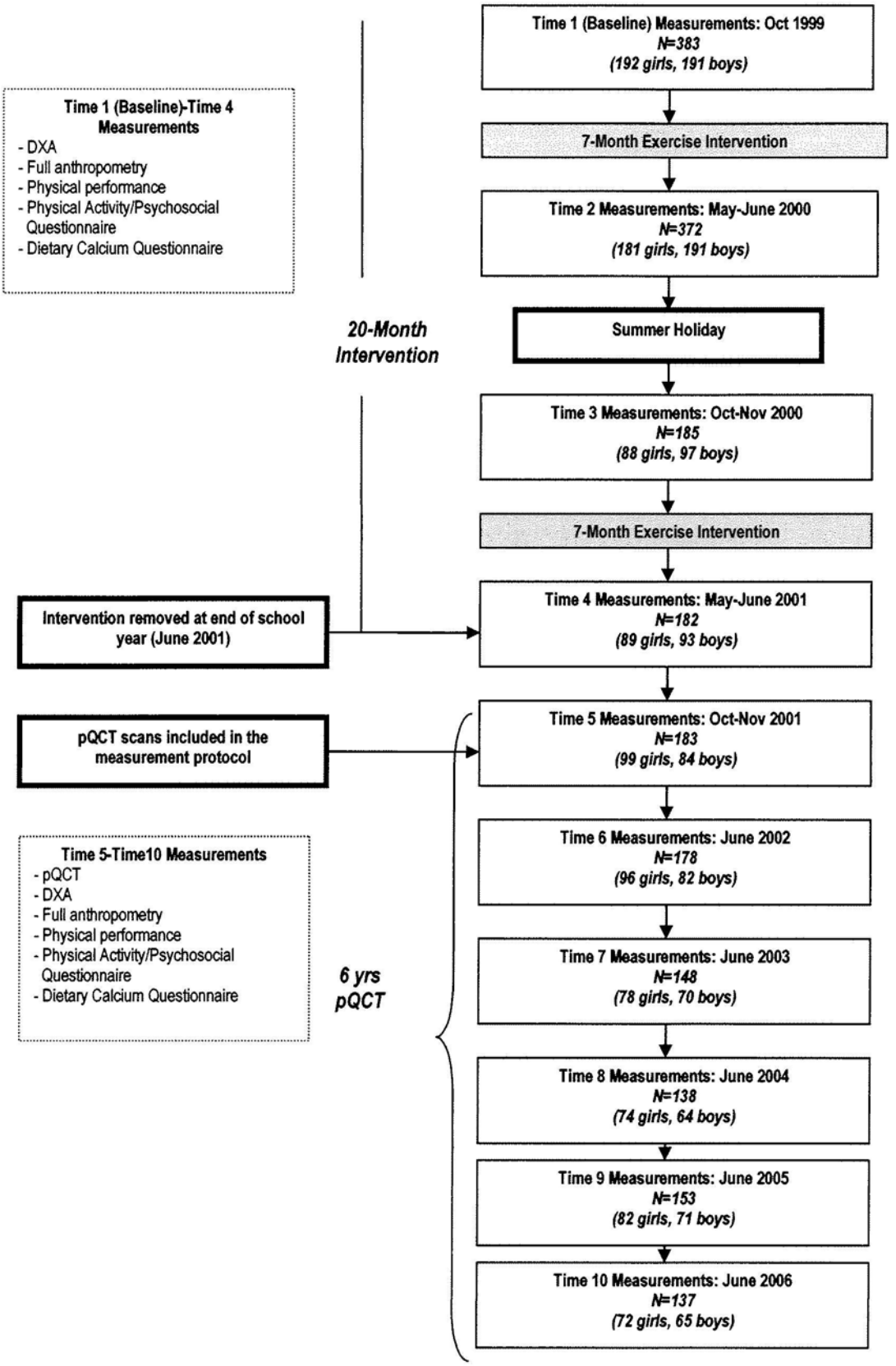

Figure 4-1: Schematic of study timeline.

4.2 Consent, Health History, Ethnicity, Randomization and Exclusion

Consent forms were distributed and collected by classroom teachers and picked up by a research assistant. All those who provided written consent underwent baseline testing. In addition, parents completed a health history questionnaire for their child and each participant completed a personal data form. These questionnaires identified medical conditions that interfer with normal physical activity or bone metabolism. Change in medical status was determined from the personal data form during each follow-up measurement. Participants were excluded from data analysis as appropriate.

In addition to identifying previous and existing medical conditions, the health history questionnaire also identified each participant's ethnicity based on parents' or grandparents' place of birth. Parents were asked to classify their own, and their child's ethnicity. Participants were classified as "Asian" if both parents or all 4 grandparents were born in Hong Kong, China, Japan, Taiwan, Philippines, or Korea; "Caucasian" if both parents or all 4 grandparents were born in North America or Europe; and "Other" if the participant had parents of other origins (i.e. Africa, India) or had 2 parents of distinct ethnicities. Schools were stratified by size and geographic location and randomly assigned to control or intervention group.

4.3 Overview of Exercise Intervention

The HBS exercise program was designed to provide 10-12 minutes of high impact (i.e. jumping, hopping) weight bearing exercises twice a week in regular physical education (PE) class and one other time inside the classroom – 3 times per week in total. Intervention teachers were provided training to implement the exercise program. All exercises were comprised of various jumping exercises (i.e. jumping jacks, lunge jumps, hopping, jumping over obstacles, platform drop jumps) that increased in frequency and intensity every week. The frequency of the jumps began at 10 and increased to a maximum of 100 jumps at the end of the first year. Children began jumping from a 10 cm platform which progressed to a 30 cm platform, and finally a 50 cm platform. Therefore, the frequency and intensity of the jumps increased progressively across the 20-month trial in all intervention schools. In the second year of the intervention, the frequency of jumps increased from 55 jumps to a maximum of 132 jumps at the end of the school year. The intensity of jumps progressed similarly to Year 1. Control participants underwent 10 minutes of stretching twice weekly prior to PE class and one additional time during regular classroom session.

4.4 Data Collection

As my thesis is a part of a larger trial, I present only the data collection methods that are relevant to this thesis.

4.4.1 Anthropometry

Stretch stature for both sitting and standing height (without shoes) was measured using standard techniques, by applying gentle upward traction from the base of the mastoid processes. Measurements were taken using a wall mounted stadiometer (Seca Model 242, Hanover, MD) and data were recorded to the nearest millimeter. Leg length was derived from the difference between standing height and sitting height. Weight was measured with participants dressed in light clothing on a calibrated electronic scale (Seca Model 840, Hanover, MD) to the nearest 0.1 kg. Duplicate measures of sitting and standing height and weight were taken unless measures differed by ±0.4 cm (height) or ±0.2 kg (weight) at which point a third measurement was taken. The average of 2 values or the median of 3 values was used for statistical analysis. Maximum calf girth and length of the tibia was measured to the nearest millimeter by standard method using an anthropometric tape. All measurements were taken by trained research assistants as well as myself.

4.4.2 pQCT Acquisition

All pQCT scans acquired during the first 4 measurement time periods (T5-T8; 2001-2004) were acquired by the same technician. The last two, time 9 and time 10 measures (2005 and 2006) were acquired by a different technician. Each participant's left leg was placed through the pQCT gantry and securely positioned (in a standardized way) on a customized leg and foot hold designed by Bone Diagnostics Inc. (Figure 4-2). A Velcro strap was placed around the front of each participant's leg and foot to help maintain the stationary position of the left leg (Figure 4-2). A 2.3 mm slice at the midshaft (50%) site of the left tibia was obtained using the XCT-2000 (Norland/Stratec Medizintechnic GmbH, Pforzheim, Germany). A scan speed of 30 mm/sec and a resolution (voxel size) of 0.5 mm in accordance with manufacturer recommendations was used to acquire the data. To locate the anatomical reference line, a 30 mm scout view was performed at the midpoint of the tibio-talar (ankle). The location of the midshaft (50% site) site was automatically adjusted to the anatomical reference line. As participants were growing, this anatomical reference line placed the measurement site in the same relative location each year. Participants were asked to remain stationary for the duration of the scan which took approximately 100 seconds to complete. However, this is contingent on the length of the bone, which may result in a slightly longer or shorter scan time. We collected data at the 50% site as it is primarily a cortical bone region and a commonly assessed pQCT site. I provide a schematic diagram to show the measurement site and a representative scan from a 16 year old girl (Figure 4-3).

The pQCT procedure is safe, painless, and the participant is exposed to a low dose of radiation. The effective dose equivalent (risk from exposure of a single tissue in terms of an equivalent risk from exposure of the whole body) is 0.22 microSV (257). This is significantly less than the radiation dose of one chest X-ray (100 microSV) and of the normal annual background radiation in Canada (~1800 microSV/year) (103). Quality assurance was performed once daily by the research assistant using a manufacturer provided cone phantom.

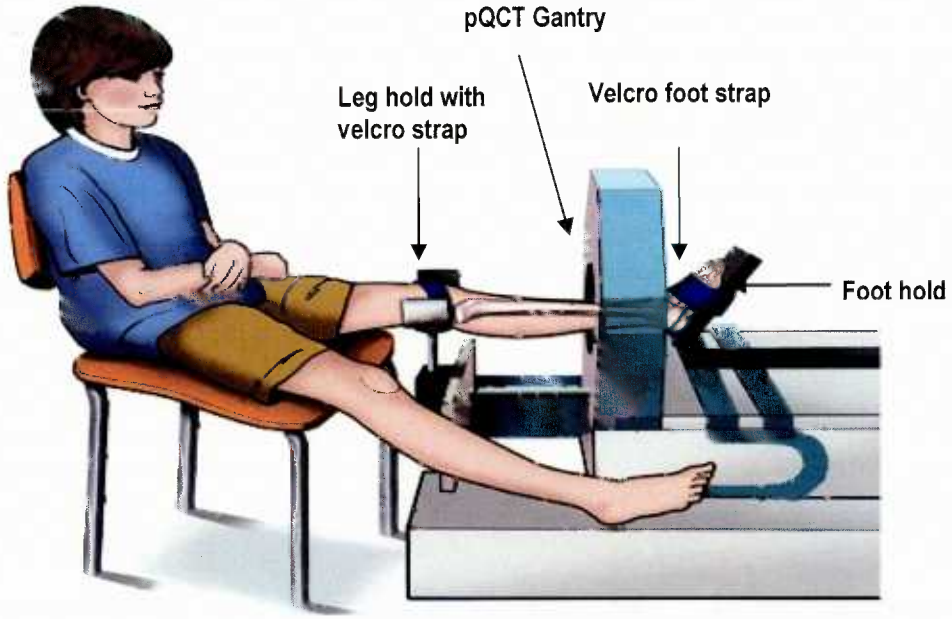

Figure 4-2: Standard positioning of the participant during a pQCT scan of the tibia. Drawing by Vicky Earle, Medical Illustrator.

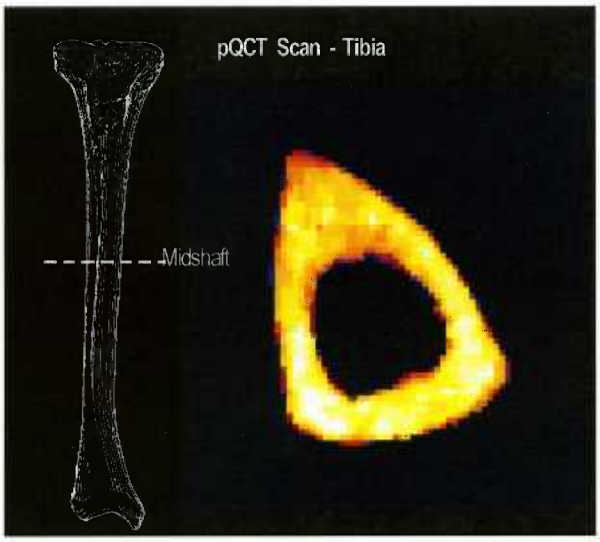

Figure 4-3: Measurement at the 50% site of the tibia (left) and a representative pQCT cross-sectional image of a 16-year old girl (right).

4.4.3 pQCT Analysis

I analyzed the pQCT scans from 2004-2006 for all individuals using the Stratec (Version 5.50) software and according to standard procedures outlined in the Stratec manual (257). For each scan, I positioned the cursor in the center of the tibia marrow cavity. I activated the edge detection algorithm with a mouse click to draw an automatic region of interest (ROI) around the tibia. The algorithm is preset by operator set modes and thresholds to determine a large number of pQCT outcome variables. The modes, thresholds and outcome variables used in this thesis are presented (Table 4-1). Currently there are no standardized analysis protocols for pQCT pediatric studies thus, the modes and thresholds chosen are similar to those used in previous studies by our group (155) and are based on the manufacturer's recommendations (257).

Table 4-1: Analysis Modes, Thresholds and Outcome Variables for pQCT Measurements at the Mid-Tibia (50% Site). All Outcomes in Bold.

Site	Analysis Mode (Threshold)	Categories	Outcome Variables
Midshaft (50%)	Peel Mode 2 (540 mg/cm^3) Cortmode/Seperation Mode 1 (default, 711 mg/cm^3) Contmode 1 (default, 711 mg/cm^3)	Geometry	**Total bone area (ToA, mm^2)** **Cortical area (CoA, mm^2)** **Medullary Canal Area (MedA, mm^2)** **Cortical density (CoD, mg/cm^3)**
Midshaft (50%)	Peel Mode 2 (540 mg/cm^3) Cortmode/Seperation Mode 1 (480 mg/cm^3)	Strength	**Polar strength-strain index (SSI, mm^3)**

4.4.3.1 Inclusion/Exclusion Criteria

All participants who had at least one pQCT scan were included in my analysis. Scans with artifacts due to participant movement were removed from analysis. In addition, scans were removed if measurement protocol was not followed (i.e. incorrect voxel size used to obtain scan). A detailed description of excluded scans is provided in *section 5.2.* (Table 5-3).

4.5 Statistical Analysis

In this section, I provide a detailed description of the statistical analyses used in this thesis. This is provided in two parts. First, I describe the analysis used to determine age at peak height velocity (*section 6.1)*. Second, I describe my statistical approach to model the data data modeling using the MLM technique to test my objectives (*section 4.5.2)*. Data were analyzed using GraphPad Prism software (Version 5.0) and STATA software, Version 9.0 (StataCorp LP, College Station, TX). Results are presented by sex for both analyses.

4.5.1 Determining Maturity Offset

To determine maturity offset, APHV and chronological age at the time of measurement must be known. I determined APHV for each participant by plotting annual change in height against their mean annual age from the last two measures. The largest change in height (velocity) was used identify the peak growth period. To achieve this I used the cubic spline procedure. This procedure employs interpolating cubic polynomials which uses information from neighboring points to obtain a degree of global smoothness to fit the curve. This form of curve fitting is preferred because it maintains the integrity of the data without transforming or modifying the data (11). Once APHV velocity was determined, maturity offset was obtained by subtracting chronological age at the time of measurement from APHV. For example, a child who reached PHV 1 year prior to the measurement date would have a maturity offset of +1. A child who reached PHV 1 year after measurement would have a maturity offset of -1. On the other hand, a child who was measured at their APHV would have a maturity offset of 0. Thus, a continuous measure of maturational age

was generated. Importantly, all children were aligned on APHV so as to compare events at bone surfaces and in the whole bone cross section.

4.5.2 Longitudinal Data Analysis

MLM was used to examine sex differences in selected pQCT outcome variables at the tibial midshaft. There are many advantages to using MLM on a longitudinal data set comprised of repeated measurements. I have described these in more detail in *section 2.6.2.* Overall, the model is comprised of two levels. The first level of analysis occurs *within* individuals where a specific model of growth is specified. The second level of analysis occurs *between* individuals and determines whether the parameters that describe growth in level one vary among individuals. Within the hierarchical structure, there is greater variability between individuals than between occasions within individuals. As each individual's data is regarded as being a random sample from the entire population, inferences about the variation between individuals are made and as such using a MLM approach is appropriate (37). A detailed description of how the model was fit is described in *Chapter 7.0.*

5 Overview of the Cohort

5.1 Participants

I describe the participants in 2 parts. First, I provide a description of the entire cohort recruited into the trial in 1999 (baseline 1). Second, I describe the cohort the year pQCT was included in the measurement protocol (baseline 2), as these participants comprise the sample for my thesis.

Baseline 1: A total of 14 schools from the Richmond BC school district were recruited to participate in the HBS. From this, a total of 383 children in grades 4-6 and their parents/guardians provided informed consent to participate in the exercise intervention and evaluation component of testing. The breakdown of this cohort by sex at each measurement time point is provided (Figure 4-1). At baseline 1, there was an even number of girls (n=192) and boys (n=191) and a balanced number of children in schools (n=7 control, n=7 intervention) that were randomized to either the intervention (n=181) or control (n=202) arms.

Descriptive characteristics for girls and boys at baseline 1 are provided (Table 5-1). One boy did not consent to the bone measurement and 2 girls and 4 boys were excluded based on medical conditions that could affect bone development. Thus, baseline descriptives are presented for 376 participants (190 girls, 186 boys) (Table 5-1). At baseline 1, girls and boys were of a similar age (girls: 10.3 ± 0.7 years; boys: 10.4 ± 0.7 years) and ethnic distribution (Girls: 35% Asian, 44% Caucasian, 20% Other; Boys: 39% Asian, 42% Caucasian, 17% Other). There was also no difference in height ($p=0.91$), weight ($p=0.54$), sitting height ($p=0.89$) or leg length ($p=0.36$) between the sexes.

Baseline 2: Descriptive characteristics for boys and girls at baseline 2 are provided (Table 5-2). Participants were of the same age (Girls: 12.1± 0.5 years; Boys: 12.1±0.5 years) and similar ethnic distribution (Girls: 33% Asian, 54% Caucasian, 13% Other; Boys: 35% Asian, 51% Caucasian, 14% Other). There was no significant difference in pQCT outcome variables between sexes, $p>0.05$ except for CoD where girls were significantly greater than boys $p<0.001$.

Table 5-1: Baseline 1 (1999) Descriptive Variables for Boys and Girls by Sex

*Descriptive variables: Mean (SD) calculated for N= 190 girls (2 exclusions: Down's syndrome, 1 polycystic kidney removal + precocious puberty).
** Descriptive variables calculated for N=186 boys (5 exclusions: 1 Downs syndrome, 1 cerebral palsy, 1 casted club foot, 1 recent heart surgery, 1 who did not consent to bone measurement portion of testing).

	N	Girls			N	Boys		
		Mean (SD)	Min.	Max.		Mean (SD)	Min.	Max
Total N	190*				186**			
#Asian/Caucasian/Other	67/84/39				77/79/30			
Age (yrs)		10.3 (0.7)	8.8	11.8		10.4 (0.6)	8.8	12.2
Height (cm)		142.2	117.0	159.0		142.3	122.0	173.0
Weight (kg)		37.0 (9.1)	20.4	70.5		37.6	20.8	80.8
Sitting height (cm)		75.3 (4.2)	65.4	87.3		75.2 (3.8)	66.0	88.6
Leg length (cm)		67.0 (4.3)	51.4	77.7		67.1 (4.4)	53.8	84.1

Table5-2: Baseline 2 (2001) Descriptive Variables and Bone Outcomes for Boys and Girls by Sex

Descriptives for anthropometric variables as well as bone outcome parameters (ToA = Total bone cross-sectional area; CoA = Cortical bone cross-sectional area; MedCanal Area = Medullary Canal area; SSI = Strength-Strain Index) provided below. Significant differences at baseline represented by * p<0.05.

	N	Girls			N	Boys		
		Mean (SD)	Minimum	Maximum		Mean (SD)	Minimum	Maximum
Total N	90				80			
#Asian/ Caucasian/Other	30/48/12				28/41/11			
Age (yrs)		12.1 (0.5)	10.8	12.8		12.1 (0.5)	10.9	13.5
Tanner Breast Stage (1/2/3/4/5)	6/33/36/13/2				N/A			
Tanner Pubic Hair Stage (1/2/3/4/5)	12/23/40/13/1				12/27/28/12/1			
Height (cm)		153.6 (7.7)	134.0	174.0		153.1 (8.8)	132.0	174.0
Weight (kg)		47.5 (10.9)	27.0	73.6		46.3 (12.4)	23.2	78.2
Sitting height (cm)		81.0 (4.2)	71.5	89.3		80.0 (4.5)	70.1	92.4
Leg length (cm)		73.5 (9.9)	61.7	155.3		73.1 (5.1)	61.4	83.6
Tibial length (mm)		352.1 (23.1)	295.0	414.0		350.6 (24.9)	285.0	400.0
ToA – 50% site (mm^2)		351.0 (56.0)	225.8	530.5		361.3 (63.1)	237.0	559.3
CoA – 50% site (mm^2)		233.9 (41.4)	145.3	380.8		236.2 (45.7)	152.8	373.3
MedCanal Area-50% site (mm^2)		117.1 (30.0)	57.0	192.3		125.6 (27.7)	70.3	221.8
CoD – 50% site (mg/cm^3)		1066.5 (36.3)*	990.7	1146.4		1035.4 (33.4)	957.4	1114.2
SSI – 50% site (mm^3)		1277.9 (293.8)	662.0	2291.0		1309.2 (346.0)	696.0	2318.0

5.2 Participants Lost to Follow-Up

To minimize attrition each year, participants were contacted by mail and telephone 1 to 2 months prior to measurement to request their return for the current measurement period. The overall attrition of the study from baseline measurements (Time 1) to the end of the 20-month intervention was 52.4% (Figure 4-1). The primary reasons for this were the withdrawal of 2 treatment schools *en bloc (-52 children)*, individual teachers withdrew their classrooms from participating (*-35 children*), children moved (*-45 children*), children did not return a consent form (*-11 children*), and significant medical conditions among children (*-6 children*). Thus, a total of 183 participants underwent baseline pQCT testing (Time 5). The overall attrition of the study from the start of pQCT measurements was 25% over the 6 year period (Figure 4-1). The details of attrition during a portion of this time period are unavailable.

During scan analysis, I excluded scans that could not be analyzed due to movement artifacts or measurement error. The number of excluded and acceptable scans is provided (Table 5-3). The number of acceptable scans incorporates both participants lost to follow-up and the scans that could not be used due to movement artifacts or measurement error.

Table 5-3: A summary of excluded and accepted pQCT scans from analysis at each time point.

Time point	Total Sample (N)	No. of Excluded Scans	No. of Acceptable Scans (Girls/Boys)
Time 5 (Baseline 2)	183	13	170 (90/80)
Time 6	178	8	170 (93/77)
Time 7	148	7	141 (76/65)
Time 8	138	9	129 (72/57)
Time 9	153	4	149 (81/68)
Time 10	137	2	135 (70/65)

5.3 Influence of the Intervention on pQCT Outcome Variables

Previous analysis by the Bone Health Research group was conducted on a subset of this cohort. At Baseline 2, bone structure and strength of the left tibia between girls involved in the 20-month exercise intervention and the control group were compared. Peripheral QCT measurements at the midshaft (50% site) were obtained from 54 girls (n=24 intervention, n=30 control). CoA (mm^2), CTh (mm), periosteal and endosteal circumference (mm), and CSMI (mm^4) values were obtained from these measurements. Despite the greater gains in femoral neck BMC in intervention girls as determined by DXA, no difference was found in bone structure and strength at the tibia between groups. In addition, no difference in age (12.2±0.5 yrs), height (154.6±8.1 cm), weight (48.8±11.2 kg) or general physical activity score was found between groups (158). To my knowledge, a similar analysis was not conducted in boys.

I sought to determine if returning participants who took part in the HBS exercise intervention differed on the key bone outcome variables used in my thesis compared with children who were initially assigned to the HBS control group. To achieve this, I produced two-way scatterplots and performed two-sample t-tests by sex and group at baseline 2 to compare selected pQCT variables between groups for children represented in the current thesis. I produced sex by group plots for ToA (mm^2), CoA (mm^2), MedA (mm^2), CoD (mg/cm^3), and SSI (mm^3) for two groups: 1. all returning participants regardless of number of scans and 2. for those with scans from either all measurement points (maximum of 6 scans) or for those missing only one scan (minimum 5 scans). There was no difference in pQCT outcomes between the whole group of intervention and control girls and boys at baseline 2 (Figure 5-1 (a-e)) or for those with 5 or 6 measurements (Figure 5-2 (a-e)), $p>0.05$. It is interesting to note that, although not significant, the control group tended to have a greater overall increase in ToA, CoA, MedA, CoD and SSI compared to the intervention group. This trend was greater for boys (Figure 5-1 (a-e)). As there was no difference in bone outcome variables between groups at baseline 2, participants were collapsed for analysis.

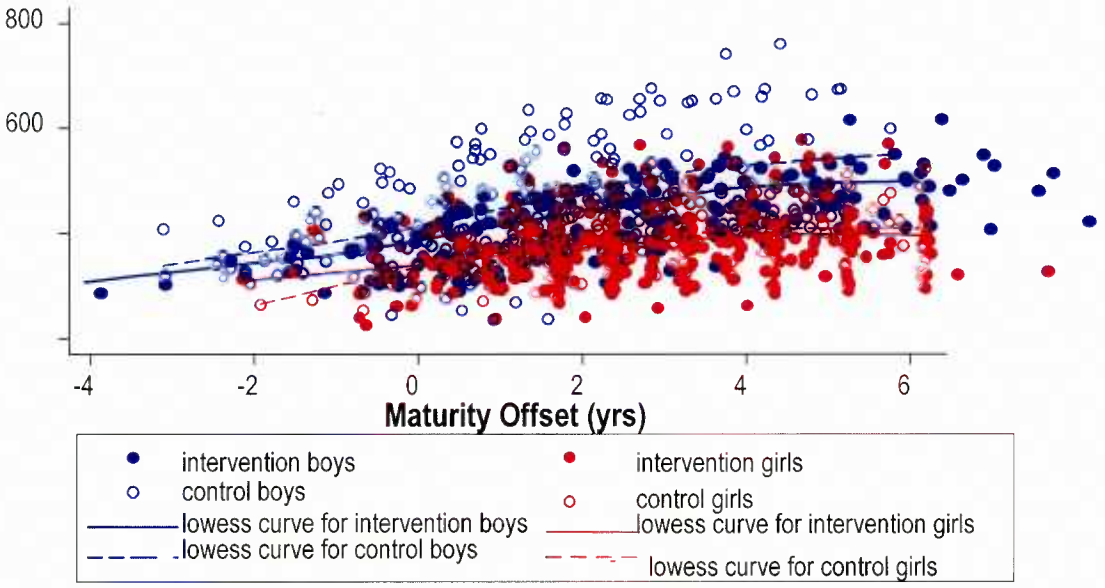

Figure 5-1 (a)

Figure 5-1: A comparison of intervention and control boys and girls by maturity offset (years) for bone; a) total area (ToA, mm^2), b) cortical area (CoA, mm^2), c) medullary canal area (MedA,mm^2), d) cortical density (CoD, mg/cm^3), and d) strength-strain index (SSI, mm^3). Boys are represented by blue circles and blue lines, girls by pink circles and pink lines. Intervention boys and girls are represented by closed circles and solid lines. Control boys and girls are represented by open circles and solid lines. All graphs suggest a minimal difference between intervention and control boys and girls.

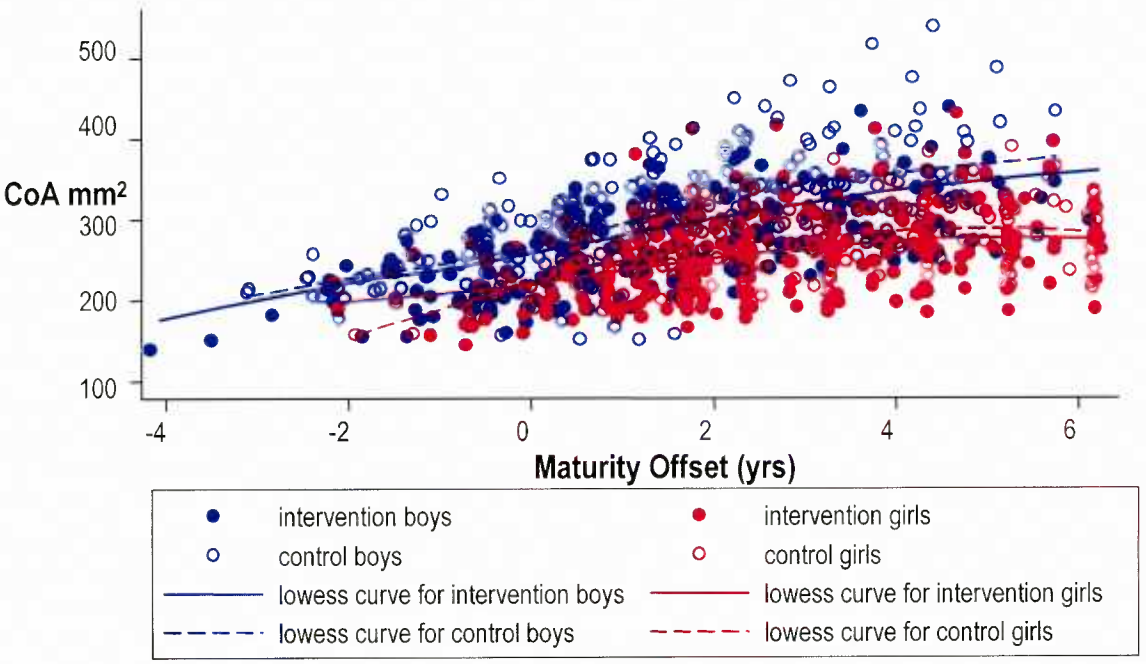

Figure 5-1 (b)

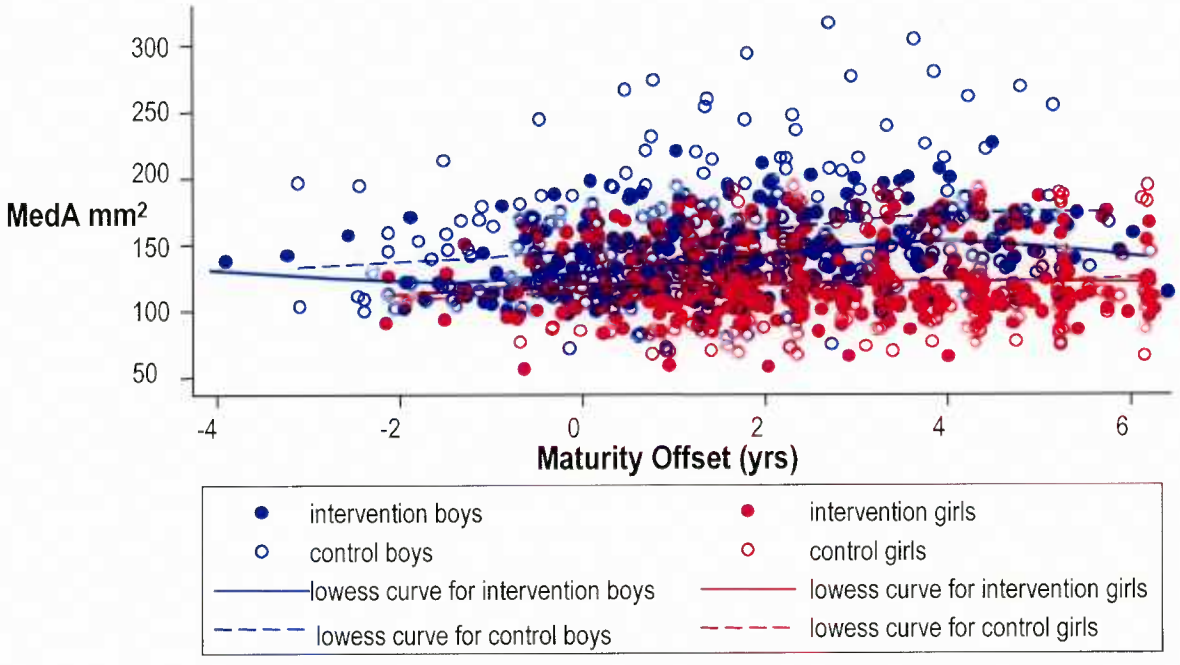

Figure 5-1 (c)

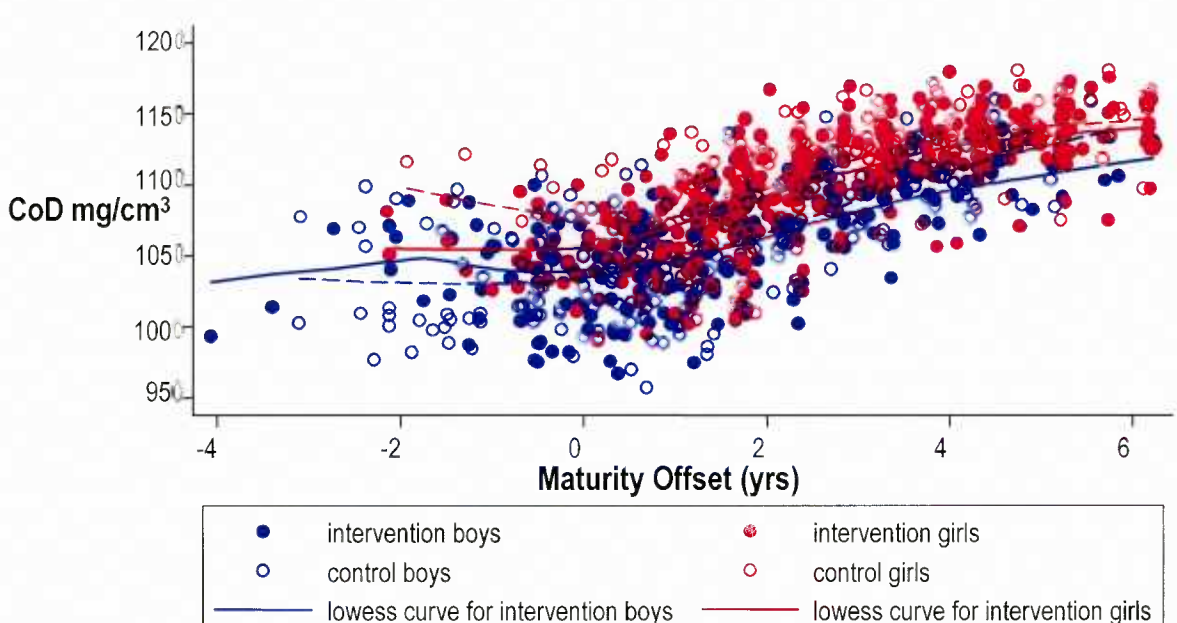

Figure 5-1 (d)

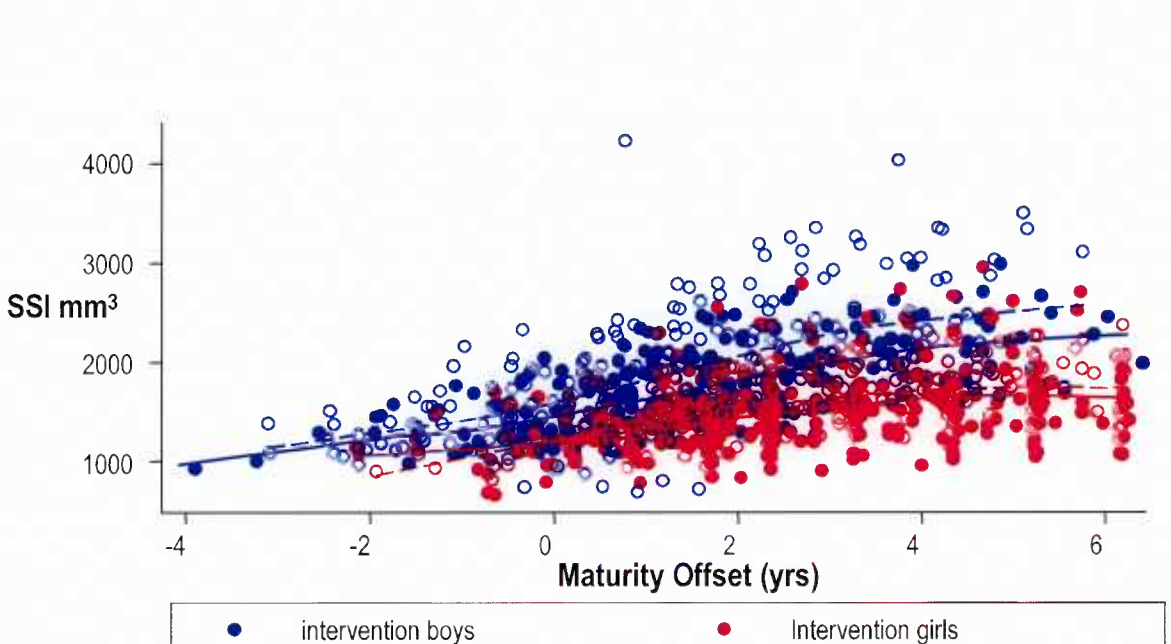

Figure 5-1 (e)

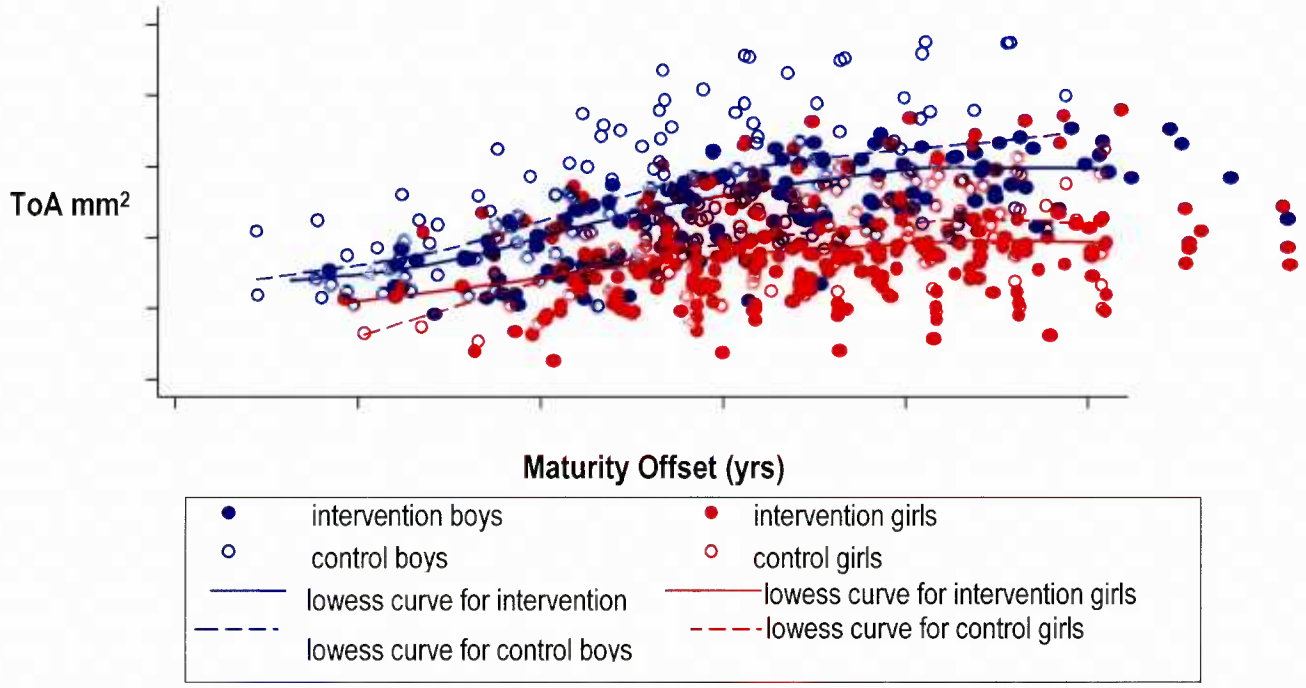

Figure 5-2 (a)

Figure 5-2: A comparison of intervention and control boys and girls with a maximum of 6 or minimum of 5 scans by maturity offset (years) for bone; a) total area (ToA, mm²), b) cortical area (CoA, mm²), c) medullary canal area (MedA, mm²), d) cortical density (CoD, mg/cm³), and d) strength-strain index (SSI, mm³). Boys are represented by blue circles and blue lines, girls by pink circles and pink lines. Intervention boys and girls are represented by closed circles and solid lines. Control boys and girls are represented by open circles and dashed lines. All graphs suggest a minimal difference between intervention and control boys and girls.

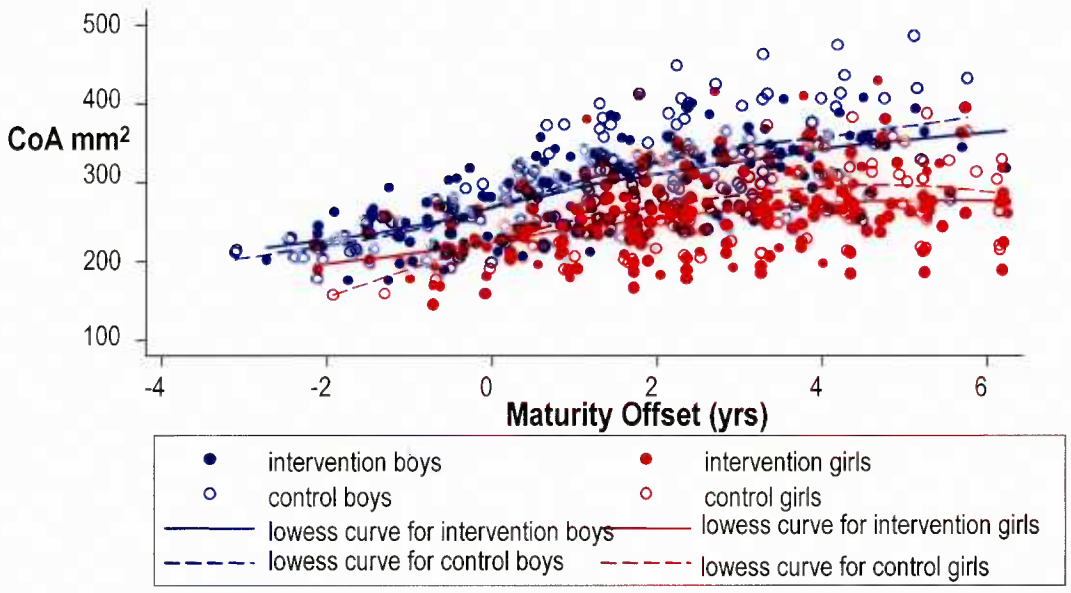

Figure 5-2 (b)

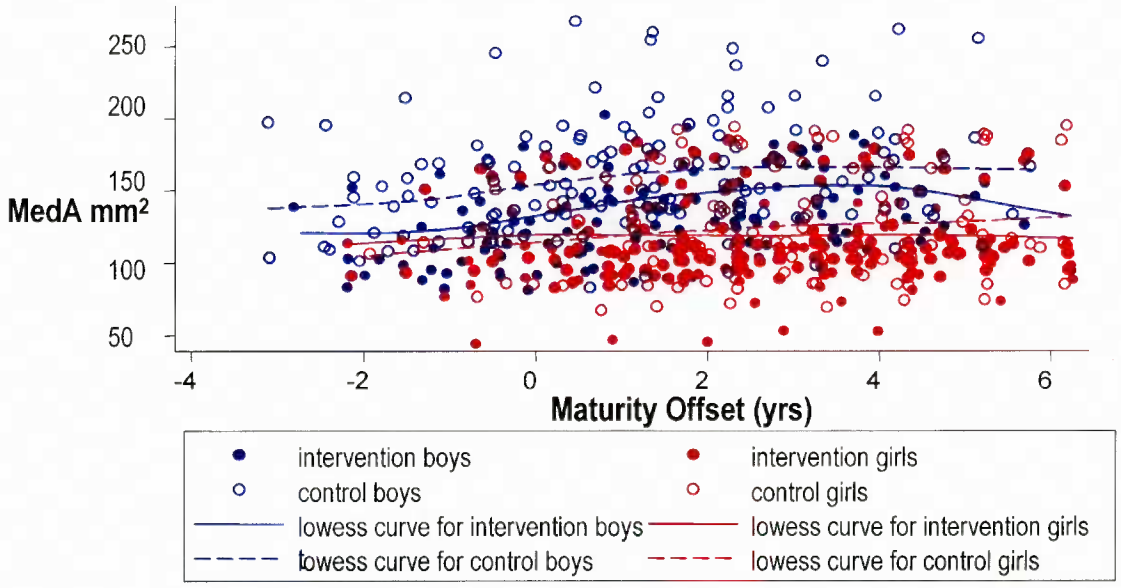

Figure 5-2 (c)

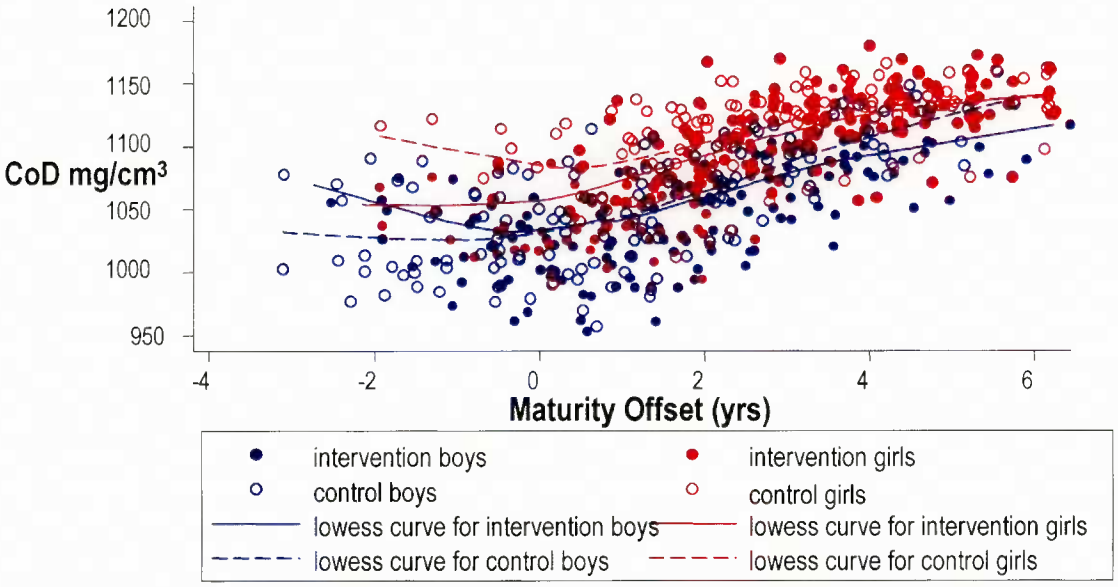

Figure 5-2 (d)

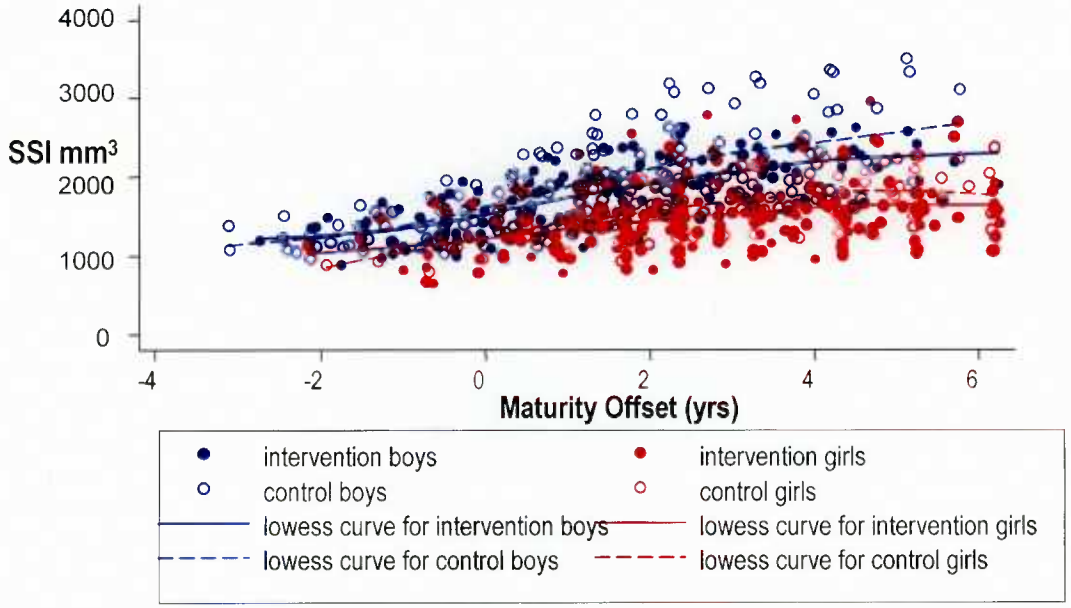

Figure 5-2 (e)

6 Age at Peak Height Velocity (APHV)

In this section, I describe the procedure that I used to determine APHV for my participants. In addition, I describe a predictive equation previously derived for the purpose of determining APHV for participants with a single measurement point and provide evidence to show why this equation cannot be used on my cohort.

6.1 Determination of APHV

APHV determination is a relatively easy, non-invasive method of aligning participants on a common maturational landmark. In this study, APHV was not derived from group data but rather individually determined. Each participant's measured height (cm) and exact chronological age was used to calculate their height velocity or height change since the last measurement. Participants' height velocity by their mean age from last two measures was then plotted using the GraphPad Prism software (Version 5.0). For the purpose of determining APHV, I used the software's scientific graphing and curve fitting capabilities to fit a cubic spline through all their data points. This software was chosen based on its ease of use, and the fact that it has been used previously to determine APHV (12). Cubic splines can be fitted to a minimum of 4 data points. Participants were separated by sex and ethnicity prior to employing the graphing procedure and all participants with ≥4 data points were fitted with a cubic spline. In order for a spline to be fitted to a number of data points, the program requires that a number of points that will define the curve (segments) be selected. The program applies a default of 40 segments. Based on my discussions with Professor (emeritus) Mirwald from the University of Saskatchewan who is a growth expert - I selected 250 data points to model the cubic spline curves.

A value (age) for APHV was calculated by the program software by identifying the greatest predicted velocity for height. I verified this value by visually assessing each curve and comparing the software-generated value to the age at peak velocity visible on each participant's graph. I present a sample of cubic spline curves for children whose age APHV was clearly identifiable in (Figure 6-1). I also present a sample of curves from which APHV was not discernible (Figure 6-2). For those participants with ≤3 measurements or those for whom peak velocity was not discernible (Figure 6-2), I initially aimed to use the Mirwald predictive equation (188) to determine APHV. I calculated APHV using the cubic spline procedure for 170 participants (90 girls, 80 boys) from which a baseline pQCT scan was obtained. I was unable to use this procedure for 13 participants (9 girls, 4 boys).

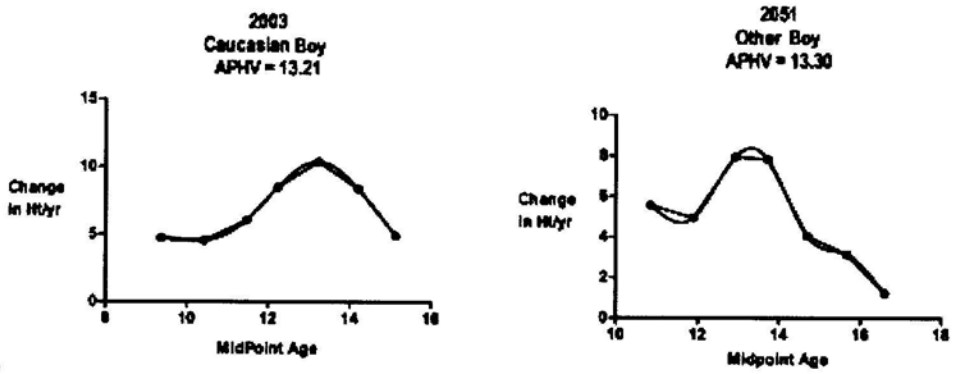

Figure 6-1: Examples of individualized cubic spline graphs with clearly identifiable peaks for a Caucasian and an Other boy. Each boy is a "normal" maturer and has reached APHV anywhere between ~13.0-13.5 years of age.

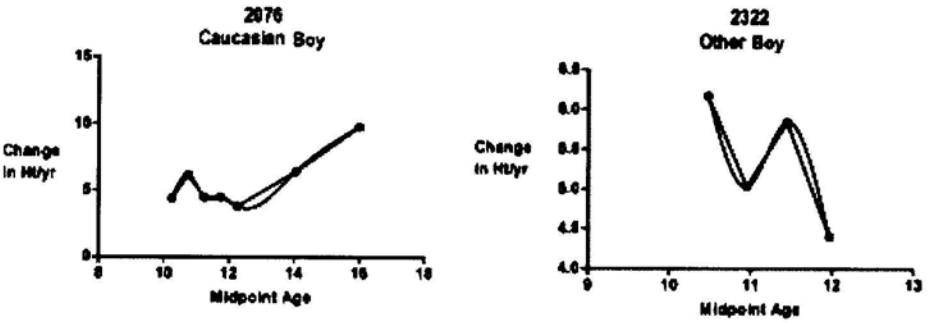

Figure 6-2: Examples of individualized cubic spline graphs where APHV cannot be determined for a Caucasian and an Other boy. From these graphs, it appears that the Caucasian boy on the left is a late maturer and has reached APHV at ~ 16 years of age or later whereas, the Other boy on the right may be an early maturer and may have reached APHV at ~ 10.5 years or earlier. He may also be a "normal" maturer and will reach APHV past 12 yrs of age. This can only be determined with additional years of measurement.

6.2 The Mirwald predictive equation

Sex dependent predictive equations were previously derived (188) to determine APHV when a limited number of measurements were available for a child or if clear peaks could not be discerned from the cubic spline graphs. These equations were validated using 2 separate studies and the R^2 shrinkage value was 0.03 or 3% for both boys and girls (188). This indicates a relatively small amount of shrinkage between the initial and comparative samples. However, the standard deviations ranged from 0.49 to 0.65 years in boys and 0.50 to 0.65 years in girls (188). To determine whether the predictive equation could be applied to my cohort, I compared the APHV values obtained using the cubic spline procedure on 206 participants for whom a clear peak was visible with the APHV values obtained using the prediction equation. Therefore, APHV derived using the cubic spline procedure served as the criterion for each participant. Results between procedures were inconsistent, with greater discrepancies observed for boys (Table 6-2 and Table 6-4). These discrepancies were ≥ +1 year for some participants and the greatest variability was noted for Asian boys (Table 6-4). The R^2 shrinkage value was 0.177 or 17.7 % for boys and 0.07 or 7% for girls. Tables comparing APHV values obtained from the cubic spline procedure and predictive equation at

Time 1 (Table 6-1 and Table 6-2) and Time 5 (Table 6-3 and Table 6-4) for all participants by sex and ethnicity are provided.

Table 6-1: Girls' mean (SD) age at peak height velocity (APHV) derived using the cubic spline procedure and from the Mirwald predictive equation at baseline.

Girls	N	APHV				N	APHV		
Cubic Spline		Mean (SD)	Minimum	Maximum	Pred.Eq'n		Mean (SD)	Minimum	Maximum
Total N	107					107			
Asian	34	11.2 (1.0)	9.6	14.1		34	11.7 (0.5)	10.6	12.6
Caucasian	58	11.4 (0.7)	9.3	12.9		58	11.7 (0.7)	10.7	15.7
Other	15	11.5 (1.3)	10.1	13.7		15	11.7 (0.6)	10.7	12.8

Table 6-2: Boys' mean (SD) age at peak height velocity (APHV) derived using the cubic spline procedure and from the Mirwald predictive equation at baseline.

Boys	N	APHV				N	APHV		
Cubic Spline		Mean (SD)	Minimum	Maximum	Pred.Eq'n		Mean (SD)	Minimum	Maximum
Total N	99					99			
Asian	34	12.3 (1.1)	10.5	15.8		34	13.2 (0.5)	12.1	14.0
Caucasian	51	13.0 (1.5)	9.8	17.0		51	13.2 (0.5)	12.1	14.2
Other	14	12.5 (1.0)	10.5	14.2		14	13.0 (0.4)	12.2	13.5

Table 6-3: Girls' mean (SD) age at peak height velocity (APHV) derived using the cubic spline procedure and from the Mirwald predictive equation at measurement occasion 5.

Girls	N	APHV				N	APHV		
Cubic Spline		Mean (SD)	Minimum	Maximum	Pred.Eq'n		Mean (SD)	Minimum	Maximum
Total N	90					99			
Asian	30	11.2 (1.0)	9.6	14.1		34	11.9 (0.5)	10.9	13.1
Caucasian	48	11.4 (0.7)	9.3	13.0		51	11.9 (0.8)	10.5	16.5
Other	12	11.5 (1.3)	10.1	13.6		19	11.8 (0.6)	10.9	12.7

Table 6-4: Boys' mean (SD) age at peak height velocity (APHV) derived using the cubic spline procedure and from the Mirwald predictive equation at measurement occasion 5.

Boys	N	APHV				N	APHV		
Cubic Spline		Mean (SD)	Minimum	Maximum	Pred.Eq'n		Mean (SD)	Minimum	Maximum
Total N	80					84			
Asian	28	12.1 (0.8)	10.9	14.4		32	13.5 (0.6)	12.4	14.7
Caucasian	41	12.7 (1.3)	9.8	16.0		41	13.6 (0.5)	12.4	15.1
Other	11	12.7 (1.1)	10.5	14.2		11	13.6 (0.4)	12.9	14.2

The predictive equation was designed as a surrogate to estimate APHV for children for whom longitudinal height measures across the age of PHV were not available. However, the discrepancies between predicted values and those obtained from the cubic spline procedure were substantial in my cohort. There are numerous possibilities that might explain these differences. First, measures of height, weight, sitting height, and leg length used to derive the prediction equation were from Caucasian boys and girls living in Saskatchewan. The equation was then validated on, and adjusted against another Caucasian cohort living in Belgium (188). Thus, the equation does not account for possible ethnic differences. This results in a cohort effect as 34% of my cohort were Asian. Sex by ethnicity cumulative distribution plots of the HBS cohort provides evidence for between and within group differences in the pattern by which all (100%) participants reached APHV. Ethnic differences in the final APHV within each sex is apparent, more so for girls than boys (Figure 6-3 and Figure 6-4).

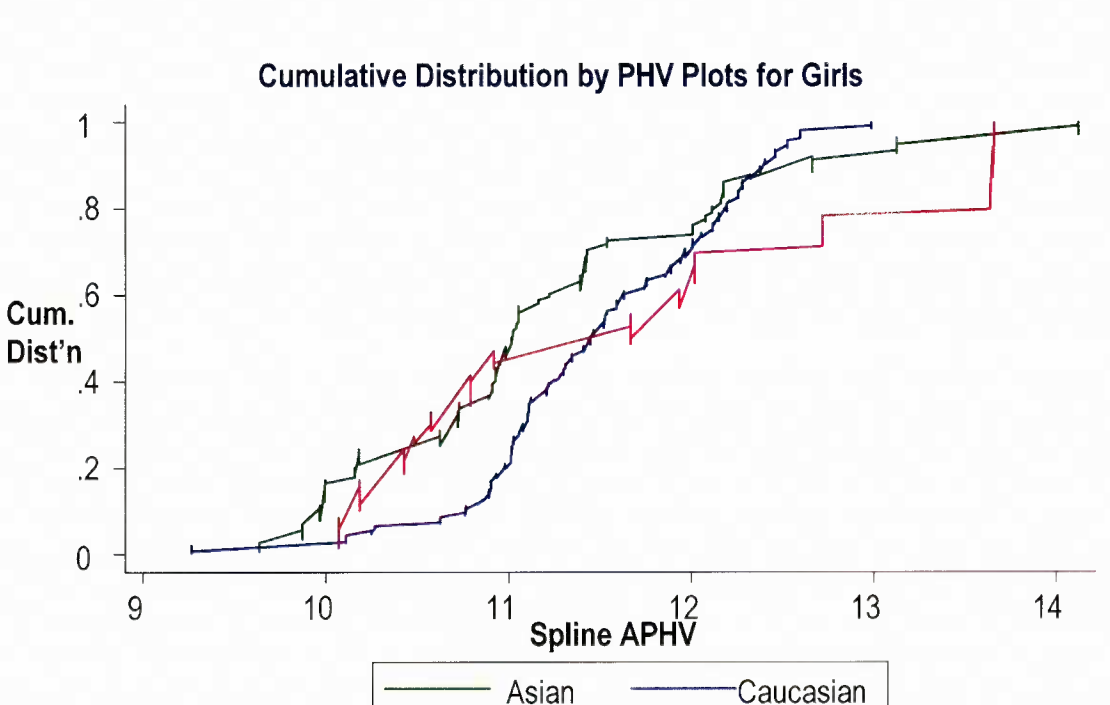

Girls by Ethnic Distribution

Figure 6-3: Cumulative distribution plots showing ethnic differences in the pattern and overall age that PHV is attained in girls.

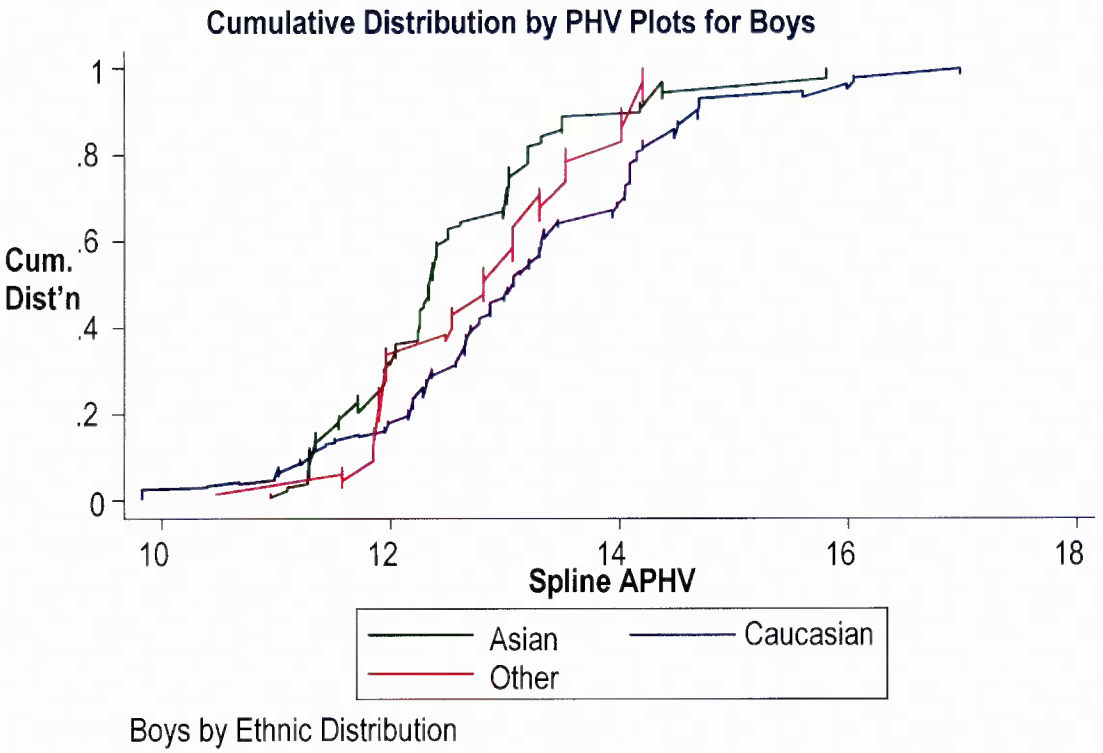

Figure 6-4: Cumulative distribution plots showing ethnic differences in the pattern and overall age that PHV is attained in boys.

The Mirwald predictive equation was derived from the U of S study participants whose APHV was 11.77 years for girls on average whereas, boys reached PHV at a mean age of 13.44 years (12). Thus, it comes to no surprise that the cubic spline generated values were similar to those obtained using the Mirwald predictive equation as this was the same cohort from which the equation was derived. However, these values differed significantly from the HBS cohort (Table 6-3 and Table 6-4) represented in this thesis.

I used the Bland-Altman procedure to verify whether the Mirwald equation could be used to predict APHV in the HBS cohort. These plots showed a linear deviation from the criterion APHV (Figure 6-5). Therefore, the predictive equation overestimated APHV if the participants had not reached PHV and underestimated it if they had reached PHV. Not surprisingly, the equation worked best when the participants' were close to age APHV. This same pattern is noted in the sex by ethnicity Bland-Altman plots (Figure 6-6). Taken together, these plots that represent the difference between predicted and actual values, suggest a systematic bias in the prediction equation. This is partly explained by the fact that the HBS cohort was younger than participants in both the derivation and validation cohorts. Further, these cohorts had maturity offset values ranging from -4 to +4, whereas, maturity offset ranged from -5 years to +5 in the HBS cohort. As many of the participants in the HBS were further away from actual APHV, the predictive equation is less likely to perform well. Malina et al., conducted a similar verification study using data from 15 Belgian female gymnasts (6.0-17.6 years of age) whom were measured annually for 6 years (166). These participants underwent vigorous training for 15 hours/week, on average (range 9-19 hours/week) for 6-7 years (166). APHV was

substantially later (12.9 ± 1.5 years) compared with recreationally active children as in the present study (166). Ideally, predictive equations should be specific to the population to whom they are being applied. For example, participants of "normal" stature do not demonstrate the same timing or relatively smaller magnitude of growth seen most often in competitive gymnasts (166) or other athletic groups who mature later (130).

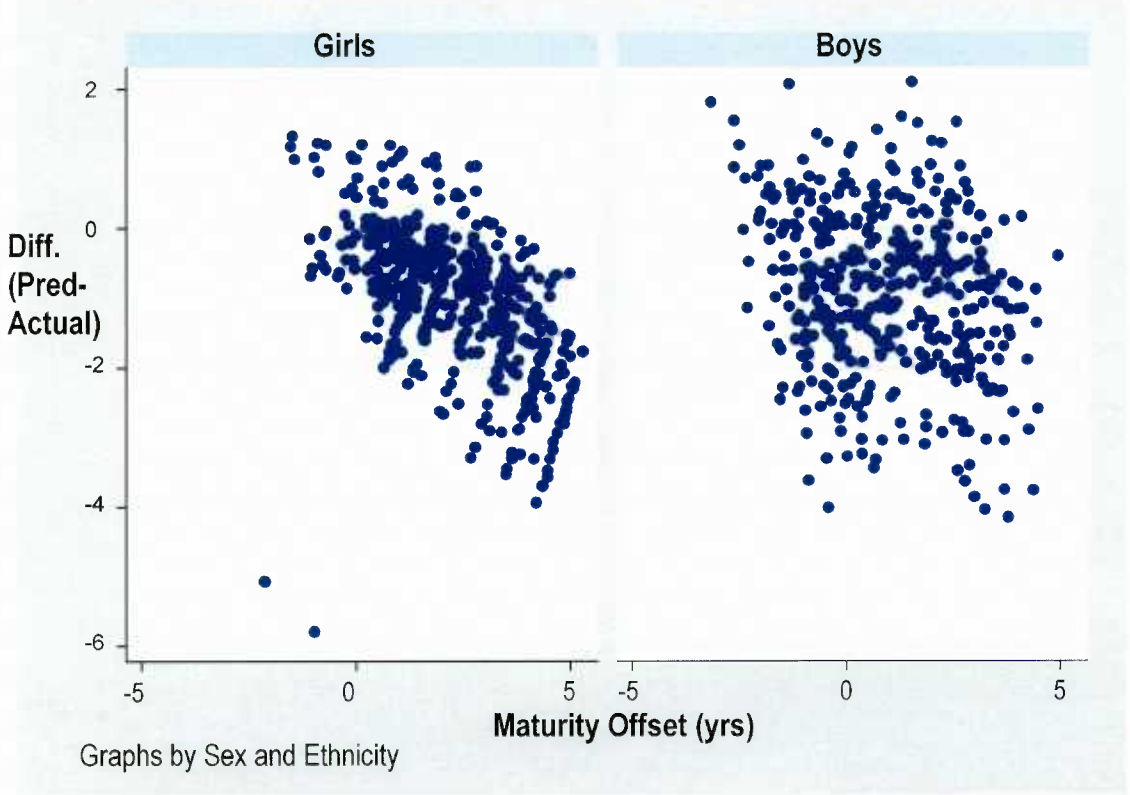

Figure 6-5: Bland-Altman procedure applied to Healthy Bones Study boys and girls. The y-axis represents the difference (Predicted years from PHV-Actual years from PHV) and the x-axis represents the calculated maturity offset (APHV-chronological age at time of measurement). Negative difference scores imply an overestimation whereas, positive scores imply an underestimation of age at maturity offset compared with those determined from the cubic spline curve-fitting procedure.

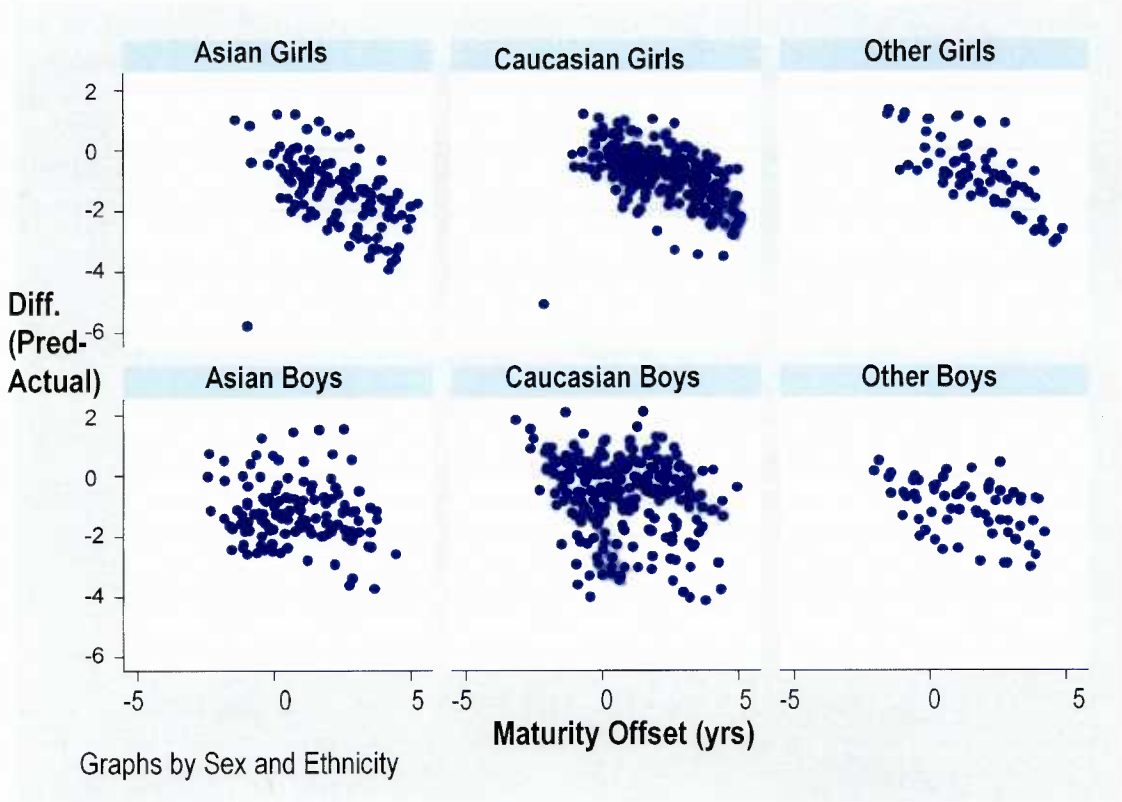

Figure 6-6: Sex by Ethnicity Bland-Altman procedure applied to Healthy Bones Study participants. The y-axis represents the difference (Predicted years from PHV-Actual years from PHV) and the x-axis represents the calculated maturity offset (APHV-chronological age at time of measurement). Negative difference scores imply an overestimation whereas, positive scores imply an underestimation of age at maturity offset compared with those determined from the cubic spline curve fitting procedure.

Lastly the Mirwald equation may have limited generalizability as it was derived from participants who were measured ~ 15 years ago and validated on participants measured ~43 years ago (188). Secular trends for patterns of linear growth have been well documented (57, 260). Specifically, height velocity has been reported to increase by 10-30 mm per decade, on average (57, 112); the greatest increases occurring in the 1960s and 1990s (236). The same trends were reported for weight. However, there is a secular trend for a *younger* age at menarche (57). The well known individual variation in the timing and tempo of growth also contributes to prediction error (166). Based on the large variability between cohorts, the Mirwald equation was not used for the current thesis. Therefore, the 13 participants for whom I was unable to discern APHV using the cubic spline procedure were excluded from the analysis.

7 Analyzing Longitudinal Data

In a longitudinal study individuals are measured repeatedly across time. As mentioned previously, most standard statistical techniques, for example, simple linear regression and the unpaired t-test, assume that each of the observations that make up a dataset are independent of each other. This assumption is inappropriate if repeated measurements are taken within individuals because observations within an individual tend to be correlated with one another. One approach to solve this problem is to create a summary statistic for each individual (177). An alternate approach is to explicitly model the correlation. Two methods commonly employed are marginal models, often referred to as generalized estimating equations (GEE), and multilevel models (37). In this section, I will discuss and compare the summary model and the multilevel modeling methods of analyzing longitudinal data. In addition, I will discuss the strengths and weaknesses of these two approaches.

7.1 Summary Measures Model

Prior to modeling the data, I first examined plots of area, density and strength versus age for each participant regardless of number of scans to determine if placing a straight line through the data points was reasonable. As I visually determined this to be reasonable, I proceeded by conducting a summary measures model (Figure 7-1). The choice of summary measure depends on the research question of interest. In this analysis of bone measurements over time we were interested in comparing the growth curves for boys and girls, thus, a natural summary measure would be the slope of the growth curve. A slope could be estimated for each individual and then compared across the sexes using a univariate statistical technique (e.g. t-test or Wilcoxon test). This method is illustrated using the outcome measure Medullary Canal Area (MedA).

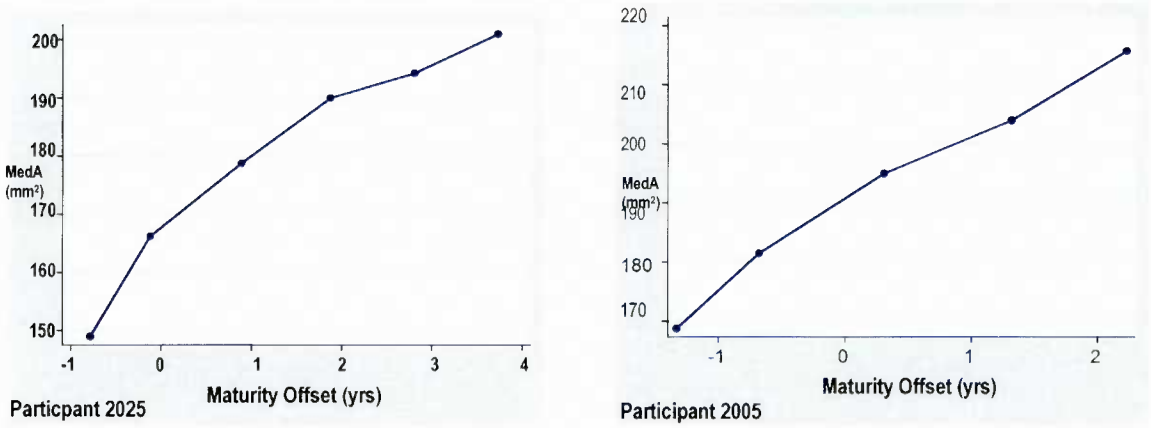

Figure 7-1: Example of medullary canal area by maturity offset plots for 2 boys randomly chosen with ≥ 5 data points. Data points were plotted for each participant in the study. It appears that a straight line is a reasonable representation over the maturity offset range.

For each participant a linear regression model was fitted,

Regression equation: $Y_{ki} = \beta_{0k} + \beta_{1k} X_{ki} + \varepsilon_{ki}$

$k=1...K$ where K is the number of participants

$i=1...nk$ where n_k is the number of observations for the k^{th} participant

β_{0k}= the intercept for the k^{th} participant

β_{1k}= the slope for the k^{th} participant

Y_{ki}= the i^{th} observation of the dependent variable (bone outcome) for the k^{th} participant

X_{ki}= the i^{th} observation of the independent variable (maturity offset) for the k^{th} participant

ε_{ki}= the residual error for each observation, $\varepsilon_{ki} \sim N(0, \sigma_k^2)$

Table 7-1 provides descriptive statistics for the MedA slopes by sex, Figure 7-2 provides a graphical summary. A two-sample t-test was used to compare the average slope between sexes (Table 7-1). On average boys had a larger MedA slope than girls, 12.2 mm^2 vs 2.5 mm^2; difference = -9.8 mm^2 in favor of boys (95%CI: -13.1 to -6.5). We note that the standard deviation and thus confidence interval values for the slopes was larger for boys than girls. This violates one of the underlying assumptions of the two-sample t-test (homogeneity of variance). However, the t-test is robust to departures from the assumption of equal variance when sample sizes are roughly the same and thus the inference remains valid (222). In addition, based on Garn's hypothesis, it is also biologically possible for both boys and girls to have a negative slope with a greater magnitude observed in girls as this would indicate significant endosteal apposition and closure of the medullary canal (Table 7-1)

The summary measures approach is simple and statistically valid but may not be fully efficient (177). As is often the case, the data collected in this study are not balanced. In a balanced design each individual would have the same number of measurements made at exactly the same time. Here we have between 1 and 6 measurements for each individual (Table 7-2) and the time between measurements is highly variable. The unbalanced nature of the data

indicates that each estimated slope has a different variance which should be taken into account in the analysis when combining the slopes to estimate the grand mean (Figure 7-2). However, the variances are not easily estimated as they are a function of the pattern of measurement times, the correlation between the measurements, and the number of measurements (79). We next consider a model which makes full use of the all data.

Table 7-1: Two sample t-test comparison of estimated medullary canal area slopes by sex.

Group	N	Mean	SD	Range	95% CI$^{\Psi}$
Girls	106	2.5	4.6	–14.9-30.0	1.6 - 3.3
Boys	94	12.2	16.5	-26.9-49.4	8.9 - 15.6
Difference (boys-girls)	-	-9.8	-	-	-13.1 - -6.5

Ψ CI = Confidence Interval

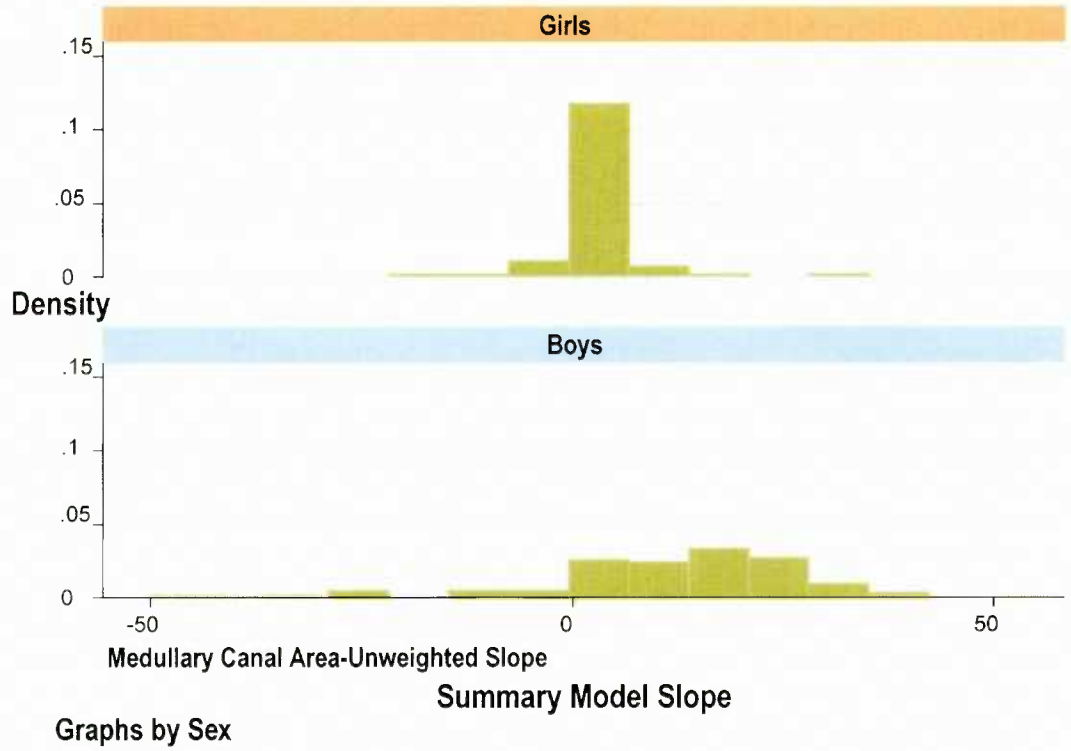

Figure 7-2: Histograms depicting sex differences in medullary canal area slope. The y-axis consists of density which is used to scale the height of the histogram bars so that the sum of their areas does not exceed the value 1. The x-axis represents the variability in the slopes. The histograms clearly depict the fact that boys have greater variability (lower graph) than girls (upper graph).

Table 7-2: Distribution of total number of measurements for each participant. A total of 98 participants (49%) have attained ≥ 5 scans.

Total No. of Scans	Frequency	Percent (%)	Cumulative Percent
6	86	43.0	43.00
5	12	6.0	49.00
4	40	20.0	69.00
3	16	8.0	77.00
2	44	22.0	99.00
1	2	1.0	100.0

7.2 Multilevel Modeling

The second form of analysis utilized a mixed linear model or MLM to compare the rate of change for selected bone outcomes between the sexes. The data are comprised of repeated measures made on a group of individuals that are said to have a hierarchical structure. These repeated measures are unique to that individual and are related to each other. The MLM was comprised of two levels. Level 1 consisted of repeated measurements within participants and level 2 consisted of measurements between participants (sex). In its simplest form, the multilevel framework allows an individual to have his or her own slope and intercept similar to traditional analysis of covariance. By allowing for variation in both intercepts and slopes within individuals, growth velocities can also vary between individuals. These models are known as random effects models. I provide an illustration of a random effects model below using MedA as the outcome.

Multilevel model equation: $Y_{ki} = (\beta_{0k} + u_k) + X_{ki}(\beta_1 + v_k) + \varepsilon_{ki}$

$k=1...K$ where k is the number of participants

$i=1...n_k$ where n_k is the number of observations for the k^{th} participant

β_{0k}= the intercept for the k^{th} participant

β_{1k}= the slope for the k^{th} participant

Y_i= the i^{th} observation of the dependent variable (bone outcome) for the k^{th} participant

X_i= the i^{th} observation of the independent variable (maturity offset) for the k^{th} participant

u_k= the random effect (intercept) for individual k, $u_k \sim N(0, \sigma_u^2)$

v_k= the random effect (slope) for individual k, $v_k \sim N(0, \sigma_v^2)$

ε_{ki}= the residual error between participants, $\varepsilon_{ki} \sim N(0, \sigma_k^2)$

Results for this mixed linear model are provided (Table 7-3). The output for MedA is obtained from the mixed-effects regression equation which is used to determine the MedA value at a specific maturity offset for a participant.

Table 7-3: Results for the mixed linear model depicting mean difference for change in medullary canal area (MedA) by sex.

MedA	Coefficient	Standard Error	95% CI$^{\Psi}$
Maturity Offset by Sex Interaction	6.4	0.4	5.6-7.1
Intercept	116.6	3.9	109.9-123.2
Maturity Offset	1.9	0.3	1.4-2.4
Sex	17.6	4.9	8.0-27.1
SD (Residual)	8.2	0.2	7.7-8.6

Ψ CI = Confidence Interval

Example Equation: Expected (Y_{ki}) = ($\beta_1 + \beta_2 x\ Sex_{ki}$) + ($\beta_3 x$ Maturity $Offset_{ki}$) + ($\beta 4 x$ Maturity $Offset_{ki} x\ Sex_{ki}$)

Bone Outcome Variable: Average MedA= (116.6 +17.6 x Sex*) + [1.9 (Maturity Offset)] + [6.4 (Maturity Offset x Sex)]

At Maturity Offset = X:

Girls MedA= [116.6 + 17.6 (0)] + (1.9 +6.4 (0)) X

Girls MedA= 116.6 + 1.9 X

Boys MedA= [116.6 +17.6 (1)] + (1.9 +6.4 (1)) X

Boys MedA= (116.6 + 17.6) + (1.9 +6.4) X

* girls=0; boys=1

This equation suggests that, when compared with girls, boys on average have a 17.6 mm^2 greater mean MedA at maturity offset = X. The estimated slope or constant rate of change for response per year increase in maturational age is $\hat{\beta}_3$ = 1.9 mm^2/yr for girls. The estimated slope for boys is ($\hat{\beta}_3 + \hat{\beta}_4$) = 8.3 mm^2/yr. Thus $\hat{\beta}_4$ is an estimate of the difference in slopes between girls and boys. Therefore, for every increment increase in maturity offset, boys' rate of change in MedA is 6.4mm^2 greater than in girls. This difference is shown in (Figure 7-3).

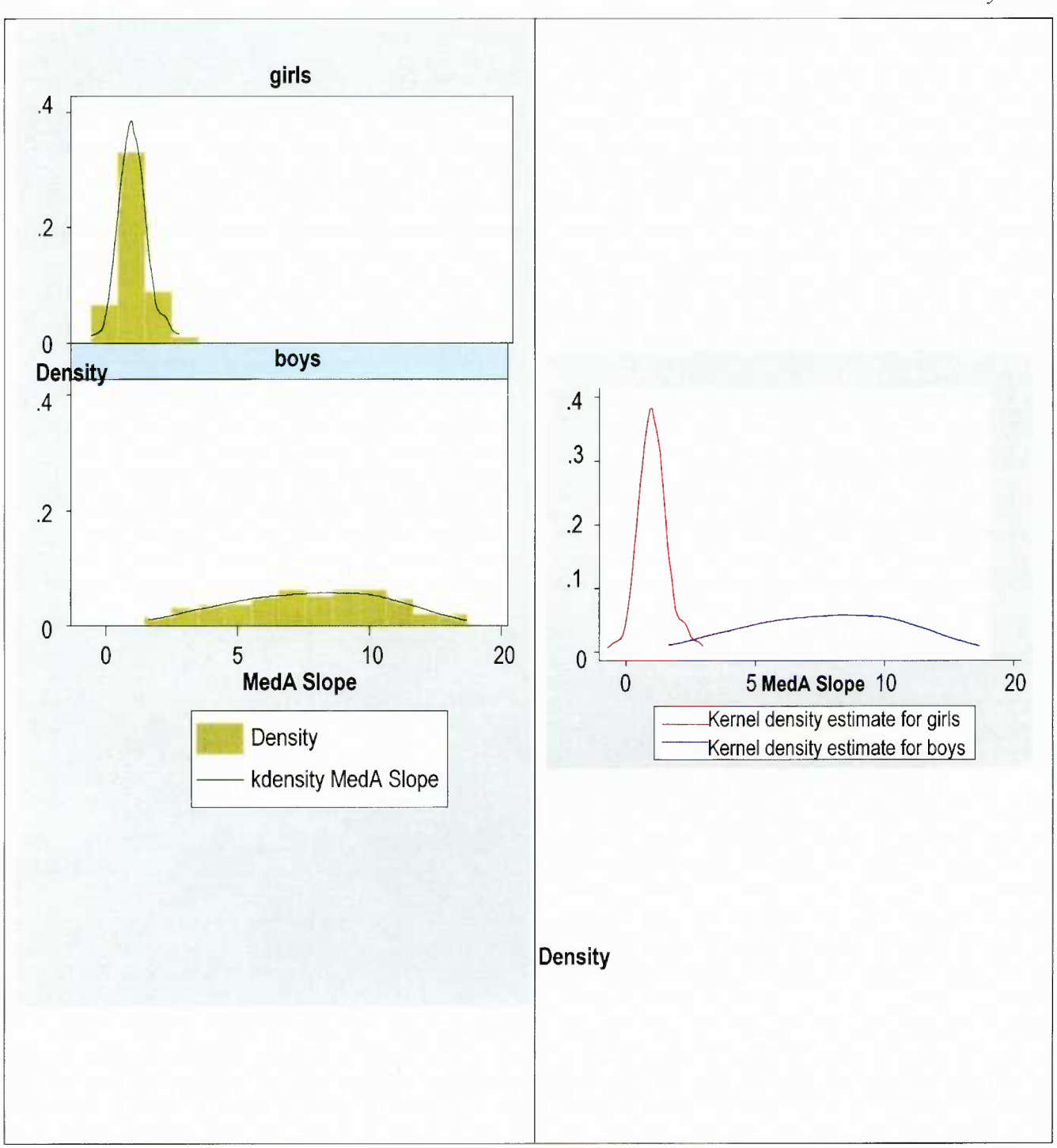

Figure 7-3: A comparison of boys and girls for change in bone for medullary canal area (MedA). The histograms on the left hand depict slope values for boys (top) and girls (bottom). A kernel density (kdensity) line is placed over the histograms to effectively show the distribution of each bone outcome variable. The graphs on the right show that boys (in blue) had significantly greater mean values ($p<0.001$) and greater variability compared with girls (in pink) for change at this site.

7.3 Comparisons between the Summary Model and the Multilevel Model

Comparison of MedA slope values from the two sample t-test and mixed model comparisons showed in both cases that boys exhibited greater rates of increase in MedA than did girls (Table 7-4). The MLM provides a greater efficiency than the summary model as the standard error is smaller-- resulting in a narrower confidence interval (Table 7-4). The multilevel approach has a number of other advantages compared with conventionally used statistical analyses (refer to *section 2.6.1)*. First, equally spaced measurement occasions for each participant and balanced data are not required. In the current study, individuals were measured at somewhat irregular intervals and some participants were measured on every occasion (6 measures) and some only twice. Thus, fitting a separate model to each of these individuals will result in unreliable estimates. A more precise model is developed by using information from the sample with complete data points. However, this would involve removing all individuals who do not have complete data during analysis. Second; multilevel modeling allows any pattern of repeated measures and will provide statistically efficient parameter estimates for missing data. The model can achieve this because the estimated coefficient for an individual is a weighted average of the average for the sample and the individual's ordinary least squares (OLS) estimate. In other words, the slope and intercepts calculated from the population data are used to pull or "shrink" towards the grand mean, the slope and intercept values of those subjects who had fewer data points (Figure 7-4). Those subjects with complete data points undergo less "shrinkage" than those subjects with fewer data points. This is illustrated for MedA (Figure 7-5). If a summary model were developed for participants with complete and balanced data this model would produce results identical to those obtained from a MLM. The mathematics for shrinkage (79) is beyond the scope of this thesis and as such has not been presented.

Table 7-4: A comparison of the difference between slope values for boys and girls obtained by two statistical analysis methods (summary model and multilevel model). The weighting of the slope values is apparent in the multilevel model method as the difference in slopes between boys and girls is smaller and the confidence intervals are tighter compared with the summary model.

Medullary Canal Area	Total N	Mean	SD	95% CI$^{\Psi}$
Summary Model Difference*	200	-9.8	1.7	-13- -6.5
Multilevel Model Difference*	202	-6.4	0.4	-7.1- -5.6

* boys>girls

$^{\Psi}$CI= Confidence Interval

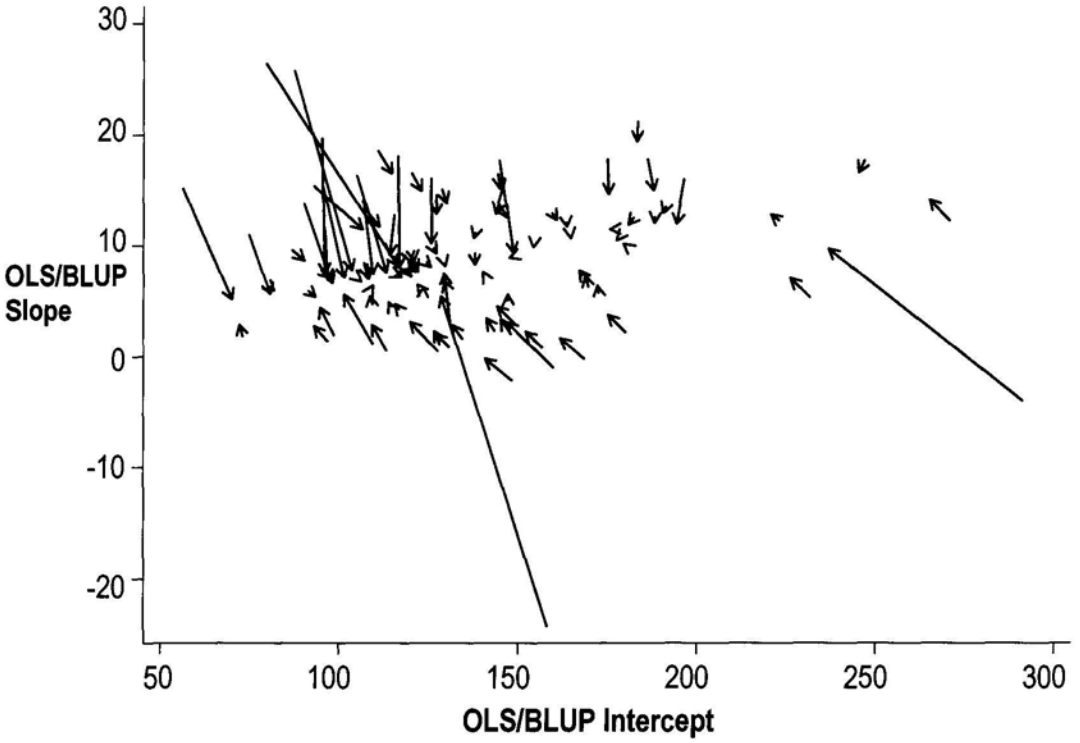

Figure 7-4: The graph depicts boys' ordinary least squares/best linear unbiased predictor (OLS/BLUP) slope by OLS/BLUP intercept for medullary canal area. The vector is created by 4 points. It starts at OLS intercept/slope and ends at BLUP intercept/slope. Thus, longer arrows depict greater "shrinkage" towards the mean slope value of zero.

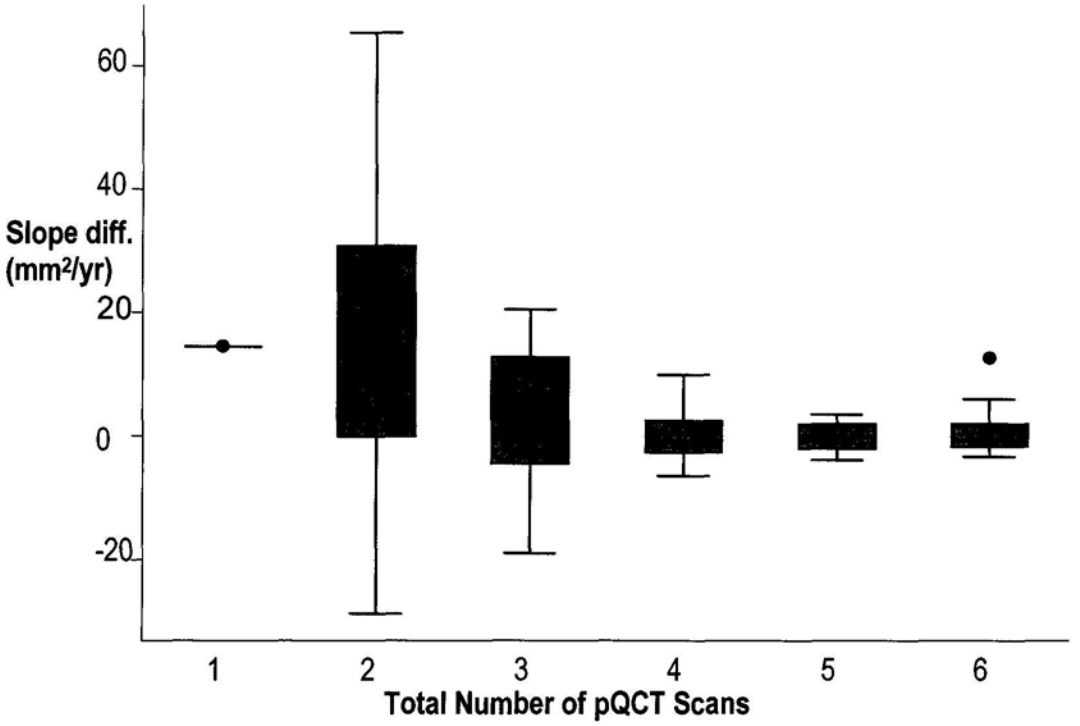

Figure 7-5: Box plots for differences in slope for medullary canal area (MedA) based on total number of scans for boys. As the number of scans measures increased the amount of shrinkage declined. The greatest amount of shrinkage is observed for those participants with 2 scans followed by those with 3 scans.

8 Results

In this chapter, I present the findings from this study, beginning with mean comparisons of sex-specific changes at each bone outcome variable while controlling for maturity offset for each participant. I will then provide the results from the MLM which examined the sex-specific changes at each bone parameter.

8.1 Bone Parameters by Maturity for Boys and Girls

Bone parameters for boys and girls are provided (Table 8-1). For almost all measured variables (ToA, CoA, MedA, SSI) boys' mean intercept values were significantly greater than those of girls, $p<0001$. The exception was CoD where girls had significantly greater values than boys, $p<0.001$. These differences are depicted in the scatterplots with lowess curves (Figure 8-1 (a-e)). These scatterplots compare boys and girls for each bone outcome variable aligned by maturity offset. These plots represent the raw data for each individual – prior to statistical modeling.

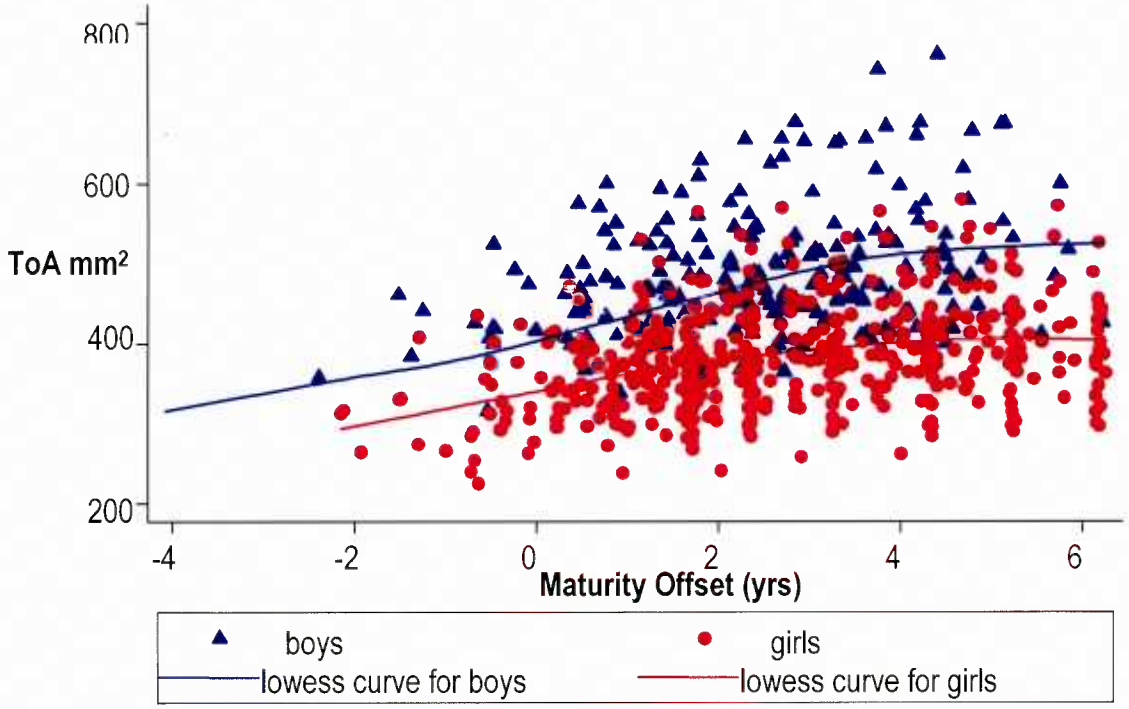

Figure 8-1 (a)

Figure 8-1: A comparison of boys and girls by maturity offset (years) for bone; a) total area (ToA, mm^2), b) cortical area (CoA, mm^2), c) medullary canal area (MedA, mm^2), d) cortical density (CoD, mg/cm^3), and e) strength-strain index (SSI, mm^3). Boys are represented by blue triangles and a blue lowess curve, girls by pink circles and a pink lowess curve. Boys had significantly greater mean values ($p<0.001$) compared with girls for all outcomes except for CoD which was significantly greater for girls compared with boys ($p<0.001$).

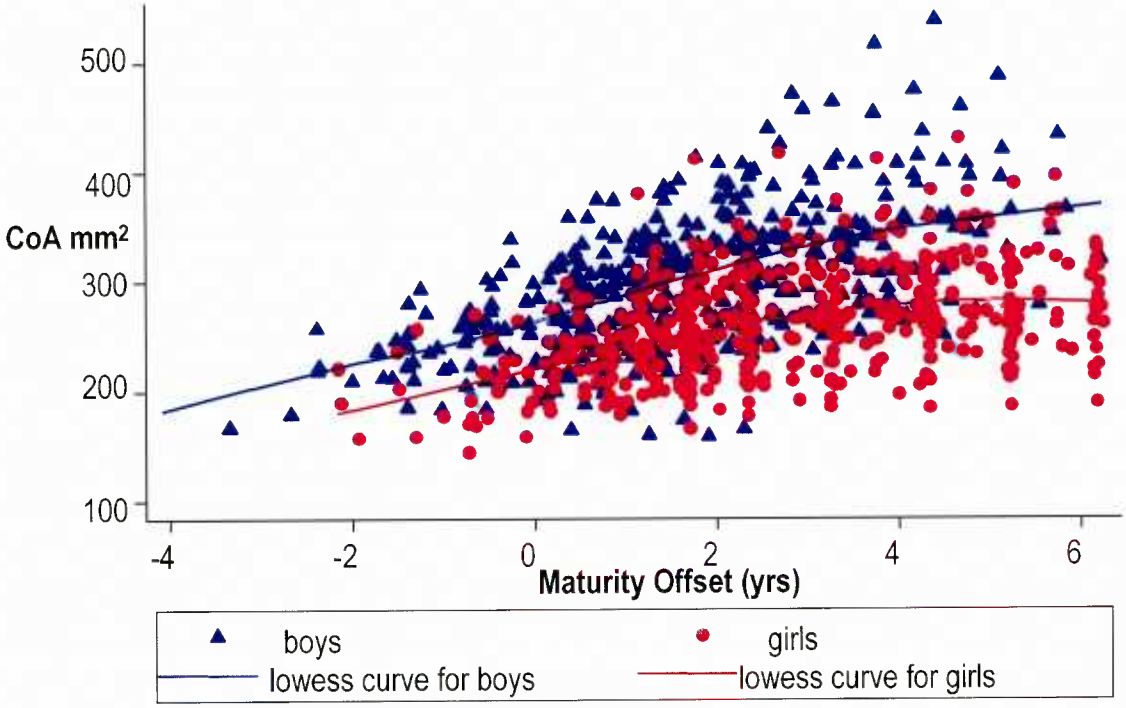

Figure 8-1 (b)

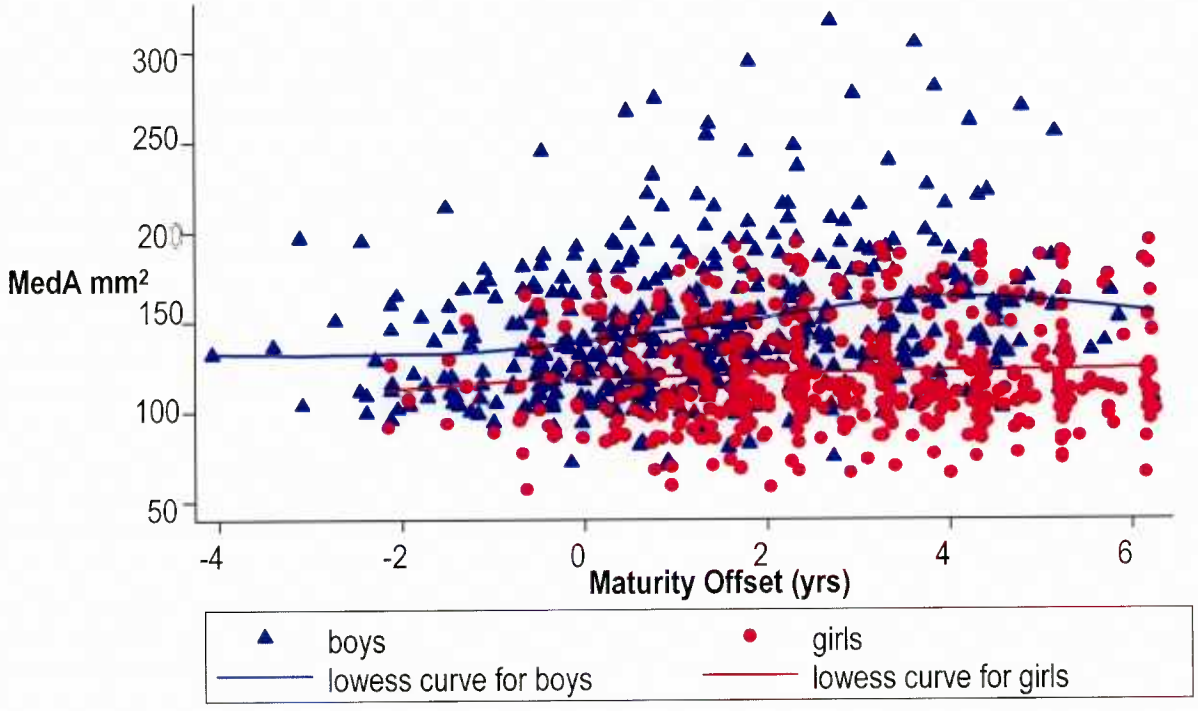

Figure 8-1 (c)

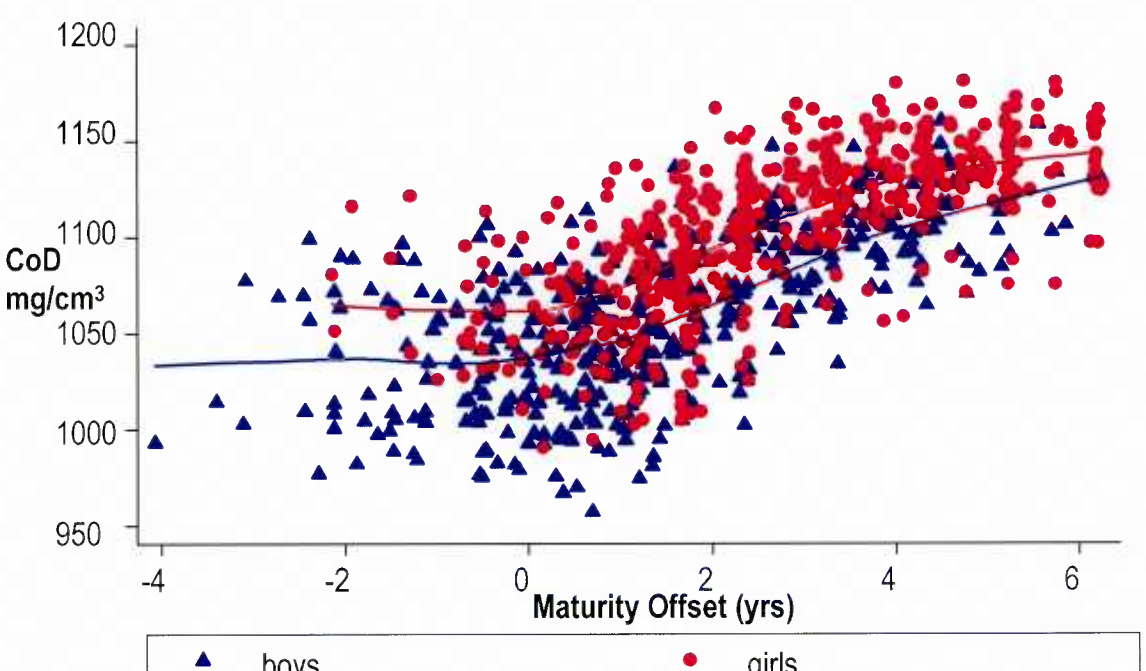

Figure 8-1 (d)

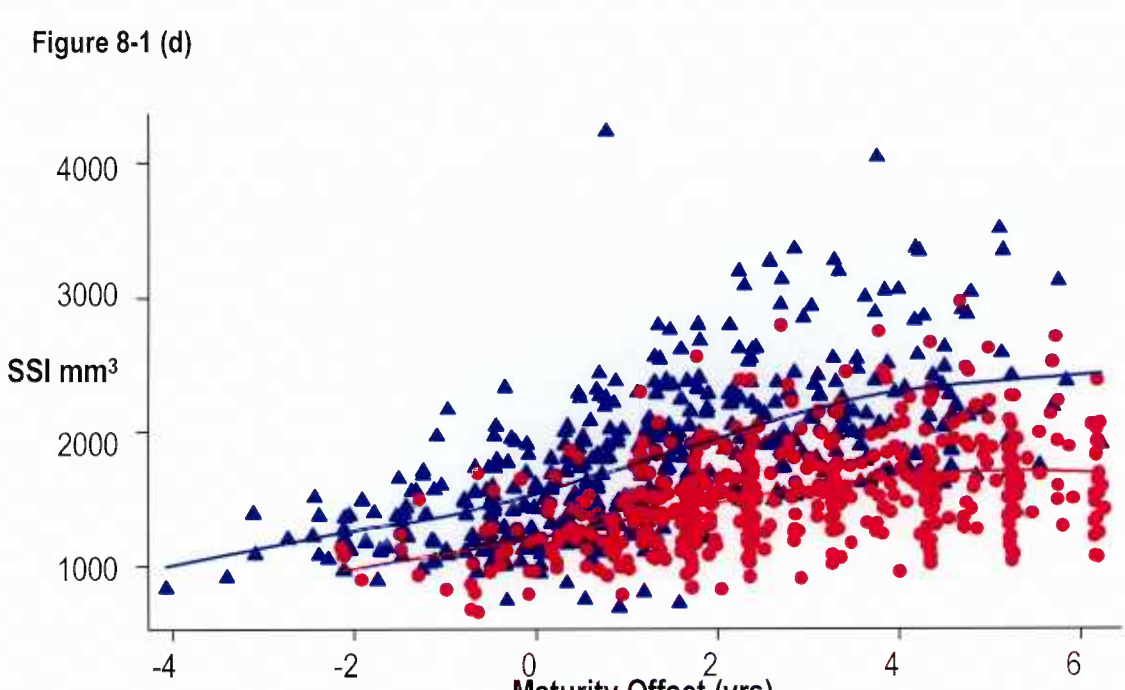

Figure 8-1 (e)

8.2 Sex-Specific Comparisons of Slopes For each Bone Parameter

Figure 8-2 and Table 8-1 show sex-specific comparisons of the mean rates of change for each bone outcome variable aligned by maturity offset for each participant. The results show that boys have a significantly greater slope when compared to girls at the ToA, CoA, MedA, and SSI sites, $p<0.001$ (Table 8-1). This coincides with the graphs of the raw values at these sites (Figure 8-1). At the CoD site, there is no significant difference in the rate of change or slope between the sexes, $p=0.904$ (Table 8-1). This is apparent when viewing Figure 8-1 and Figure 8-2. The magnitude of the difference in slopes between boys and girls was calculated to be 60.8% for ToA, 55.7% for CoA, 75.6% for MedA, 1.3% for CoD, and 54.7% for SSI.

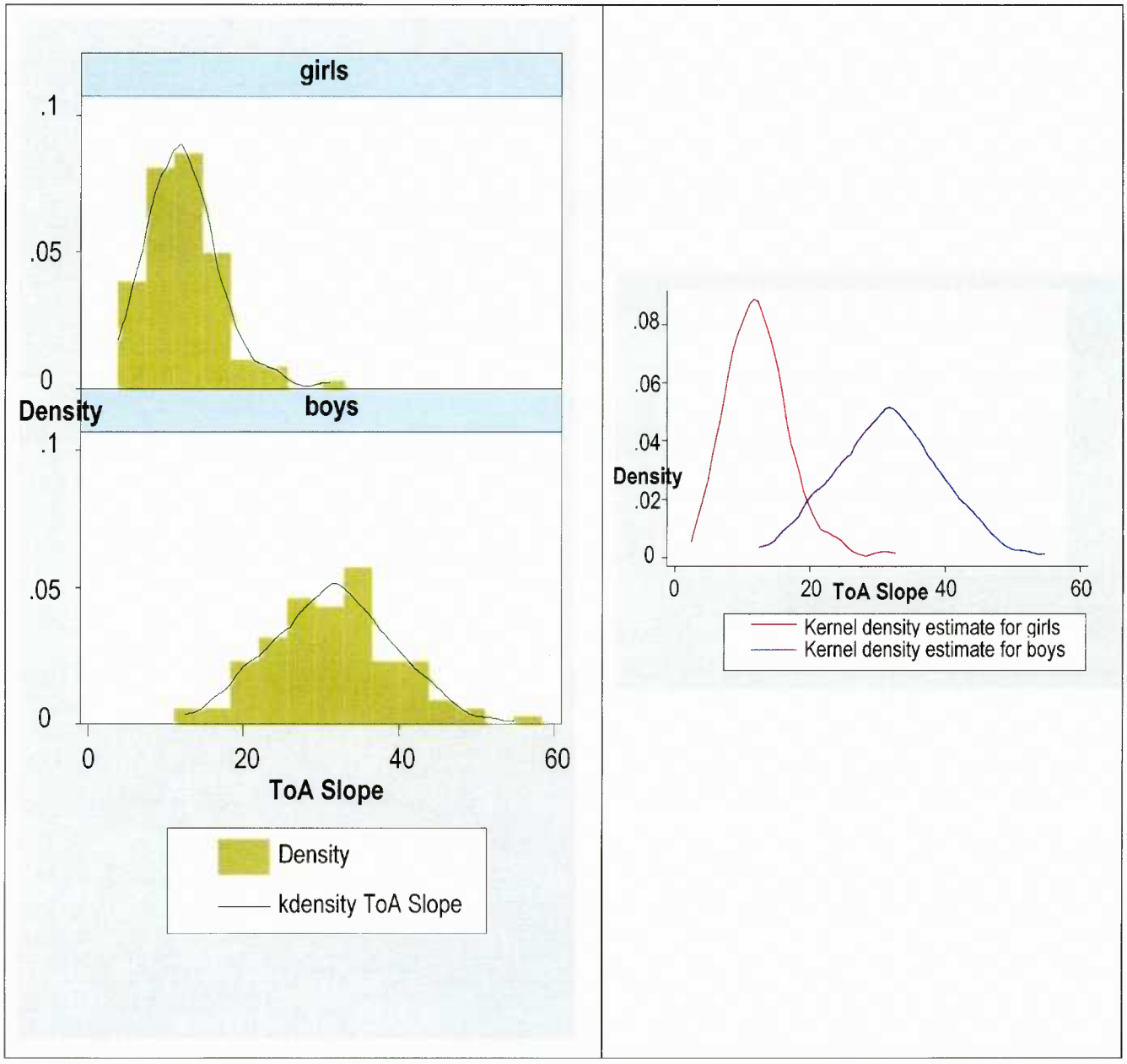

Figure 8-2 (a)

Figure 8-2: A comparison of boys and girls for change in bone; a) total area (ToA, mm^2), b) cortical area (CoA, mm^2), c) cortical density (CoD, mg/cm^3), and d) strength-strain index (SSI, mm^3). The histograms on the left hand depict slope values for boys (top) and girls (bottom). A kernel density (kdensity) line is placed over the histograms to effectively show the distribution of each bone outcome variable. The graphs on the right show that boys (in blue) had significantly greater mean slope values ($p<0.001$) and greater variability compared with girls (in pink) for change in all bone outcomes, except for CoD where there was no difference between the sexes ($p=0.094$). The graph for medullary canal area can be found in Figure 7-3 page 84.

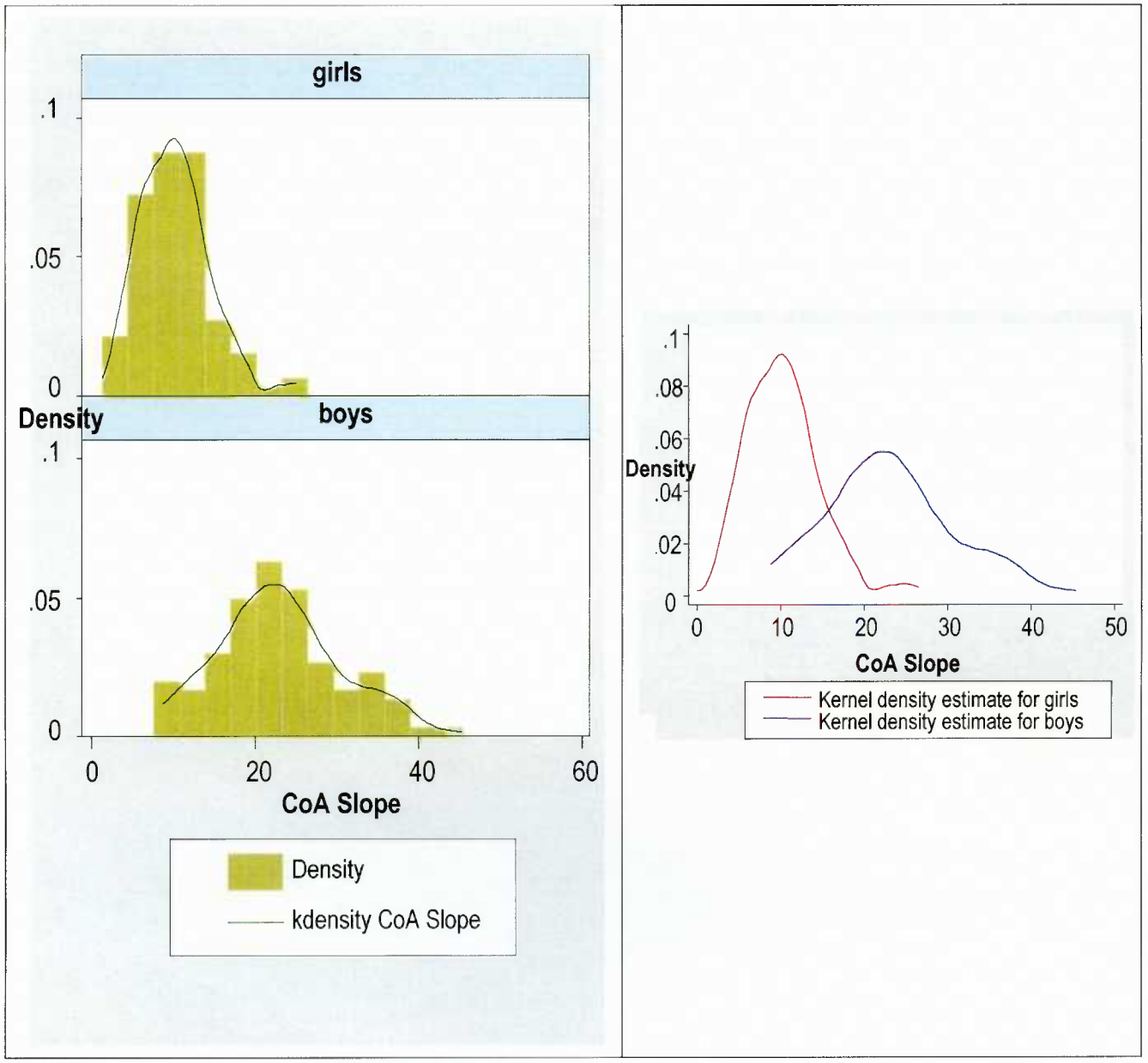
girls
boys
Density
.1
.05
0
0
20
40
60
CoA Slope
Density
kdensity CoA Slope
.1
.08
.06
.04
.02
0
10
20
30
40
50
CoA Slope
Kernel density estimate for girls
Kernel density estimate for boys

Figure 8-2 (b)

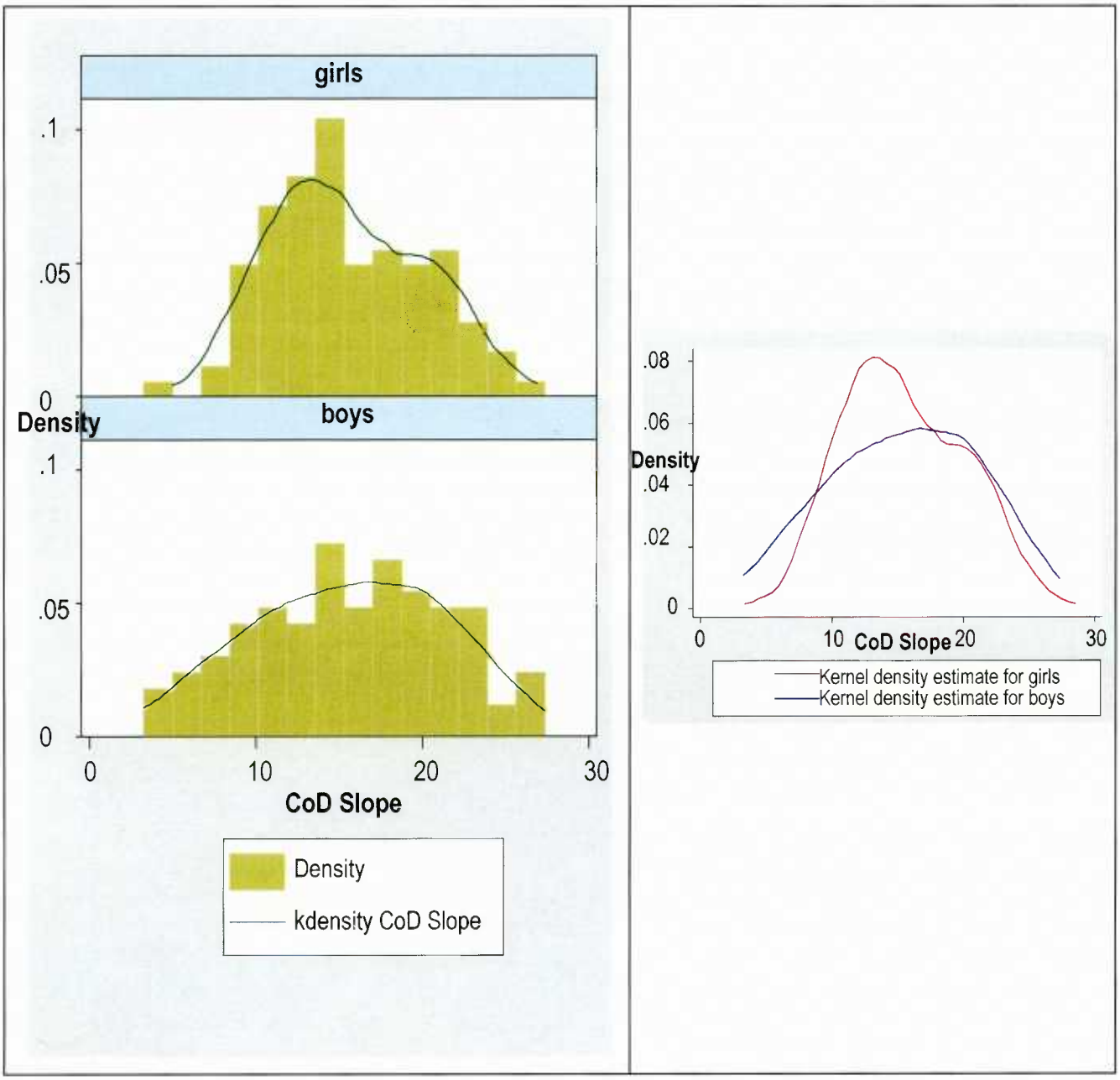
girls
boys
Density
.1
.05
0
0
10
20
30
CoD Slope
Density
kdensity CoD Slope
.08
.06
.04
.02
Kernel density estimate for girls
Kernel density estimate for boys

Figure 8-2 (c)

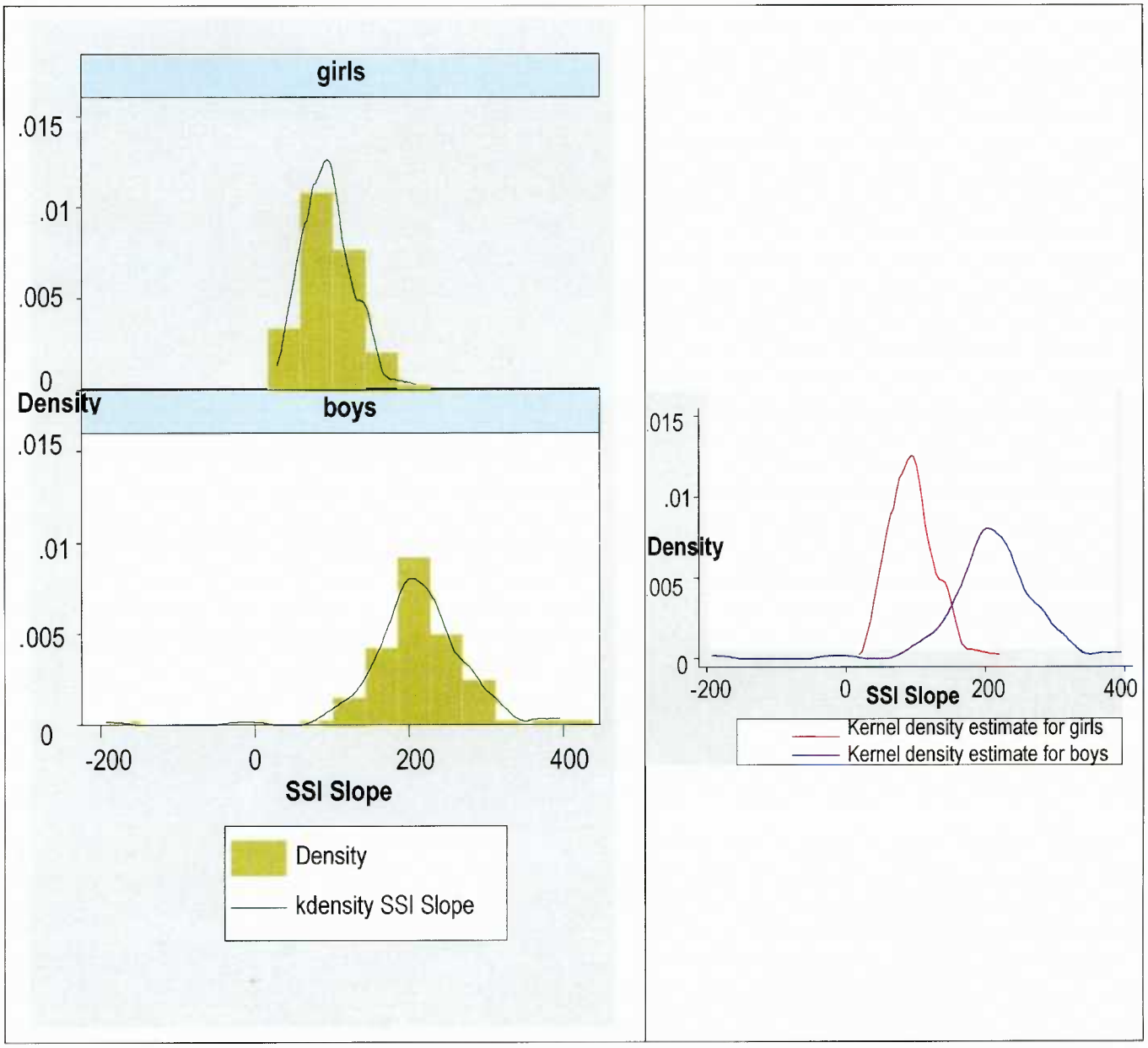
girls
boys
Density
.015
.01
.005
0
-200
0
200
400
SSI Slope
Density
kdensity SSI Slope
Kernel density estimate for girls
Kernel density estimate for boys

Figure 8-2 (d)

Table8-1: Mean slope (± 95% confidence intervals (CI)) and intercept values (SE) for boys and girls for total area (ToA, mm²), cortical area (CoA, mm²), medullary canal area (MedA, mm²), cortical density (CoD, mg/cm³) and strength-strain index (SSI, mm³). Boys had significantly greater slope and intercept values for all bone outcomes except for CoD, where girls had a significantly greater intercept and the difference in slope between the sexes was not significant.

	Boys (n=96)					Girls (n=106)					
Outcome Variable	Slope (SE)	95% CI	Intercept (SE)	95% CI		Slope (SE)	95% CI	Intercept (SE)	95% CI	Slope P Value	Intercept P Value
ToA mm²	31.4 (1.3)	28.9-34.0	397.9 (7.6)	383.0-412.9		12.3 (0.7)	11.0-13.6	352.8 (5.1)	342.8-362.7	<0.001	<0.001
CoA mm²	23.0 (1.1)	20.8-25.3	261.7 (4.8)	252.3-271.1		10.2 (0.6)	9.1-11.4	236.0 (3.8)	228.6-243.5	<0.001	<0.001
MedA mm²	8.2 (0.6)	7.0-9.4	136.3 (3.9)	128.7-143.9		2.0 (0.2)	1.6-2.5	116.8 (2.7)	111.5-122.2	<0.001	<0.001
CoD mg/cm³	15.6 (0.9)	13.7-17.5	1034.8 (3.7)	1027.6-1041.9		15.4 (0.7)	14.1-16.7	1063.7 (3.9)	1056.0-1071.3	0.904	<0.001
SSI mm³	209.5 (11.1)	187.8 (231.2)	1523.8 (48.9)	1427.9-1619.6		94.8 (4.4)	86.1-103.4	1276.5 (26.1)	1225.4-1327.6	<0.001	<0.001

9 Discussion

In this chapter, I discuss the findings of this thesis with a focus on a number of key areas: 1) descriptive characteristics of participants; 2) sex differences in bone surface changes at the periosteum and endosteum; 3) sex-specific comparisons of cortical density and the strength strain index; 4) methodological techniques employed that have strengthened my findings; 5) unique aspects and strengths of the study; 6) limitations of my study; and 7) future directions.

9.1 Descriptive Characteristics of Participants at Baseline 2 (2001)

Overall, children in the current study were healthy. Boys and girls were the same age, on average, at baseline. There was no significant difference in standing or sitting height, body weight, tibial length or total leg length between the sexes. There were a similar number of boys and girls in each Tanner stage with the exception of Tanner stage 3, where 9.4% more girls than boys resided. Age at peak height velocity (APHV) was on average, one year earlier for girls (11.4 ± 0.9 years) compared with boys (12.5 ± 1.2 years). Age at PHV for girls occurred at approximately the same time as mean age of menarche (11.6 ± 0.1 years, data not shown).

For comparison, I looked to a key study of Caucasian participants conducted in Canada (the University of Saskatchewan Bone Mineral Accrual Study (U of S)) that assessed bone parameters and *change* in these parameters (by dual energy x-ray absorptiometry (DXA)) over 6 years (1991-1997). Participants in my study were slightly older, taller, heavier and from a number of different ethnic backgrounds (Caucasian (52%), Asian (34%) and mixed or other ethnicities (14%)) (9).

This section assesses studies which have determined APHV for children of different ethnicites. Table 9-1 provides a summary of sex by ethnicity APHV's. For girls, the U of S study reported that age of menarche lagged behind PHV by approximately one year (12, 18) and coincided with the timing of peak bone mass accrual (10, 12). The small discrepancy between studies may be a function of the mixed ethnic HBS cohort. This is supported by the APHV I noted for HBS Caucasian girls (11.4 ± 0.7 years) which compared closely with APHV for the Caucasian girls (11.8 years, standard deviation not provided) in the U of S Study. Age at PHV for Caucasian girls in both these studies was slightly older than for girls residing in the United States (APHV, 10.9 years, standard deviation not provided) (258).

For boys, there was a greater difference in APHV for Caucasians between studies. In the HBS, the APHV for Caucasian boys was 12.7 ± 1.3 years, compared with 13.4 years (standard deviation not provided) in the U of S trial. There are many possible reasons for this some of which are discussed below. It is important to note that APHV was determined by a similar method in both studies (12). Asian girls reached APHV at 11.2 ± 1.0 years, and girls of Other ethnicities reached APHV at 11.5 ± 1.3 years, on average. Matsumoto et. al., estimated APHV in Japanese children using the proportional distribution method. Age at PHV was 10.5 years in Japanese girls, on average (standard

deviation not provided) (176). A difference in APHV was noted between boys of different ethnicities in the HBS trial. Asian and Other boys were approximately 6 months younger at PHV (APHV, 12.1 ±0.8 years), on average, compared with Caucasian boys. By comparison, age at PHV in Asian boys was similar to Japanese boys (mean age 12 years, standard deviation not provided) (176).

There are a number of other possible explanations for these differences in APHV. These include measurement protocol (stretch stature versus relaxed stature), secular trends in growth, time of year of measurement, genetics related to ethnicity and activity levels of participants. I comment on each briefly. First, participants in the U of S study (12) were measured from 1991-1997 – a full decade prior to the start of the HBS. This may partially explain the APHV differences between Caucasian participants as height has been reported to increase by 10-30 mm/decade (57, 101). There is also a known seasonal variation in growth in height (57). Second, Japanese children may be genetically different from both Caucasian children and the Asian children in my study who were of primarily Hong Kong origin. Third, physical activity levels may have been different between groups. Extreme activity levels have been known to influence the rate of growth. Belgian female gymnasts (n= 13, 6.0-17.6 years of age) underwent vigorous training for 15 hours/week, on average (range 9-19 hours/week) for 6-7 years (166). Age at PHV was substantially later (APHV, 12.9 ± 1.5 years) compared with recreationally active children, as in the present study (166).

The considerable variability with respect to the timing of PHV within and between sexes is an accepted tenet within the growth literature. One of the forefathers of human growth research, Professor Robert Malina, reported that PHV was commonly attained within a wide range for both girls (9.3-15.0 years) and boys (12.0-15.8 years) (165). This known variability in the timing of growth among children who are the same chronological age also highlights the need to control for maturational differences by using a common maturational indicator, such as APHV.

Table 9-1: Ages at PHV for Asian and Caucasian children who participated in longitudinal growth and development studies. Data from my thesis are bolded for comparison.

Authors/year study published	Ethnicity	Location	Boys Mean APHV (years)	Standard Deviation	Girls Mean APHV (years)	Standard Deviation
Bailey et al, 1999 (12)	Caucasian	Saskatchewan	13.4	Not Provided	11.8	Not Provided
Malina et al, 2006 (165)	Caucasian	Belgium	N/A	N/A	12.9	1.5
Ahamed 2007	**Caucasian**	**Vancouver**	**12.7**	**1.3**	**11.4**	**0.7**
Matsumoto et al, 1990 (176)	Japanese	Japan	12.0	Not Provided	10.5	Not Provided
Ahamed 2007	**Asian**	**Vancovuer**	**12.1**	**0.8**	**11.2**	**1.0**

For bone variables at baseline, there was no significant difference between boys and girls for ToA, CoA, MedA, or SSI. However, girls had significantly greater CoD than boys ($p<0.05$). This is consistent with previous studies that measured change in CoD over 20 months in girls who were mean age 11.9 years (133) and either prepubertal (Tanner Stage 1) or early/peri pubertal (Tanner Stage 2 and 3) (154).

9.2 Sex-Differences at the Periosteal and Endosteal Surfaces of Growing Bone

The questions I address in this thesis build upon previous work that aimed to quantify sex specific differences at the endosteal and periosteal surfaces of growing bone. Total area represented bone modelling on the periosteal (outer) surface and medullary canal area represented modelling activity on the endosteal (inner) surface (Figure 8-1 (a) and (c)). Cortical area was also assessed to represent cortical bone between the periosteum and endosteum. Therefore, if values for any two of these variables were known, the other could be derived (e.g. CoA=ToA-MedA).

Total area

After boys and girls were aligned by maturity offset (APHV-chronological age), boys had substantially larger bones than girls did ($p<0.001$). This was represented by the 11% greater mean intercept values for boys' ToA (Table 8-1). There was substantial bone formation for both sexes on the periosteal surface, however boys accrued 2.6 times as much bone as girls did (61%, $p<0.001$) (Table 8-1). Figure 8-1 (a) depict boys' larger bones (greater ToA values). Figure 8-2 (a) shows that boys have both greater rates of change represented as the mean slope (19 mm^2/year) and greater variability in their slope compared with girls (Table 8-1). This is similar to Garn's findings where boys had greater periosteal apposition from childhood to late adolescence at the second metacarpal than did girls (84, 91, 92).

This increased bone size whereby bone is distributed further from the neutral axis confers a considerable strength advantage to boys (discussed under SSI). My results across 56 months extend the findings of Kontulainen et al. who demonstrated similar changes but of a smaller magnitude at the periosteal surface in this cohort at the mid-tibia over 20 months (8% difference between boys and girls in the early and peri pubertal years and a 14% difference between sexes in early post puberty) (133).

Cortical area

For CoA, boys had significantly greater values (approximately 10% greater, $p<0.001$) compared with girls (Table 8-1). There was substantial cortical bone accrued for both sexes; however, boys gained approximately 2 times as much bone as girls did (56%, $p<0.001$). Not surprisingly, there was a direct relationship between the increase in ToA and the increase in CoA ($r=0.9126$). As was shown for ToA, the rate of change for boys was of a greater magnitude (13.0 mm^2/year) and was of greater variability (CI= 21-25mm^2) than in girls (CI= 9-11mm^2). From Figure 8-1 (b), it appears as though CoA continues to rise throughout pubertal growth but the rate at which this occurs slows from 3 years post APHV onwards. The implications of these trends to the health of adult men and women are not clear. It seems important to assess the children in the present study through their adolescent years into early adulthood to establish a clear steady state for CoA. Ideally, these children might be followed prospectively until they reach an older age when bone strength begins to decline.

Medullary canal area

Garn examined the second metacarpals of pubertal boys and girls by applying radiogrammetric techniques to planar radiographic images. The metacarpal demonstrated significant endosteal apposition (depicted by a decline in MedA width) in pubertal girls compared with boys (84, 91, 92). The theory most recently proposed to explain this sex difference is referred to as the "estrogen-driven bone packing" theory (123). This theory suggests that during puberty girls "pack bone" at the endosteum for reproductive requirements later in life. Specifically, it is proposed that "packing" occurs to meet the increased calcium needs of fetal development during pregnancy and the demands of lactation after birth (123, 221, 242). Thus, during puberty which occurs earlier in girls compared with boys, it has been suggested that estrogen promotes enhanced endosteal apposition and diminished endosteal resorption in both sexes -- and this effect is thought to be greater in girls (50, 192, 225, 249).

Our results do not support the notion of enhanced *bone formation* at the endosteal surface in girls during the pubertal years as reported by Garn and others (84, 91, 92). Figure 8-1(c) and Figure 7-3 depict that in girls, on average, endosteal *resorption* predominated (as represented by a small net increase in MedA) across all biological ages. Medullary expansion in boys (8.2 mm^2) was 4 times that of girls (2.0 mm^2) across the 6-year measurement timeframe. Therefore, although the data do not provide support the notion of increased endosteal bone *formation* in girls they do suggest that girls' bone was preserved through diminished endosteal bone *resorption*.

Results from the current study were similar to a prospective trial conducted on the HBS cohort over a shorter period (132). Boys and girls exhibited significant increases in ToA and CoA at the mid-tibia over a 20-month measurement period. Medullary cavity area also increased for all maturity groups in both sexes, but these changes were statistically significant in EARLY and PERI groups only, $p<0.05$. Thus, once again it seems likely that both bone formation and resorption are occurring at the endosteal surface during growth, although my study was not able to directly characterize the balance between these events. However, endosteal, resorption appears to dominate in both sexes but is of a lesser magnitude in girls.

Does estrogen have a role to play in endosteal bone formation?

It has been postulated that estrogen may modulate bone formation at the endosteal surface in women (123, 242). However, the mechanistic action of estrogen on bone is controversial and complex as it can influence the response to mechanical loading (67, 128), can increase the production of bone resorbing cytokines (150) and inhibit osteoclast function (117, 119), among other effects. Nature provides a means for us to indirectly evaluate estrogen effects on bone. From conception to child birth estrogen levels of the mother increase steadily (149). For the "bone packing" theory to hold true, increased parity should result in less bone on the endosteal surface (increased MedA) as bone would be made available to support the demands of the developing fetus. In addition, women who breast fed their infants might be expected to lose more bone during lactation compared with women who did not breast feed. However, studies in pregnant and lactating women do not support this notion (92, 185, 251).

Garn conducted a study on 41 pregnant women aged 35-70 years of age, of Dominican origin, who had ≥10 children, on average. Radiographs of the midshaft of the second metacarpal were obtained during and after their pregnancies. From these images it appeared that bone loss during or after pregnancy was not observed, compared with 112 nonparous same-aged women. On the contrary, some of the multiparous women experienced endosteal apposition (bone gain) during their first trimester. In addition, there was no bone loss during lactation in breastfeeding women compared with those who did not breast feed (92).

To further illustrate the independent effects of pregnancy and lactation on bone, Holmberg-Marttila et. al., examined changes in femoral neck BMC in two women during, immediately after and 1 year post pregnancy (118). One of the women had an adequate calcium supply and the other a low calcium supply and high calcium demand due to excessive lactation (123). During pregnancy both women had decreased bone mineral content (~4% as measured by DXA) at the femoral neck (FN). After pregnancy and during post-natal amenorrhea, FN BMC decreased ~8% in the woman with low calcium intake whereas no additional loss in FN BMC was observed in the woman with normal calcium intake. Bone mineral increased in both mothers one year post partum. However, only the woman with normal calcium intakes regained her pre-pregnancy bone status (123). Although results have been mixed (68, 105, 250), this simple case study suggests that bone conservation may depend on adequate nutrition before, during and after pregnancy (92, 123). However, these results must be interpreted with caution as the sample consisted of only two

women. Overall, results obtained from studies conducted on adult women do not support the notion that pregnancy and/or lactation has a long term negative impact on bone mass (92, 185, 251). Conversely, young/adolescent mothers have been found to decrease their bone mass at the lumbar spine during pregnancy and never regained their pre-pregnancy bone status (6, 55). Similar findings to *young* women have been observed in *animals* that were assessed after pregnancy; bone mass at the endocortical surface in rats declined substantially (40, 107, 187, 213).

There are a number of other possible explanations for the differences in findings between studies. First, it is likely that rates of bone formation and resorption are specific to different sectors of a bone as well as between different anatomical regions of the whole skeleton (137, 201). Thus, it may not be prudent to compare events at the metacarpals (as per Garn) with our findings at the tibia. Second, discrepancies between studies may be attributed to significant limitations that have been associated with estimating bone parameters using 2-dimensional radiographs, as used in Garn's studies (269). Finally, despite the relatively large sample sizes, Garn's studies were cross-sectional, compared with the prospective design of the current study (92).

9.3 Sex-Differences in Cortical Density and the Strength Strain Index

The strength-strain index (SSI) provides a surrogate measure for bone strength. It is important to examine the density of cortical bone in combination with bone geometry in order to better understand the mechanical properties of bone such as its resistance to bending, compression forces and its propensity to fail under certain loads (91).

Cortical density

Our results suggest that girls had significantly denser cortical bone at the tibial midshaft compared with boys ($p<0.001$) (Table 8-1). However, there was no difference in the rate of change in CoD between boys and girls over the measurement timeframe ($p=0.904$) (Figure 8-2 (c) and Table 8-1). The advantage we note for girls with respect to CoD was already apparent at pre and early puberty (2 years prior to PHV) (Figure 8-1 (d)). It is possible that one bone-region may be undergoing resorption while another region is simultaneously undergoing formation -- resulting in no net gain in bone. In a companion study, we found that both sexes had the greatest density in the posterior cortex while the least dense bone was in the in the anterior cortex (Cooper et al., unpublished data). This sexual dimorphism in CoD has been reported previously at both the tibial midshaft (132, 133, 154) and the proximal radius (239).

Schoenau et al. conducted a cross-sectional pQCT study that examined sex differences in CoD at the proximal radius. Participants were comprised of 362 males and females across a wide age range (6-23 years) and 107 of their parent's (29-40 years old) (239). Pubertal girls and pre-menopausal women had ~ 3-4% greater CoD at the radius; girls were compared with same age and maturity boys (239). One limitation of this study was that children were matched by age rather than by maturity. Further, although Tanner Staging was used to control for maturity it is a

relatively crude measure of maturational status as maturity levels of children may vary *within* Tanner stages (18, 256). Regardless, these results are similar to those that I report for the HBS cohort.

Other studies have reported that females experience decreased intracortical remodeling (123) and consequently increased CoD (31, 32, 237, 239) at various skeletal sites. These events coincide with the cyclical secretion of estrogen after menarche in girls and women. On the other hand, androgens in boys and men enhance metabolic activity such as intracortical remodeling (123). Intracortical remodeling may then lead to increased porosity (238) and along with greater periosteal apposition the result would be a less dense but larger bone. Given the greater contribution of geometry as compared with density to bone strength, this configuration in men (a significantly larger but less dense bone) would theoretically provide a greater resistance to structural failure (33, 242).

Strength-strain index (SSI)

Bone density, bone mineral content, bone size and shape all contribute to bone strength (33), but their relative contribution to bone strength in children is largely unknown. I used SSI as a surrogate measure for bone strength in the current study. On average, boys had significantly greater SSI (16%) and increased their SSI significantly more (55%) than girls did over the study period (both, $p<0.001$ (Figure 8-1 (e), Figure 8-2 (d), (Table 8-1)). In boys, the surge of testosterone increases the magnitude and prolongs duration of the pubertal growth spurt and boys experience greater gains in height and weight across puberty. Boys also accrue more muscle mass and have larger bones after puberty, compared with girls (165). The resistance of bone to bending is directly proportional to the distribution of mass about the neutral bending axis, also referred to as area moment of inertia (33). Further, a small increase in the external diameter of a long bone (increased bone size) improves its resistance to bending and torsional loading and dramatically increases bone's strength (33). Thus, boys' larger bones (as denoted by greater CoA and ToA in the current study) and their enhanced rates of change in these parameters (Table 8-1), compared with girls, contribute to boys greater SSI. If this advantage were to persist, it would provide boys and men a bone strength advantage throughout life (34, 145-147, 195).

I reported significantly greater CoD for girls in the current study. Their smaller bones theoretically experience less mechanical stresses which could lead to a decreased number of microcracks in cortical bone, less intracortical bone remodeling and less porosity – resulting in more dense bones (239). However, given the lesser contribution of CoD (as compared to ToA) to SSI, girls' more dense bones only partially compensates for their size disadvantage, compared with boys. In adults it has been suggested that it is men's larger bone size and not differences in density or the amount of bone within the periosteum and endosteum that explains their greater bone strength as compared with women (242).

9.4 Methodological and Statistical Techniques Employed

In this section I focus my discussion on; 1) methods used to assess maturity and 2) pQCT methodology at the tibial midshaft.

9.4.1 Methods used to Assess Maturity

I previously presented the many ways to assess maturity in children (s*ection 2.1.2*). As stated earlier, Tanner staging is the method most commonly used to assess maturity in non-clinical settings and in pediatric bone studies (18, 165, 256). Although self-report Tanner staging is non-invasive and compares well with a physician's rating of maturity by direct observation (165), it is also prone to error. Bias is introduced as young children may overestimate or underestimate their stage of sexual maturity based on their overall size or adiposity (18, 27). In addition, Tanner staging may reduce the variation in the sample as it is a categorical variable and does not account for the continuing process of growth or the differences in the timing and tempo of maturation (133, 165). For example, a 14 year old girl in the later stage, and a 12 year old girl in the early stage, of Tanner stage 3 will fall into the same maturity category. In reality the level of maturity could be quite different between them (18, 165).

For girls, Tanner stages are based on breast and pubic hair development and these events are not perfectly aligned with the Tanner stage ratings of genitalia and pubic hair in boys. So it is often not possible to make direct comparisons at a given Tanner stage between the sexes. Ideally, multiple measures of hormones analyzed from blood samples would be taken to assess children's maturity status -- but it is often not possible to collect blood samples in a healthy cohort of children. Further, age of menarche provides a precise maturity time point within girls – but there is not an obvious equivalent event for boys. Finally, hand-wrist X-rays can provide accurate assessment of developmental age but depends upon the technique used (Greulich Pyle or Tanner Whitehouse II) and the experience of the rater (18).

The timing of peak growth in height is a somatic event experienced by all children at approximately the same maturational time point (165). At APHV children on average have achieved 80% of their adult height (165). However, although height and weight are relatively simple measures, PHV can only be determined from longer-term longitudinal data that transverses peak linear growth. As these data are time consuming and expensive to collect very few studies are able to utilize this approach.

For the current study, where possible, age at PHV was determined for every child using the cubic spline procedure. Children for whom age at PHV was determined had ≥4 height measurements. I was unable to determine APHV for 13 participants who had only three (1 girl) or four (8 girls and 4 boys) data points. The girls were comprised of Caucasian, Asian, and Other ethnicities (3 each) and the 4 boys were all of Asian ethnicity. These children were excluded from analysis. A strength of my study was that I was then able to align boys and girls on APHV to compare their bone parameters at each maturational age. This procedure, however, has some limitations. A number of

analytical techniques have been used to determine APHV; however, as no standardized protocol has yet been published. There may also be differences in outcomes based on the number of data points available to generate the cubic spline procedure.

9.4.2 Peripheral QCT Methodology

Peripheral QCT is a relatively novel technique that has been has been used in a relatively small number of pediatric bone trials. Although the manufacturer recommends standard (default) analysis protocols, the user can choose from many analysis options depending on the site (for example, mid or distal radius or tibia) and the population being measured. Currently, consensus has not been reached in the scientific literature as to the standard modes or thresholds that should be used to analyze pediatric pQCT scans. Therefore, we followed the manufacturer's recommendations when analyzing scans collected from children in the HBS cohort (257).

9.5 Limitations

I acknowledge that this study has a number of limitations. First, as in any repeated measures study of growing children it is not possible to locate the exact same bone site between measurements. This is a function of a change in long bone length which is unequal at the two long bone ends. Fifty-seven per cent of longitudinal growth of the tibia occurs at the proximal metaphyses and 43% occurs at the distal metaphysis (3, 101). However, by using the same anatomical landmark, it was possible to find the same *relative* point along the length of the tibia at each measurement.

Second, although we were fortunate to have the scans across all years collected by only 2 technologists, there may have been some differences between them. The first technologist acquired the pQCT scans from 2001-2004 and another individual acquired the scans for the 2005 and 2006 measurement periods. To reduce measurement error, the second technologist was trained by the first individual who also monitored measurement technique during the first few days of data collection. We were unable to undertake a precision study to determine the reproducibility of scan acquisition between the 2 measurers. The same technologist (YA) analyzed pQCT scans from 2004-2006 and SSI for all scans.

Third, as discussed, we used the recommended protocols to acquire the pQCT scans (132, 133, 154, 158). However, studies from the Healthy Bones Lab conducted by Kontulainen et. al. (133) and Cooper et. al., (unpublished data) noted regional differences in cortical bone density within a bone cross-section. Thus, the conservative choice of a relatively high threshold to ensure only cortical bone was recognized, may have resulted in the exclusion of voxels that contained cortical bone of lower density. This may be especially true of children who are undergoing higher rates of remodeling as compared with adults.

The outcomes of any study that uses an imaging system to assess tissue may be subject to partial volume effects (PVE). To minimize the PVE, half filled or low density voxels are often "peeled" from along the edges of bony contour, and excluded from analysis (133). The risk with this approach is that low density cortical bone may be inappropriately excluded from the analysis, resulting in an overestimation of cortical bone density. Therefore, I attempted to minimize the partial volume effect in two ways during scan analysis. First, I manually placed a region of interest (ROI) along the bone edge to more precisely identify the outer edge of bone. Second, I used a filter in combination with the Peel Mode 2 protocol. Filtering does not completely control for, but helps to reduce the PVE (257).

Fourth, to identify the important biological events along the growth trajectory, including bone development, long-term longitudinal data are needed. Further, to discern a specific growth event and to make comparisons between boys and girls requires that there be data points on either side of the event or time period of interest. This becomes a challenge as the timing of these events is different, on average, between the sexes. In the current study, although the mean age for both boys and girls was 12.1 (±0.5) years at baseline, girls were more advanced with respect to their maturity. This was illustrated by the earlier age of PHV for girls (11.4 ± 0.9 years) compared with boys (12.5 ± 1.2 years). Therefore, I was unable to capture and compare boys and girls in prepuberty (maturity offset -3 or - 4) as most girls had already advanced beyond this maturity stage. Similarly I was unable to compare boys and girls in post-puberty, as most boys had not yet reached that maturational stage. It seems important to follow these boys and girls until adult status is reached.

Fifth, the results of my study are specific to the midshaft of the tibia and do not necessarily represent events at other anatomical regions of the skeleton. Therefore it is possible that although I was unable to discern *net* endosteal apposition in girls' tibiae, endosteal apposition may occur at other skeletal sites that I did not measure in my study.

Finally, we experienced considerable attrition (55%) between the first and second year of the trial (Baseline 1). This was in most part due to the withdrawl by teachers in two treatment schools. Attrition between years apart from this time point averaged approximately 6%/year. Although we know that for the largest percentage of children (17%) attrition was due to a move or transition from elementary to high school – we do not have these data for all children.

9.6 Unique Aspects and strength of this study

This study has a number of unique aspects. First, it is the longest prospective trial in the world to assess bone geometry, density and estimate bone strength (measured as SSI). Second, pQCT is a relatively novel instrument that improves upon a number of longitudinal studies that used dual energy x-ray absorptiometry (a planar technique) to assess bone mass accrual during growth. It overcomes many limitations of DXA and evaluates both cortical and trabecular bone compartments and assesses a number of bone parameters that underpin bone strength. Third, to my knowledge, this is the first study to describe bone surface and strength changes at the tibial midshaft

over a period of 5 years using pQCT. Fourth, using the richness of longitudinal data, I was able to align all children on a common maturational landmark, APHV. Only one other study, the U of S bone mineral accrual study (9) that described bone mass accrual by DXA across 7 years has achieved this. Finally, I feel that by using multilevel modeling techniques I have strengthened the statistical analysis used in my study. As a Masters student this is my first experience with more advanced statistical modeling. Therefore, I provided a clear illustration of this technique and compared it with a simpler statistical model (Chapter 7). In summary, this thesis has been strengthened by the use of a longitudinal data set, by using a 3 dimensional imaging device, by aligning all participants by age of PHV and by utilizing MLM statistical technique

9.7 Future Directions

Studies that assess boys and girls across the entire period of growth are rare. However, unless we better understand the biological events that strengthen the skeleton during growth we will be unable to understand how these events might predispose individuals to fracture in later life. Thus, it is important to understand the differences between how bone strength is developed in individuals of the same sex and between boys and girls.

To gain a better understanding, longer term studies that cover the entire growth period from prepuberty to late puberty and into adulthood are needed. It seems important that the HBS cohort be followed forward until the children reach skeletal maturity. This would provide the opportunity to further examine events on the endosteal and periosteal surfaces of bone. Ideally, I would add a younger group of children (ages 7-10 years) to this sample and follow the entire cohort into later life to see how the events of childhood and adolescence effect bone loss with aging.

Given the multiethnic nature of Vancouver we are in the unique position to compare differences across ethnicities. Although this was not the focus of my study it would provide some insights into differences between Asian and Caucasian children who live in Vancouver. It would also allow us to explore how ethnic differences in lifestyle factors (diet and exercise) influence bone strength accrual.

Finally, the multi-level analysis I undertook to represent the data was only a starting point. It would be interesting to develop a more complex multilevel model to see how (and to what extent) other factors such as overall size, timing of maturity (early versus late maturers) and lifestyle factors such as diet and exercise effect the bone strength trajectory.

10 Summary

I address each of my original hypotheses below.

H_1 Boys and girls exhibit endosteal formation during adolescence but the magnitude of this is greater in girls. Experimentally this will be represented by a reduction in the cross-sectional area of the medullary canal (MedA).

Our results do not support the notion of enhanced *bone formation* at the endosteal surface in girls during the pubertal years. Rather, endosteal resorption predominated (as represented by a small net increase in MedA) across all maturational ages. Medullary expansion in boys (8.2 mm^2) was 4 times that of girls (2.0 mm^2) across the 6-year measurement timeframe. Although the data do not provide support the notion of increased endosteal bone *formation* in girls they do suggest that girls' bone was preserved through diminished endosteal bone *resorption*.

H_2 Boys and girls exhibit periosteal formation during adolescence but the magnitude of this is greater in boys. Experimentally this will be represented by an increase in periosteal diameter as measured by total area (ToA).

Although both boys and girls were found to undergo periosteal formation, boys had substantially larger bones than girls did ($p<0.001$). This was represented by 11% greater mean intercept values for boys' ToA. In addition, boys accrued 2.6 times as much bone as girls (61%, $p<0.001$).

For CoA, boys had significantly greater values (approximately 10 % greater, $p<0.001$) compared with girls. There was substantial cortical bone accrued for both sexes, however boys accrued approximately 2 times as much bone as girls did (56%, $p<0.001$).

H_3 Boys and girls exhibit gains in volumetric bone density during adolescent growth. The magnitude of this increase is greater in girls.

Girls had significantly denser cortical bone at the tibial midshaft compared with boys ($p<0.001$). However, there was no difference in the rate of change in CoD between boys and girls over the measurement timeframe ($p=0.904$).

H_4 Boys and girls will exhibit increases in bone strength accrual during adolescent growth. The magnitude of this increase will be greater in boys.

Boys had significantly greater SSI (16%) as determined from their significantly larger mean intercept and increased their SSI significantly more (55%) than girls did over the study period (both, $p<0.001$).

11 Conclusion

As the skeleton grows it becomes stronger in both boys and girls. However, strength is conferred somewhat differently between the sexes. In boys, strength is a function of a larger bone size and increased periosteal dimensions while girls have more dense, but smaller bones. The relative contribution of each of these parameters, size and density, to overall bone strength is not well understood for children – although central biomechanical tenets would confer the strength advantage to boys. Laboratory experiments that test bone specimens from across the lifespan to failure would provide further insight into this question.

References

1. Adams, J. C., Hamblen, D.L. An Outline of Fractures. Edinburg: Churchill Livingstone; 1992.
2. Alaranta, H., An, K., et al. Orthopaedic Basic Science. Biology and Biomechanics of the Musculoskeletal System. USA: American Academy of Orthopaedic Surgeons; 2000.
3. Anderson, M., Green, W. T., and Messner, M. B. The classic. Growth and predictions of growth in the lower extremities by Margaret Anderson, M.S., William T. Green, M.D. and Marie Blail Messner, A.B. from the Journal of Bone and Joint Surgery, 45A:1, 1963. Clin Orthop Relat Res:7-21; 1978.
4. Arnett, T. R., Henderson, B. Methods in Bone Biology. Bone Histomorphometry. USA: Springer; 1997.
5. Ashe, M. C., Liu-Ambrose, T., Khan, K. M., White, N., and McKay, H. A. Optimizing results from pQCT: reliability of operator-dependent pQCT variables in cadavers and humans with low bone mass. J Clin Densitom 8:335-40; 2005.
6. Atkinson, P. J., and West, R. R. Loss of skeletal calcium in lactating women. J Obstet Gynaecol Br Commonw 77:555-60; 1970.
7. Augat, P., Gordon, C. L., Lang, T. F., Iida, H., and Genant, H. K. Accuracy of cortical and trabecular bone measurements with peripheral quantitative computed tomography (pQCT). Phys Med Biol 43:2873-83; 1998.
8. Bachrach, L. K., Hastie, T., Wang, M. C., Narasimhan, B., and Marcus, R. Bone mineral acquisition in healthy Asian, Hispanic, black, and Caucasian youth: a longitudinal study. J Clin Endocrinol Metab 84:4702-12; 1999.
9. Bailey, D. A. The Saskatchewan Pediatric Bone Mineral Accrual Study: bone mineral acquisition during the growing years. Int J Sports Med 18 Suppl 3:S191-4; 1997.
10. Bailey, D. A., Baxter-Jones, A. D., Mirwald, R. L., and Faulkner, R. A. Bone growth and exercise studies: The complications of maturation. J Musculoskelet Neuronal Interact 3:335-7; discussion 356; 2003.
11. Bailey, D. A., Martin, A. D., McKay, H. A., Whiting, S., and Mirwald, R. Calcium accretion in girls and boys during puberty: a longitudinal analysis. J Bone Miner Res 15:2245-50; 2000.
12. Bailey, D. A., McKay, H.A., Mirwald, R.L., Crocker, P.R.E., Faulkner, R.A. A Six-Year Longitudinal Study of the Relationship of Physical Activtiy to Bone Mineral Accrual in Growing Children: The University of Saskatchewan Bone Mineral Accrual Study. Journal of Bone and Mineral Research 14:1672-1676; 1999.
13. Bailey, D. A., Wedge, J. H., McCulloch, R. G., Martin, A. D., and Bernhardson, S. C. Epidemiology of fractures of the distal end of the radius in children as associated with growth. J Bone Joint Surg Am 71:1225-31; 1989.
14. Baron, J. A., Barrett, J. A., and Karagas, M. R. The epidemiology of peripheral fractures. Bone 18:209S-213S; 1996.
15. Bass, S., Delmas, P. D., Pearce, G., Hendrich, E., Tabensky, A., and Seeman, E. The differing tempo of growth in bone size, mass, and density in girls is region-specific. J Clin Invest 104:795-804; 1999.
16. Baxter-Jones, A. D., Mirwald, R. L., McKay, H. A., and Bailey, D. A. A longitudinal analysis of sex differences in bone mineral accrual in healthy 8-19-year-old boys and girls. Ann Hum Biol 30:160-75; 2003.
17. Baxter-Jones, A. D., Mirwald, R. Multilevel modelling. Methods in Human Growth Research: Cambridge University Press; 2004.
18. Baxter-Jones, A. D., Sherar, L.B. Chapter 1: Growth and maturation. Paediatric Exercise Physiology. London: Churchill Livingston; 2006.
19. Baxter-Jones, A. D., Thompson, A.M., Malina, R.M. Growth and maturation in elite young female athletes. Sports Medicine and Arthroscopy Review 10:42-49; 2002.

20. Bennell, K. L., Khan, K.M., Matthews, B., et al. Activity-associated differences in bone mineral are evident before puberty: a cross-sectional study of 130 novice dancers and controls. Pediatric Exercise Science 12:91-122; 2000.
21. Bernard, G. W., and Pease, D. C. An electron microscopic study of initial intramembranous osteogenesis. Am J Anat 125:271-90; 1969.
22. Bertram, J. E., and Swartz, S. M. The 'law of bone transformation': a case of crying Wolff? Biol Rev Camb Philos Soc 66:245-73; 1991.
23. Billewicz, W. Z., and McGregor, I. A. A birth-to-maturity longitudinal study of heights and weights in two West African (Gambian) villages, 1951-1975. Ann Hum Biol 9:309-20; 1982.
24. Birkenhager-Frenkel, D. H., Nigg, A.L. Age-related bone loss as reflected by changes of interstitial bone thickness. Calcif Tissue Int 52:S60; 1993.
25. Black, S., Williams, S.M., Jones, I.E., Goulding, A. Children who avoid drinking cow milk have low dietary intakes and poor bone health. American Journal of Clinical Nutrition 76:675-680; 2002.
26. Bogin, B., Wall, M., MacVean, R.B. Longitudinal growth of high socioeconomic Guatemalan children analyzed by the Preece-Baines Function: An international comparison. Am J Human Biol. 2:271-281; 1990.
27. Bonat, S., Pathomvanich, A., Keil, M. F., Field, A. E., and Yanovski, J. A. Self-assessment of pubertal stage in overweight children. Pediatrics 110:743-7; 2002.
28. Bonjour, J. P., Carrie, A. L., Ferrari, S., Clavien, H., Slosman, D., Theintz, G., and Rizzoli, R. Calcium-enriched foods and bone mass growth in prepubertal girls: a randomized, double-blind, placebo-controlled trial. J Clin Invest 99:1287-94; 1997.
29. Bonjour, J. P., Rizzoli, R. Bone acquisition in adolescence. Osteoporosis. USA: Academic Press; 1996.
30. Bonjour, J. P., Theintz, G., Buchs, B., Slosman, D., and Rizzoli, R. Critical years and stages of puberty for spinal and femoral bone mass accumulation during adolescence. J Clin Endocrinol Metab 73:555-63; 1991.
31. Bousson, V., Bergot, C., Meunier, A., Barbot, F., Parlier-Cuau, C., Laval-Jeantet, A. M., and Laredo, J. D. CT of the middiaphyseal femur: cortical bone mineral density and relation to porosity. Radiology 217:179-87; 2000.
32. Bousson, V., Meunier, A., Bergot, C., Vicaut, E., Rocha, M. A., Morais, M. H., Laval-Jeantet, A. M., and Laredo, J. D. Distribution of intracortical porosity in human midfemoral cortex by age and gender. J Bone Miner Res 16:1308-17; 2001.
33. Bouxsein, M. L. Determinants of skeletal fragility. Best Pract Res Clin Rheumatol 19:897-911; 2005.
34. Bouxsein, M. L., Coan, B. S., and Lee, S. C. Prediction of the strength of the elderly proximal femur by bone mineral density and quantitative ultrasound measurements of the heel and tibia. Bone 25:49-54; 1999.
35. Bowman, B. M., and Miller, S. C. Skeletal mass, chemistry, and growth during and after multiple reproductive cycles in the rat. Bone 25:553-9; 1999.
36. Bowman, B. M., Siska, C. C., and Miller, S. C. Greatly increased cancellous bone formation with rapid improvements in bone structure in the rat maternal skeleton after lactation. J Bone Miner Res 17:1954-60; 2002.
37. Boyle, M. H., and Willms, J. D. Multilevel modelling of hierarchical data in developmental studies. J Child Psychol Psychiatry 42:141-62; 2001.
38. Bradney, M., Pearce, G., Naughton, G., Sullivan, C., Bass, S., Beck, T., Carlson, J., and Seeman, E. Moderate exercise during growth in prepubertal boys: changes in bone mass, size, volumetric density, and bone strength: a controlled prospective study. J Bone Miner Res 13:1814-21; 1998.
39. Bravo, G., Gauthier, P., Roy, P.M., et al. Impact of a 12-month exercise program on the physical and psychological health of osteopenic women. J Am Geriatr Soc 44:756-762; 1996.

40. Brommage, R., and DeLuca, H. F. Regulation of bone mineral loss during lactation. Am J Physiol 248:E182-7; 1985.
41. Brown, T., and Townsend, G. C. Adolescent growth in height of Australian aboriginals analysed by the Preece-Baines function: a longitudinal study. Ann Hum Biol 9:495-505; 1982.
42. Brundtland, G. H., Liestol, K., and Walloe, L. Height, weight and menarcheal age of Oslo schoolchildren during the last 60 years. Ann Hum Biol 7:307-22; 1980.
43. BuckWalter, J. A., Einhorn, T.A., Simon, S.R. Orthopaedic Basic Science. Biology and the Biomechanics of the Musculoskeletal System; 2000.
44. Burr, D. B. Bone material properties and mineral matrix contributions to fracture risk or age in women and men. J Musculoskelet Neuronal Interact 2:201-4; 2002.
45. Burr, D. B. The contribution of the organic matrix to bone's material properties. Bone 31:8-11; 2002.
46. Burr, D. B., Martin, R. B., Schaffler, M. B., and Radin, E. L. Bone remodeling in response to in vivo fatigue microdamage. J Biomech 18:189-200; 1985.
47. Burr, D. B., Turner, C.H., Naick, P., Forwood, M.R. Ambrosius, W., Hasan, M.S., Pidaparti, R. Does microdamage accumulation affect the mechanical properites of bone? J Biomech 31:337-345; 1998.
48. Burstein, A. H., Reilly, D. T., and Martens, M. Aging of bone tissue: mechanical properties. J Bone Joint Surg Am 58:82-6; 1976.
49. Cann, C. E., Genant, H. K., Kolb, F. O., and Ettinger, B. Quantitative computed tomography for prediction of vertebral fracture risk. Bone 6:1-7; 1985.
50. Carani, C., Qin, K., Simoni, M., Faustini-Fustini, M., Serpente, S., Boyd, J., Korach, K. S., and Simpson, E. R. Effect of testosterone and estradiol in a man with aromatase deficiency. N Engl J Med 337:91-5; 1997.
51. Carter, D. M., van der Meulen, M.C.H., Beaupre, G.S. Skeletal development: mechanical consequences of growth, aging, and disease. Osteoporosis. New York: Academic Press; 1996.
52. Carter, D. R. Mechanical loading history and skeletal biology. J Biomech 20:1095-109; 1987.
53. Carter, D. R., Bouxsein, M. L., and Marcus, R. New approaches for interpreting projected bone densitometry data. J Bone Miner Res 7:137-45; 1992.
54. Carter, D. R., and Hayes, W. C. Bone compressive strength: the influence of density and strain rate. Science 194:1174-6; 1976.
55. Chan, G. M., Ronald, N., Slater, P., Hollis, J., and Thomas, M. R. Decreased bone mineral status in lactating adolescent mothers. J Pediatr 101:767-70; 1982.
56. Chevalley, T., Rizzoli, R., Jans, D., Ferrari, S., Bonjour, J.P. Interaction between calcium intake and menarcheal age on bone mass gain: An 8-year follow-up study from pre-puberty to post-menarche. J Clin Endocrinol Metab 99:1287-1294; 2005.
57. Cole, T. J. Secular trends in growth. Proceedings of the Nutritional Society 59:317-324; 2000.
58. Cooper, R. R., Milgram, J. W., and Robinson, R. A. Morphology of the osteon. An electron microscopic study. J Bone Joint Surg Am 48:1239-71; 1966.
59. Courtney, A. C., Hayes, W. C., and Gibson, L. J. Age-related differences in post-yield damage in human cortical bone. Experiment and model. J Biomech 29:1463-71; 1996.
60. Crowder, C., and Austin, D. Age ranges of epiphyseal fusion in the distal tibia and fibula of contemporary males and females. J Forensic Sci 50:1001-7; 2005.
61. Currey, J. D. Bone strength: what are we trying to measure? Calcif Tissue Int 68:205-10; 2001.
62. Currey, J. D. Changes in the impact energy absorption of bone with age. J Biomech 12:459-69; 1979.
63. Currey, J. D. Physical characteristics affecting the tensile failure properties of compact bone. J Biomech 23:837-44; 1990.

64. Currey, J. D., Brear, K., and Zioupos, P. The effects of ageing and changes in mineral content in degrading the toughness of human femora. J Biomech 29:257-60; 1996.
65. Currey, J. D., and Butler, G. The mechanical properties of bone tissue in children. J Bone Joint Surg Am 57:810-4; 1975.
66. Daly, R. M. The effect of exercise on bone mass and structural geometry during growth. Med Sport Sci 51:33-49; 2007.
67. Damien, E., Price, J. S., and Lanyon, L. E. Mechanical strain stimulates osteoblast proliferation through the estrogen receptor in males as well as females. J Bone Miner Res 15:2169-77; 2000.
68. Dent, C. E., and Friedman, M. Pregnancy and idiopathic osteoporosis. Q J Med 34:341-57; 1965.
69. Dickenson, R. P., Hutton, W. C., and Stott, J. R. The mechanical properties of bone in osteoporosis. J Bone Joint Surg Br 63-B:233-8; 1981.
70. Dimeglio, A. Growth in pediatric orthopaedics. J Pediatr Orthop 21:549-55; 2001.
71. Dimeglio, A., Bonnel, F. Growth and development of the knew. The Immature Knee: Masson; 1998.
72. Drapeau, M. S., and Streeter, M. A. Modeling and remodeling responses to normal loading in the human lower limb. Am J Phys Anthropol 129:403-9; 2006.
73. Duke, P. M., Litt, I. F., and Gross, R. T. Adolescents' self-assessment of sexual maturation. Pediatrics 66:918-20; 1980.
74. Einhorn, T. A. Bone strength: the bottom line. Calcif Tissue Int 51:333-9; 1992.
75. Eriksen, E. F., Mosekilde, L., and Melsen, F. Effect of sodium fluoride, calcium, phosphate, and vitamin D2 on trabecular bone balance and remodeling in osteoporotics. Bone 6:381-9; 1985.
76. Evans, R. A., Marel, G.M., Lancaster, E.K., Kos, S., Evans, M., Wong, S.Y.P. Bone mass is low in relatives of osteoporotic patients. Ann. Intern. Med 109:870-873.; 1998.
77. Faulkner, R. A., Bailey, D. A., Drinkwater, D. T., McKay, H. A., Arnold, C., and Wilkinson, A. A. Bone densitometry in Canadian children 8-17 years of Age. Calcif Tissue Int 59:344-51; 1996.
78. Ferretti, J. L. Peripheral quantitative computed tomography for evaluating structural and mechanical properties of small bone. Mechanical testing of bone and the bone implant interface. Washington DC: CRC Press; 2000.
79. Fitzmaurice, G. M. Applied Longitudinal Analysis. Simple Linear Rgression: A Model for the Mean. USA: Jon Wiley & Sons, Inc.; 1962.
80. Foundation, N. O. Osteoporosis facts. USA; 1994.
81. Frank, J. D., Ryan, M., Kalscheur, V.L., Ruauz-Mason, C.P., Hozak, R.R., Muir, P. Aging and accumulation of microdamage in canine bone. Bone 30:201-206; 2002.
82. Frantz, A. G., and Rabkin, M. T. Effects of estrogen and sex difference on secretion of human growth hormone. J Clin Endocrinol Metab 25:1470-80; 1965.
83. Freemont, A. J. Basic bone cell biology. Int J Exp Pathol 74:411-6; 1993.
84. Frisancho, A. R., Garn, S.M., Ascoli, W. Subperiosteal and endosteal bone apposition during adolescence. Human Biology 42:639-664; 1970.
85. Frost, H. M. Bone's mechanostat: a 2003 update. Anat Rec A Discov Mol Cell Evol Biol 275:1081-101; 2003.
86. Frost, H. M. Bone "mass" and the "mechanostat": a proposal. Anat Rec 219:1-9; 1987.
87. Frost, H. M. Introduction to a new skeletal physiology.: Pajaro Group; 1995.
88. Frost, H. M. The mechanostat: a proposed pathogenic mechanism of osteoporoses and the bone mass effects of mechanical and nonmechanical agents. Bone Miner 2:73-85; 1987.
89. Frost, H. M. Perspectives: a proposed general model of the "mechanostat" (suggestions from a new skeletal-biologic paradigm). Anat Rec 244:139-47; 1996.
90. Frost, H. M. Skeletal structural adaptations to mechanical usage (SATMU): 4. Mechanical influences on intact fibrous tissues. Anat Rec 226:433-9; 1990.
91. Garn, S. M. The Course of Bone Gain and the Phases of Bone Loss. Orthopedic Clinics of North America 3:503; 1972.

92. Garn, S. M. The Earlier Gain and Later Loss of Cortical Bone. In Nutritional Perspective. USA: Charles C thomas; 1970.
93. Genant, H. K., Engelke, K., Fuerst, T., Gluer, C. C., Grampp, S., Harris, S. T., Jergas, M., Lang, T., Lu, Y., Majumdar, S., Mathur, A., and Takada, M. Noninvasive assessment of bone mineral and structure: state of the art. J Bone Miner Res 11:707-30; 1996.
94. Genant, H. K., Faulkner, K. G., and Gluer, C. C. Measurement of bone mineral density: current status. Am J Med 91:49S-53S; 1991.
95. Gill, G. G., Abbott, L.C. Practical method of predicting the growth of the femur and tibia in the child. Archives of Surgery 45:286-315; 1942.
96. Gilsanz, V., Boechat, M. I., Gilsanz, R., Loro, M. L., Roe, T. F., and Goodman, W. G. Gender differences in vertebral sizes in adults: biomechanical implications. Radiology 190:678-82; 1994.
97. Gilsanz, V., Boechat, M. I., Roe, T. F., Loro, M. L., Sayre, J. W., and Goodman, W. G. Gender differences in vertebral body sizes in children and adolescents. Radiology 190:673-7; 1994.
98. Gilsanz, V., Gibbens, D. T., Roe, T. F., Carlson, M., Senac, M. O., Boechat, M. I., Huang, H. K., Schulz, E. E., Libanati, C. R., and Cann, C. C. Vertebral bone density in children: effect of puberty. Radiology 166:847-50; 1988.
99. Gilsanz, V., Kovanlikaya, A., Costin, G., Roe, T. F., Sayre, J., and Kaufman, F. Differential effect of gender on the sizes of the bones in the axial and appendicular skeletons. J Clin Endocrinol Metab 82:1603-7; 1997.
100. Gong, E. J., Heald, F.P. Modern nutrition in health and disease. Diet, nutrition and adolescence. Philadel[hia: Lea & Febiger; 1994.
101. Gong, G., Johnston, M.L., Barger-Lux, M.J., Heaney, R.P. Association of Bone Dimensions with a Parathyroid Hormone Gene Polymorphism in Women. Osteoporos Int 9:307-311; 1999.
102. Goulding, A., Cannan, R., Williams, S. M., Gold, E. J., Taylor, R. W., and Lewis-Barned, N. J. Bone mineral density in girls with forearm fractures. J Bone Miner Res 13:143-8; 1998.
103. Grasty, R. L., and LaMarre, J. R. The annual effective dose from natural sources of ionising radiation in Canada. Radiat Prot Dosimetry 108:215-26; 2004.
104. Grimston, S. K., Morrison, K., Harder, J. A., and Hanley, D. A. Bone mineral density during puberty in western Canadian children. Bone Miner 19:85-96; 1992.
105. Gruber, H. E., Gutteridge, D. H., and Baylink, D. J. Osteoporosis associated with pregnancy and lactation: bone biopsy and skeletal features in three patients. Metab Bone Dis Relat Res 5:159-65; 1984.
106. Guglielmi, G., Grimston, S. K., Fischer, K. C., and Pacifici, R. Osteoporosis: diagnosis with lateral and posteroanterior dual x-ray absorptiometry compared with quantitative CT. Radiology 192:845-50; 1994.
107. Hagaman, J. R., Ambrose, W. W., and Hirsch, P. F. A scanning electron microscopic and photon absorptiometric study of the development, prolongation, and pattern of recovery from lactation-induced osteopenia in rats. J Bone Miner Res 5:123-32; 1990.
108. Haines, R. W. The histology of epiphyseal union in mammals. J Anat 120:1-25; 1975.
109. Hall, B. K. the embryonic development of bone. American Science 76:174-181; 1988.
110. Hangartner, T. N., and Gilsanz, V. Evaluation of cortical bone by computed tomography. J Bone Miner Res 11:1518-25; 1996.
111. Hauspie, R. C., Steendijk, R. Application of growth models in the analysis of pathological growth data: The cause of hypophosphatemic vitamin D--resistant rickets. Am J Human Biol. 5:181-192; 1993.
112. Hauspie, R. C., Vercauteren, M., and Susanne, C. Secular changes in growth and maturation: an update. Acta Paediatr Suppl 423:20-7; 1997.
113. Hayes, W. C. Biomechanics of cortical and trabecular bone: implications for assesment for fracture risk. Basic Orthopaedic Biomechanics. New York, USA: Raven Press Limited; 1991.

114. Heaney, R. P. Bone mass, the mechanostat, and ethnic differences. J Clin Endocrinol Metab 80:2289-90; 1995.
115. Heaney, R. P., Abrams, S., Dawson-Hughes, B., Looker, A., Marcus, R., Matkovic, V., Weaver, C. Peak Bone Mass. Osteoporosis International 11:985-1009; 2000.
116. Heinonen, A., Oja, P., Sievanen, H., et al. Effect of two training regimes on bone mineral density in healthy perimenopausal women: a randomised controlled trial. Journal of Bone and Mineral Research 12:483-490; 1998.
117. Hofbauer, L. C., Khosla, S., Dunstan, C. R., Lacey, D. L., Spelsberg, T. C., and Riggs, B. L. Estrogen stimulates gene expression and protein production of osteoprotegerin in human osteoblastic cells. Endocrinology 140:4367-70; 1999.
118. Holmberg-Marttila, D., Sievanen, H., and Tuimala, R. Changes in bone mineral density during pregnancy and postpartum: prospective data on five women. Osteoporos Int 10:41-6; 1999.
119. Hughes, D. E., Dai, A., Tiffee, J. C., Li, H. H., Mundy, G. R., and Boyce, B. F. Estrogen promotes apoptosis of murine osteoclasts mediated by TGF-beta. Nat Med 2:1132-6; 1996.
120. Hunziker, E. B. Mechanism of Longitudinal Bone Growth and Its Regulation by Growth Plate Chondrocytes. Microscopy Research and Technique 28:505-519; 1994.
121. Ilich, J. Z., Hangartner, T.A., Skugor, M., Roche, A.F., Goel, P., and Matkovic, V. Skeletal age as a determinant of bone mass in young females. Skeletal Radiol 25:431-439; 1996.
122. Jaglal, S. B., McIsaac, W. J., Hawker, G., Jaakkimainen, L., Cadarette, S. M., and Chan, B. T. Patterns of use of the bone mineral density test in Ontario, 1992-1998. Cmaj 163:1139-43; 2000.
123. Jarvinen, T. L., Kannus, P., and Sievanen, H. Estrogen and bone--a reproductive and locomotive perspective. J Bone Miner Res 18:1921-31; 2003.
124. Jarvinen, T. L., Kannus, P., Sievanen, H., Jolma, P., Heinonen, A., and Jarvinen, M. Randomized controlled study of effects of sudden impact loading on rat femur. J Bone Miner Res 13:1475-82; 1998.
125. Jarvinen, T. L. N., Kannus, P., Sievanen, H. Have the DXA-based exercise studies seriously underestimated the effects of mechanical loading on bone? (Letter). Journal of Bone and Mineral Research 14:1634-1635; 1999.
126. Jaworski, Z. F. G., Duck, B., Sekaly, G. Cell kinetics underlying skeletal growth and bone tissue turnover. Bone Histomorphometry: Techniques and Interpretation. Boca Ranton, FL: CRC Press; 1981.
127. Jee, W. S. The Skeletal tissues. Cell and Tissue Biology. Baltimore, MD: Urban & Schwarzenburg; 1988.
128. Jessop, H. L., Sjoberg, M., Cheng, M. Z., Zaman, G., Wheeler-Jones, C. P., and Lanyon, L. E. Mechanical strain and estrogen activate estrogen receptor alpha in bone cells. J Bone Miner Res 16:1045-55; 2001.
129. Kemper, H. C., Twisk, J. W., van Mechelen, W., Post, G. B., Roos, J. C., and Lips, P. A fifteen-year longitudinal study in young adults on the relation of physical activity and fitness with the development of the bone mass: The Amsterdam Growth And Health Longitudinal Study. Bone 27:847-53; 2000.
130. Khan, K. M., McKay, H.A., Kannus, P., Bailey, D., Wark, J., Bennell, K. Physical Activity and Bone Health. U.S.A.: Human Kinetics; 2001.
131. Kimmel, D. B. A paradigm for skeletal strength homeostasis. J Bone Miner Res 8 Suppl 2:S515-22; 1993.
132. Kontulainen, S. A., Macdonald, H. M., Khan, K. M., and McKay, H. A. Examining bone surfaces across puberty: a 20-month pQCT trial. J Bone Miner Res 20:1202-7; 2005.
133. Kontulainen, S. A., Macdonald, H. M., and McKay, H. A. Change in cortical bone density and its distribution differs between boys and girls during puberty. J Clin Endocrinol Metab 91:2555-61; 2006.

134. Kovacs, C. S., and Kronenberg, H. M. Maternal-fetal calcium and bone metabolism during pregnancy, puerperium, and lactation. Endocr Rev 18:832-72; 1997.
135. Kroke, A., Manz, F., Kersting, M., Remer, T., Sichert-Hellert, W., Alexy, U., and Lentze, M. J. The DONALD Study. History, current status and future perspectives. Eur J Nutr 43:45-54; 2004.
136. Kunkele, J., and Kenagy, G. J. Inefficiency of lactation in primiparous rats: the costs of first reproduction. Physiol Zool 70:571-7; 1997.
137. Lai, Y. M., Qin, L., Hung, V. W., and Chan, K. M. Regional differences in cortical bone mineral density in the weight-bearing long bone shaft--a pQCT study. Bone 36:465-71; 2005.
138. Landin, L. A. Fracture patterns in children. Analysis of 8,682 fractures with special reference to incidence, etiology and secular changes in a Swedish urban population 1950-1979. Acta Orthop Scand Suppl 202:1-109; 1983.
139. Lang, P., Steiger, P., Faulkner, K., Gluer, C., and Genant, H. K. Osteoporosis. Current techniques and recent developments in quantitative bone densitometry. Radiol Clin North Am 29:49-76; 1991.
140. Lasky, M. A., Lyttle, K.D., Flaxman, M.E., et al. The influence of tissue depth and composition on the performance of the Lunar dual-energy X-ray absorptiometry whole body scanning mode. Eur J Clin Nutr 46:39-45.; 1992.
141. Li, J., Mashiba, T., and Burr, D. B. Bisphosphonate treatment suppresses not only stochastic remodeling but also the targeted repair of microdamage. Calcif Tissue Int 69:281-6; 2001.
142. Liberman, U. A., Weiss, S. R., Broll, J., Minne, H. W., Quan, H., Bell, N. H., Rodriguez-Portales, J., Downs, R. W., Jr., Dequeker, J., and Favus, M. Effect of oral alendronate on bone mineral density and the incidence of fractures in postmenopausal osteoporosis. The Alendronate Phase III Osteoporosis Treatment Study Group. N Engl J Med 333:1437-43; 1995.
143. Lieberman, D. E., Pearson, O. M., Polk, J. D., Demes, B., and Crompton, A. W. Optimization of bone growth and remodeling in response to loading in tapered mammalian limbs. J Exp Biol 206:3125-38; 2003.
144. Lilley, J., Walters, B. G., Heath, D. A., and Drolc, Z. In vivo and in vitro precision for bone density measured by dual-energy X-ray absorption. Osteoporos Int 1:141-6; 1991.
145. Lochmuller, E. M., Burklein, D., Kuhn, V., Glaser, C., Muller, R., Gluer, C. C., and Eckstein, F. Mechanical strength of the thoracolumbar spine in the elderly: prediction from in situ dual-energy X-ray absorptiometry, quantitative computed tomography (QCT), upper and lower limb peripheral QCT, and quantitative ultrasound. Bone 31:77-84; 2002.
146. Lochmuller, E. M., Groll, O., Kuhn, V., and Eckstein, F. Mechanical strength of the proximal femur as predicted from geometric and densitometric bone properties at the lower limb versus the distal radius. Bone 30:207-16; 2002.
147. Lochmuller, E. M., Lill, C. A., Kuhn, V., Schneider, E., and Eckstein, F. Radius bone strength in bending, compression, and falling and its correlation with clinical densitometry at multiple sites. J Bone Miner Res 17:1629-38; 2002.
148. Lochmuller, E. M., Miller, P., Burklein, D., Wehr, U., Rambeck, W., and Eckstein, F. In situ femoral dual-energy X-ray absorptiometry related to ash weight, bone size and density, and its relationship with mechanical failure loads of the proximal femur. Osteoporos Int 11:361-7; 2000.
149. Lockwood, C. J. The initiation of parturition at term. Obstet Gynecol Clin North Am 31:935-47, xii; 2004.
150. Lorenzo, J. A., Naprta, A., Rao, Y., Alander, C., Glaccum, M., Widmer, M., Gronowicz, G., Kalinowski, J., and Pilbeam, C. C. Mice lacking the type I interleukin-1 receptor do not lose bone mass after ovariectomy. Endocrinology 139:3022-5; 1998.
151. Lorrain, J., Paiement, G., Chevrier, N., Lalumiere, G., Laflamme, G. H., Caron, P., and Fillion, A. Population demographics and socioeconomic impact of osteoporotic fractures in Canada. Menopause 10:228-34; 2003.

152. Luke, D. A. Multilevel Modelling. Quantitative Applications in the Social Sciences: Sage Publications Inc.; 2001.
153. Luliano-Burns, S. S., L., Naughton, G., Gibbons, K. Regional specificity of exercise and calcium during skeletal growth in girls: a randomized controlled trial. Journal of Bone and Mineral Research 18:156-162; 2003.
154. Macdonald, H., Kontulainen, S., Petit, M., Janssen, P., and McKay, H. Bone strength and its determinants in pre- and early pubertal boys and girls. Bone 39:598-608; 2006.
155. Macdonald, H. M., Kontulainen, S. A., Mackelvie-O'Brien, K. J., Petit, M. A., Janssen, P., Khan, K. M., and McKay, H. A. Maturity- and sex-related changes in tibial bone geometry, strength and bone-muscle strength indices during growth: a 20-month pQCT study. Bone 36:1003-11; 2005.
156. Macdonald, H. M., Kontulainen, S.A., MacKelvie-O'Brien, Petit, M.A., Janssen, P., Khan, K.M. McKay, H.A. Matuirty and sex-related changes in tibial bone geometry, strength and bone-muscle strength indices during growth: A 20-month pQCT study. Bone 36:1303-1311; 2004.
157. Macdonald, H. M., Kontulainen, S.A., MacKelvie-O'Brien, Petit, M.A., Janssen, P., Khan, K.M. McKay, H.A. Maturity and sex-related changes in tibial bone geometry, strength and bone-muscle strength indices during growth: A 20-month pQCT study. Bone 36:1303-1311; 2005.
158. Macdonald, H. M., Mackelvie, K.J., MacLean, L.B., McKay, H.A. Does tibial bone structure differ between girls who completed a 20-month exercise intervention and controls? Medicine & Science in Sports & Exercise 35:S360; 2003.
159. MacKelvie, K. J., Khan, K. M., and McKay, H. A. Is there a critical period for bone response to weight-bearing exercise in children and adolescents? a systematic review. Br J Sports Med 36:250-7; discussion 257; 2002.
160. Mackelvie, K. J., McKay, H. A., Khan, K. M., and Crocker, P. R. Lifestyle risk factors for osteoporosis in Asian and Caucasian girls. Med Sci Sports Exerc 33:1818-24; 2001.
161. Mackelvie, K. J., McKay, H. A., Khan, K. M., and Crocker, P. R. A school-based exercise intervention augments bone mineral accrual in early pubertal girls. J Pediatr 139:501-8; 2001.
162. MacKelvie, K. J., McKay, H. A., Petit, M. A., Moran, O., and Khan, K. M. Bone mineral response to a 7-month randomized controlled, school-based jumping intervention in 121 prepubertal boys: associations with ethnicity and body mass index. J Bone Miner Res 17:834-44; 2002.
163. MacKelvie, K. J., Petit, M. A., Khan, K. M., Beck, T. J., and McKay, H. A. Bone mass and structure are enhanced following a 2-year randomized controlled trial of exercise in prepubertal boys. Bone 34:755-64; 2004.
164. Mahmoodi, S., Sharif, B. S., Chester, E. G., Owen, J. P., and Lee, R. Skeletal growth estimation using radiographic image processing and analysis. IEEE Trans Inf Technol Biomed 4:292-7; 2000.
165. Malina, R. B., C. Growth, Maturation, and Physical Activitiy. Human Kinetics. Champaign, IL; 1991.
166. Malina, R. M., Claessens, A.L., Van Aken, Katrijn, Thomis, M., Lefevre, J., Philippaerts, R., Beunen, G.P. Maturity Offest in Gymnasts: Application of a Prediction Equation. Med Sci Sports Exerc 38:1342-1347; 2006.
167. Marieb, E. N. Human Anatomy & Physiology. Menlo Park, California: Benjamin/Cummings Science Publishing; 1998.
168. Martin, R. B. Determinants of the mechanical properties of bones. Journal of Biomechanics 24:79-88; 1991.
169. Martin, R. B. Fatigue damage, remodeling, and the minimization of skeletal weight. J Theor Biol 220:271-6; 2003.
170. Martin, R. B. Is all cortical bone remodeling initiated by microdamage? Bone 30:8-13.; 2002.
171. Martin, R. B., Burr, D.B., Sharkey, N.A. Skeletal Tissue Mechanics. New York: Springer; 1998.
172. Martini, F., Timmons, M.J. Human Anatomy. U.S.A.: Prentice Hall; 1995.
173. Marvaso, V., Bernard, R.F. The third metacarpal styloid process in humans: origins and functions. American Journal of Anatomy 149:453-468; 1977.

174. Matkovic, V., Ciganovic, M., Tominac, C., and Kostial, K. Osteoporosis and epidemiology of fractures in Croatia. An international comparison. Henry Ford Hosp Med J 28:116-26; 1980.
175. Matkovic, V., Jelic, T., Wardlaw, G. M., Ilich, J. Z., Goel, P. K., Wright, J. K., Andon, M. B., Smith, K. T., and Heaney, R. P. Timing of peak bone mass in Caucasian females and its implication for the prevention of osteoporosis. Inference from a cross-sectional model. J Clin Invest 93:799-808; 1994.
176. Matsumoto, K., Konishi, H., Shiraishi, T., Morioka, I., Miyamoto, K., Yoshida, Y., Miyashita, K, Takeda, S. A comparative study on three methods for measuring the subischial leg length. Jouran lof Wakayama Medical Society (in Japanese) 41:353-358; 1990.
177. Matthews, J. N., Altman, D. G., Campbell, M. J., and Royston, P. Analysis of serial measurements in medical research. Bmj 300:230-5; 1990.
178. Mazess, R. B., Barden, H. S., Bisek, J. P., and Hanson, J. Dual-energy x-ray absorptiometry for total-body and regional bone-mineral and soft-tissue composition. Am J Clin Nutr 51:1106-12; 1990.
179. McKay, H. A., Bailey, D. A., Mirwald, R. L., Davison, K. S., and Faulkner, R. A. Peak bone mineral accrual and age at menarche in adolescent girls: a 6-year longitudinal study. J Pediatr 133:682-7; 1998.
180. McKay, H. A., Bailey, D.A., Wilkinson, A.A., Houston, C.S. Familial comparison of bone mineral density in the lumbar spine and proximal femur. Bone and Mineral 24:95-107; 1994.
181. McKay, H. A., MacLean, L., Petit, M., MacKelvie-O'Brien, K., Janssen, P., Beck, T., Khan, K.M. "Bounce at the Bell": a novel program of short bouts of exercise improves proximal femur bone mass in early pubertal children. British Journal of Sports Medicine 39:521-526; 2005.
182. McKay, H. A., Petit, M. A., Schutz, R. W., Prior, J. C., Barr, S. I., and Khan, K. M. Augmented trochanteric bone mineral density after modified physical education classes: a randomized school-based exercise intervention study in prepubescent and early pubescent children. J Pediatr 136:156-62; 2000.
183. McKern, T. W., Stewart, T.D. Skeletal age changes in young American males, analysed from the standpoint of age identification. United States of America; 1957.
184. Meema, H. E., and Meema, S. Cortical bone mineral density versus cortical thickness in the diagnosis of osteoporosis: a roentgenologic-densitometric study. J Am Geriatr Soc 17:120-41; 1969.
185. Melton, L. J., 3rd, Thamer, M., Ray, N. F., Chan, J. K., Chesnut, C. H., 3rd, Einhorn, T. A., Johnston, C. C., Raisz, L. G., Silverman, S. L., and Siris, E. S. Fractures attributable to osteoporosis: report from the National Osteoporosis Foundation. J Bone Miner Res 12:16-23; 1997.
186. Miller, J. Z., Slemenda, C. W., Meaney, F. J., Reister, T. K., Hui, S., and Johnston, C. C. The relationship of bone mineral density and anthropometric variables in healthy male and female children. Bone Miner 14:137-52; 1991.
187. Miller, S. C., Shupe, J. G., Redd, E. H., Miller, M. A., and Omura, T. H. Changes in bone mineral and bone formation rates during pregnancy and lactation in rats. Bone 7:283-7; 1986.
188. Mirwald, R. L., Baxter-Jones, A.D.G., Bailey, D.A., Beunen, G.P. An assessment of maturity from anthropometric measurements. Medicine & Science in Sports & Exercise 34:689-694; 2002.
189. Molgaard, C., Thomsen, B. L., and Michaelsen, K. F. Whole body bone mineral accretion in healthy children and adolescents. Arch Dis Child 81:10-5; 1999.
190. Mori, S., and Burr, D. B. Increased intracortical remodeling following fatigue damage. Bone 14:103-9; 1993.
191. Mori, S., Harruff, R., Ambrosius, W., and Burr, D. B. Trabecular bone volume and microdamage accumulation in the femoral heads of women with and without femoral neck fractures. Bone 21:521-6; 1997.

192. Morishima, A., Grumbach, M. M., Simpson, E. R., Fisher, C., and Qin, K. Aromatase deficiency in male and female siblings caused by a novel mutation and the physiological role of estrogens. J Clin Endocrinol Metab 80:3689-98; 1995.
193. Morris, F. L., Naughton, G.A., Gibbs, J.L., Carlson, J.S., Wark, J.D. Prospective Ten-Month Exercise Intervention in Premenarcheal Girls: Positive Effects on Bone and Lean Mass. Journal of Bone and Mineral Research 12:1453-1462; 1997.
194. Mosekilde, L., and Mosekilde, L. Sex differences in age-related changes in vertebral body size, density and biomechanical competence in normal individuals. Bone 11:67-73; 1990.
195. Muller, M. E., Webber, C. E., and Bouxsein, M. L. Predicting the failure load of the distal radius. Osteoporos Int 14:345-52; 2003.
196. Muthen, B. O., Curran, P.J. General longitudinal modeling of individual differences in experimental designs: A latent variable framework for analysis and power estimation. Psychological Methods 2:371-402.; 1997.
197. Neer, C. S., 2nd, and Horwitz, B. S. Fractures of the proximal humeral epiphysial plate. Clin Orthop Relat Res 41:24-31; 1965.
198. Nelson, D. A., and Koo, W. W. Interpretation of absorptiometric bone mass measurements in the growing skeleton: issues and limitations. Calcif Tissue Int 65:1-3; 1999.
199. Neu, C. M., Rauch, F., Rittweger, J., Manz, F., and Schoenau, E. Influence of puberty on muscle development at the forearm. Am J Physiol Endocrinol Metab 283:E103-7; 2002.
200. Nilsson, A., Ohlsson, C., Isaksson, O. G., Lindahl, A., and Isgaard, J. Hormonal regulation of longitudinal bone growth. Eur J Clin Nutr 48 Suppl 1:S150-8; discussion S158-60; 1994.
201. Nonaka, K., Fukuda, S., Aoki, K., Yoshida, T., and Ohya, K. Regional distinctions in cortical bone mineral density measured by pQCT can predict alterations in material property at the tibial diaphysis of the Cynomolgus monkey. Bone 38:265-72; 2006.
202. O'Connor, J. A., Lanyon, L. E., and MacFie, H. The influence of strain rate on adaptive bone remodelling. J Biomech 15:767-81; 1982.
203. Ogden, J. A. Injury to the growth mechanisms of the immature skeleton. Skeletal Radiol 6:237-53; 1981.
204. Ortner, D. J. Aging effects on osteon remodeling. Calcif Tissue Res 18:27-36; 1975.
205. Orwoll, E. S., and Oviatt, S. K. Longitudinal precision of dual-energy x-ray absorptiometry in a multicenter study. The Nafarelin/Bone Study Group. J Bone Miner Res 6:191-7; 1991.
206. Papadimitropoulos, E. A., Coyte, P.C., Josse, R.G., Greenwood, C.E. Current and projected rates of hip fracture in Canada. Canadian Medical Association Journal 157:1357-1363.; 1997.
207. Parfitt, A. M. Osteonal and hemi-osteonal remodeling: the spatial and temporal framework for signal traffic in adult human bone. J Cell Biochem 55:273-86; 1994.
208. Parfitt, A. M. Quantum concept of bone remodeling and turnover: implications for the pathogenesis of osteoporosis. Calcif Tissue Int 28:1-5; 1979.
209. Parfitt, A. M. Targeted and nontargeted bone remodeling: relationship to basic multicellular unit origination and progression. Bone 30:5-7; 2002.
210. Parfitt, A. M. The two faces of growth: benefits and risks to bone integrity. Osteoporos Int 4:382-98; 1994.
211. Parfitt, A. M., Travers, R., Rauch, F., and Glorieux, F. H. Structural and cellular changes during bone growth in healthy children. Bone 27:487-94; 2000.
212. Pearson, O. M., Lieberman, D.E. The Aging of Wolff's "Law": Ontogeny and Responses to Mechanical Loading in Cortical Bone. Yearbook of Physical Anthropology 47:63-99; 2004.
213. Peng, T. C., Kusy, R. P., Garner, S. C., Hirsch, P. F., and De Blanco, M. C. Influence of lactation and pregnancy + lactation on mechanical properties and mineral content of the rat femur. J Bone Miner Res 2:249-57; 1987.

214. Petrtyl, M., Hert, J., and Fiala, P. Spatial organization of the haversian bone in man. J Biomech 29:161-9; 1996.
215. Plotnikoff, R., Williams, P., Fein, A. Effects of a school capacity-building intervention on children's heart health: evaluation of the Coalfields Healthy Heartbeat School Project in New South Wales, Australia. Health Education Journal 58:389-400.; 1999.
216. Polig, E., and Jee, W. S. A model of osteon closure in cortical bone. Calcif Tissue Int 47:261-9; 1990.
217. Price, J. S., Oyajobi, B.O., Russell, R.G.G. The cell biology of bone growth. European Journal of Clinical Nutrition 48:S131*S149; 1994.
218. Pritchett, J. W. Longitudinal growth and growth-plate activity in the lower extremity. Clin Orthop Relat Res:274-9; 1992.
219. Pyle, S. I., Hoerr, N.L. Radiographic Atlas of Skeletal Development of the Knee. United States of America: Springfield Press; 1955.
220. Raab, D. M., Crenshaw, T. D., Kimmel, D. B., and Smith, E. L. A histomorphometric study of cortical bone activity during increased weight-bearing exercise. J Bone Miner Res 6:741-9; 1991.
221. Raisz, L. G., and Seeman, E. Causes of age-related bone loss and bone fragility: an alternative view. J Bone Miner Res 16:1948-52; 2001.
222. Ramsey, F. L. The statistical sleuth: a course in methods of data analysis. Mathematical Statistics. Pacific Grove, CA: Wadsworth Group; 2002.
223. Rauch, F., and Schoenau, E. The developing bone: slave or master of its cells and molecules? Pediatr Res 50:309-14; 2001.
224. Rauch, F., and Schoenau, E. Skeletal development in premature infants: a review of bone physiology beyond nutritional aspects. Arch Dis Child Fetal Neonatal Ed 86:F82-5; 2002.
225. Riggs, B. L., Khosla, S., and Melton, L. J., 3rd A unitary model for involutional osteoporosis: estrogen deficiency causes both type I and type II osteoporosis in postmenopausal women and contributes to bone loss in aging men. J Bone Miner Res 13:763-73; 1998.
226. Riggs, B. L., Wahner, H. W., Dunn, W. L., Mazess, R. B., Offord, K. P., and Melton, L. J., 3rd Differential changes in bone mineral density of the appendicular and axial skeleton with aging: relationship to spinal osteoporosis. J Clin Invest 67:328-35; 1981.
227. Riggs, B. L., Wahner, H. W., Melton, L. J., 3rd, Richelson, L. S., Judd, H. L., and Offord, K. P. Rates of bone loss in the appendicular and axial skeletons of women. Evidence of substantial vertebral bone loss before menopause. J Clin Invest 77:1487-91; 1986.
228. Ritchie, L. D., Fung, E. B., Halloran, B. P., Turnlund, J. R., Van Loan, M. D., Cann, C. E., and King, J. C. A longitudinal study of calcium homeostasis during human pregnancy and lactation and after resumption of menses. Am J Clin Nutr 67:693-701; 1998.
229. Robling, A. G., Burr, D. B., and Turner, C. H. Recovery periods restore mechanosensitivity to dynamically loaded bone. J Exp Biol 204:3389-99; 2001.
230. Robling, A. G., Castillo, A. B., and Turner, C. H. Biomechanical and molecular regulation of bone remodeling. Annu Rev Biomed Eng 8:455-98; 2006.
231. Ruff, C., Holt, B., and Trinkaus, E. Who's afraid of the big bad Wolff? "Wolff's law" and bone functional adaptation. Am J Phys Anthropol 129:484-98; 2006.
232. Schaffler, M. B., Choi, K., and Milgrom, C. Aging and matrix microdamage accumulation in human compact bone. Bone 17:521-25; 1995.
233. Scheuer, L., Black, S. The Juvenile Skeleton. Great Britian: Elsevier Academic Press; 2004.
234. Schiessl, H., Ferretti, J.L., Tysarczkk-Niemeyer, G., Willnecker, J. Noninvasive bone strength index as analyzed by peripheral quantitative computed tomography (pQCT). Pediatric Osteology: New Developments in Diagnostics and Therapy. Amsterdam: Elsevier; 1996.
235. Schiessl, H., Frost, H. M., and Jee, W. S. Estrogen and bone-muscle strength and mass relationships. Bone 22:1-6; 1998.

236. Schmidt, I. M., Jorgensen, M. H., and Michaelsen, K. F. Height of conscripts in Europe: is postneonatal mortality a predictor? Ann Hum Biol 22:57-67; 1995.
237. Schoenau, E., Neu, C. M., Mokov, E., Wassmer, G., and Manz, F. Influence of puberty on muscle area and cortical bone area of the forearm in boys and girls. J Clin Endocrinol Metab 85:1095-8; 2000.
238. Schoenau, E., Neu, C. M., Rauch, F., and Manz, F. The development of bone strength at the proximal radius during childhood and adolescence. J Clin Endocrinol Metab 86:613-8; 2001.
239. Schoenau, E., Neu, C. M., Rauch, F., and Manz, F. Gender-specific pubertal changes in volumetric cortical bone mineral density at the proximal radius. Bone 31:110-3; 2002.
240. Schonau, E. Problems of bone analysis in childhood and adolescence. Pediatr Nephrol 12:420-9; 1998.
241. Schwandt, P., Geiss, H. C., Ritter, M. M., Ublacker, C., Parhofer, K. G., Otto, C., Laubach, E., Donner, M. G., Haas, G. M., and Richter, W. O. The prevention education program (PEP). A prospective study of the efficacy of family-oriented life style modification in the reduction of cardiovascular risk and disease: design and baseline data. J Clin Epidemiol 52:791-800; 1999.
242. Seeman, E. Clinical review 137: Sexual dimorphism in skeletal size, density, and strength. J Clin Endocrinol Metab 86:4576-84; 2001.
243. Seeman, E. Growth in bone mass and size--are racial and gender differences in bone mineral density more apparent than real? J Clin Endocrinol Metab 83:1414-9; 1998.
244. Seeman, E. Pathogenesis of bone fragility in women and men. Lancet 359:1841-50; 2002.
245. Seeman, E., Hopper, J. L., Bach, L. A., Cooper, M. E., Parkinson, E., McKay, J., and Jerums, G. Reduced bone mass in daughters of women with osteoporosis. N Engl J Med 320:554-8; 1989.
246. Seeman, E., Tsalamandris, C., Formica, C., Hopper, J. L., and McKay, J. Reduced femoral neck bone density in the daughters of women with hip fractures: the role of low peak bone density in the pathogenesis of osteoporosis. J Bone Miner Res 9:739-43; 1994.
247. Sherar, L. B., Baxter-Jones, A. D., and Mirwald, R. L. Limitations to the use of secondary sex characteristics for gender comparisons. Ann Hum Biol 31:586-93; 2004.
248. Sievanen, H., Loskue, V., Rauhio, A., Kannus, P., Heinonen, A., Vuori, I. Peripheral quantitative computed tomography in human long bones: evaluation of in vitro and in vivo precision. Journal of Bone and Mineral Research 1998:871-882.; 1998.
249. Smith, E. P., Boyd, J., Frank, G. R., Takahashi, H., Cohen, R. M., Specker, B., Williams, T. C., Lubahn, D. B., and Korach, K. S. Estrogen resistance caused by a mutation in the estrogen-receptor gene in a man. N Engl J Med 331:1056-61; 1994.
250. Smith, R., Stevenson, J. C., Winearls, C. G., Woods, C. G., and Wordsworth, B. P. Osteoporosis of pregnancy. Lancet 1:1178-80; 1985.
251. Smith, R. W. Dietary and hormonal factors in bone loss. Fed Proc 26:1737-1746; 1967.
252. Southard, R. N., Morris, J. D., Mahan, J. D., Hayes, J. R., Torch, M. A., Sommer, A., and Zipf, W. B. Bone mass in healthy children: measurement with quantitative DXA. Radiology 179:735-8; 1991.
253. Specker, B., and Binkley, T. Randomized trial of physical activity and calcium supplementation on bone mineral content in 3- to 5-year-old children. J Bone Miner Res 18:885-92; 2003.
254. Specker, B. L. Influence of rapid growth on skeletal adaptation to exercise. J Musculoskelet Neuronal Interact 6:147-53; 2006.
255. Specker, B. L., Brazerol, W., Tsang, R. C., Levin, R., Searcy, J., and Steichen, J. Bone mineral content in children 1 to 6 years of age. Detectable sex differences after 4 years of age. Am J Dis Child 141:343-4; 1987.
256. Stang, J., Story, M. Adolescent Growth and Development. Guidelines for Adolescent Nutrition Services.; 2005.
257. Stratec XCT 2000 Manual, Software Version 5.50.; 2000.

258. Tanaka, C., Murata, M., Homma, M., Kawahara, T. Reference charts of body proportion for Japanese girls and boys. Annals of Human Biology 31:681-689; 2004.
259. Tanner, J. M. Foetus into Man. Cambridge: Harvard Press; 1978.
260. Tanner, J. M. Growth as a measure of the nutritional and hygienic status of a population. Hormone Research 38:106-115; 1992.
261. Tanner, J. M., and Davies, P. S. Clinical longitudinal standards for height and height velocity for North American children. J Pediatr 107:317-29; 1985.
262. Tanner, J. M., and Whitehouse, R. H. Clinical longitudinal standards for height, weight, height velocity, weight velocity, and stages of puberty. Arch Dis Child 51:170-9; 1976.
263. Tanner, J. M., Whitehouse, R. H., and Takaishi, M. Standards from birth to maturity for height, weight, height velocity, and weight velocity: British children, 1965. II. Arch Dis Child 41:613-35; 1966.
264. Thum, Y. M. Hierarchical linear models for multivariate outcomes. Journal of Education and Behavioural Statistics 27:77-108.; 1997.
265. Tickle, C. Vertebrate development. On making a skeleton. Nature 368:587-8; 1994.
266. Tortora, G. J. Principles of Human Anatomy. New York: Harpor and Row Publishers; 1989.
267. Tuck, S. P., Pearce, M. S., Rawlings, D. J., Birrell, F. N., Parker, L., and Francis, R. M. Differences in bone mineral density and geometry in men and women: the Newcastle Thousand Families Study at 50 years old. Br J Radiol 78:493-8; 2005.
268. Turner, C. H., and Burr, D. B. Basic biomechanical measurements of bone: a tutorial. Bone 14:595-608; 1993.
269. Van Gerven, D. O., Armelagos, G.J., Bartley, M.H. Roentgenographic and direct measurement fo femoral cortical involution in a prehistoric Mississippian population. American Journal of Physical Anthropology 1:23-38; 1969.
270. Van Loan, M. D., Keim, N.L., Berg, K., et al. Evaluation of body composition by dual energy x-ray absorptiometry and two different software packages. Med Sci Sports Exerc 27:587-591.; 1995.
271. Vinz, H. [Change in the resistance properties of compact bone tissue in the course of aging]. Gegenbaurs Morphol Jahrb 115:257-72; 1970.
272. Vinz, H. [Firmness of pure bone substance. Approximation method for the determination of bone tissue firmness related to the cavity-free cross section]. Gegenbaurs Morphol Jahrb 117:453-60; 1972.
273. Wang, Q., Markku, A, Nicholson, P., Lyytikainen, A, Suuriniemi, M, Helkala, E, Suominen, H, Cheng, S. Growth Patterns at Distal Radius and Tibial Shaft in Pubertal Girls: A 2-Year Longitudinal Study. Journal of Bone and Mineral Research 20:954-961; 2005.
274. Wiktorowicz, M. E., Goeree, R., Papaioannou, A., Adachi, J. D., and Papadimitropoulos, E. Economic implications of hip fracture: health service use, institutional care and cost in Canada. Osteoporos Int 12:271-8; 2001.
275. Willett, J. B., Sayer, A.G. Using covariance structure analysis to detect correlates and predictors of individual change over time. Psychological Bulletin 116:363-381.; 1994.
276. Zemel, B. S., Johnston, F.E. Application of the Preece-Bains Growth Model to Cross-Sectional Data: Problems of Validity and Interpretation. American Journal of Human Biology 6:563-570; 1994.